

**DISTRIBUTED SECONDARY VOLTAGE CONTROL FOR AC MICROGRIDS USING  
SPARSITY-PROMOTING METHOD**

by

**Thamer Zeed H Alharbi**

B.S., King Saud University, 2007

M.S., University of Adelaide, 2011

Submitted to the Graduate Faculty of  
the Swanson School of Engineering in partial fulfillment  
of the requirements for the degree of  
Doctor of Philosophy

University of Pittsburgh

2019

UNIVERSITY OF PITTSBURGH  
SWANSON SCHOOL OF ENGINEERING

This dissertation was presented

by

**Thamer Zeed H Alharbi**

It was defended on

December 11, 2018

and approved by

Brandon Grainger, PhD, Assistant Professor  
Department of Electrical and Computer Engineering

Gregory Reed, PhD, Professor  
Department of Electrical and Computer Engineering

Ervin Sejdic, PhD, Associate Professor  
Department of Electrical and Computer Engineering

Mingui Sun, PhD, Professor  
Department of Neurological Surgery

Dissertation Director: Zhi-Hong Mao, PhD, Professor  
Department of Electrical and Computer Engineering

Copyright © by Thamer Zeed H Alharbi  
2019

# **DISTRIBUTED SECONDARY VOLTAGE CONTROL FOR AC MICROGRIDS USING SPARSITY-PROMOTING METHOD**

Thamer Zeed H Alharbi, PhD

University of Pittsburgh, 2019

In hierarchal control structure of microgrids, the control problem is decoupled into three control layers with specific goals at each layer; namely, primary control, secondary control, and tertiary control. While the higher control layer manages the economic aspects of operation, the objective of the primary control layer is to stabilizing the system and maintaining a proper load sharing between the DGs (distributed generators). This can be achieved via droop-controlled techniques that does not require any communication links between the DGs. However, this level of control will cause a voltage deviation (from nominal values) at each connected generator, which is resulted in power deficiency. Hence, the goal of the secondary control layer is to regulate these deviations caused by the primary control level with a minimum impact on the established power sharing property; preferably, at minimum communication links to have more reliable, secure and efficient system, which is a challenging task to realize. In this dissertation, a distributed secondary voltage control will be presented, that is able to successfully achieve the standard secondary control objectives for small/medium scale AC inverter-based & droop-controlled microgrids using sparsity-promoting method. In this framework, the problem of designing a distributed secondary controller is formulated as an optimal control problem with an additional term added to the

standard objective function ( $H_2$  norm of the closed-loop system) to include sparsity structure. The solution of this optimization problem is a candidate  $K$  (state-feedback matrix) for the state-feedback controller  $u=-Kx$  that minimizes the objective function (i.e. able to optimize performance as a regulator, lower the control effort, and eliminate insignificant elements to achieve a desired level of sparsity) while maintaining closed-loop stability of the system. To verify the effectiveness of the proposed distributed secondary voltage controller to achieve its objectives with satisfactory results, a simulated model of a typical microgrid system has been used and tested under various operation conditions.

## TABLE OF CONTENTS

<b>PREFACE.....</b>	<b>xii</b>
<b>1.0 INTRODUCTION.....</b>	<b>1</b>
<b>1.1 RESEARCH OBJECTIVES.....</b>	<b>2</b>
<b>1.2 PREVIOUS WORK .....</b>	<b>2</b>
<b>1.3 SUMMARY OF CONTRIBUTION .....</b>	<b>3</b>
<b>1.4 IMPACT .....</b>	<b>5</b>
<b>2.0 MICROGRID: STATE OF THE ART.....</b>	<b>7</b>
<b>2.1 HIERARCHICAL CONTROL OF DROOP-CONTROLLED AC MICROGRIDS</b> <b>.....</b>	<b>9</b>
<b>2.1.1 Primary Control.....</b>	<b>11</b>
<b>2.1.2 Secondary Control .....</b>	<b>13</b>
<b>2.1.2.1 Centralized methods.....</b>	<b>14</b>
<b>2.1.2.2 Decentralized methods .....</b>	<b>19</b>
<b>2.1.2.3 Localized methods .....</b>	<b>21</b>
<b>2.1.3 Tertiary Control.....</b>	<b>30</b>
<b>3.0 SPARSITY-PROMOTING OPTIMAL CONTROL VIA ALTERNATING DIRECTION</b> <b>METHOD OF MULTIPLIERS.....</b>	<b>31</b>
<b>3.1 PROBLEM FORMULATION OF DESIGNING A DISTRIBUTED STATE</b> <b>FEEDBACK CONTROLLER .....</b>	<b>34</b>

3.2	<b>SOLVING THE DESIGN PROBLEM USING ADMM OPTIMIZATION ALGORITHM .....</b>	<b>37</b>
3.2.1	<b>Performance Optimization Iteration.....</b>	<b>40</b>
3.2.2	<b>Sparsity Optimization Iteration.....</b>	<b>41</b>
3.3	<b>FURTHER ENHANCEMENT FOR FINAL HEURISTIC SOLUTION .....</b>	<b>41</b>
3.4	<b>SUMMARIES AND OVERALL FLOWCHART OF THE ALGORITHM .....</b>	<b>42</b>
3.5	<b>AN ILLUSTRATED EXAMPLE.....</b>	<b>45</b>
4.0	<b>DISTRIBUTED SECONDARY VOLTAGE CONTROL (DSVC) FOR AC MICROGRID USING SPARSITY-PROMOTING APPROACH.....</b>	<b>48</b>
4.1	<b>REDUCED SMALL-SIGNAL STATE-SPACE MODEL OF INVERTER-BASED MICROGRID.....</b>	<b>48</b>
4.2	<b>OPTIMIZATION PROBLEM OF DISTRIBUTED STATE-FEEDBACK SECONDARY CONTROLLER.....</b>	<b>59</b>
4.3	<b>SPARSITY PROMOTING VIA ADMM.....</b>	<b>60</b>
4.4	<b>CHOOSING THE DESIGN PARAMETERS .....</b>	<b>62</b>
4.4.1	<b>Augmented tunable error states for nominal voltage tracking and improved reactive power sharing (<math>ei</math>) .....</b>	<b>62</b>
4.4.2	<b>State Weight Matrix (Q).....</b>	<b>65</b>
4.4.3	<b>Control Weight Matrix (R) .....</b>	<b>65</b>
4.4.4	<b>Disturbance Matrix (Bw).....</b>	<b>66</b>
4.4.5	<b>Desired Level of Sparsity (d).....</b>	<b>66</b>
4.5	<b>SIMULATION AND RESULTS.....</b>	<b>67</b>
4.5.1	<b>Test System Description .....</b>	<b>67</b>
4.5.2	<b>Design Guides .....</b>	<b>67</b>
4.5.3	<b>Test Procedure and Results.....</b>	<b>70</b>

4.5.3.1 Voltage Levels Restoration and Power Correction in homogenous Setup (identical line impedances) .....	70
4.5.3.2 Voltage Levels Restoration, Power Correction, and Reactive Power Sharing in Heterogeneous Setup (different line impedances).....	74
4.5.3.3 Reliability Against Generators Interruptions .....	81
<b>5.0 CONCLUSION AND FUTURE WORK .....</b>	<b>84</b>
<b>5.1 CONCLUSION.....</b>	<b>84</b>
<b>5.2 FUTURE WORK.....</b>	<b>87</b>
<b>APPENDIX.....</b>	<b>89</b>
<b>BIBLIOGRAPHY.....</b>	<b>95</b>

## LIST OF TABLES

Table 4-1 System parameters.....	69
Table 4-2. Number of nonzero elements and performance degradation compared to the equivalent centralized controller, case (1).....	73
Table 4-3. Number of nonzero elements and performance degradation compared to the equivalent centralized controller, case (2).....	77

## LIST OF FIGURES

Figure 2-1. Schematic diagram of a typical islanded microgrid. ....	8
Figure 2-2. Hierarchical levels of controlling a microgrid [11].....	10
Figure 2-3. Objectives of each control's level in the hierarchal control structure of a microgrid. ....	11
Figure 2-4. Droop-controlled based primary control of DG inverter [58].....	13
Figure 2-5. Communication structures in secondary control of a microgrid. ....	14
Figure 2-6. Centralized structure of secondary and tertiary controls in a microgrid [7]. ....	15
Figure 2-7. Potential Function Method (PFM) based secondary control of a microgrid [34]. ....	18
Figure 2-8. Decentralized structure of Estimator-based secondary control of a microgrid [44]. ..	21
Figure 2-9. Distributed secondary control of a microgrid: strongly connected communication topology [36].....	23
Figure 2-10. Distributed cooperative secondary control of a microgrid: pre-specified topology with a spanning tree [51].....	27
Figure 2-11. Distributed secondary control of a microgrid via distributed averaging: neighboring-basis communication topology [55].....	29
Figure 3-1. A generic distributed plant controlled by a distributed controller with sparse communication structure.....	32
Figure 3-2. Communication structures for controlling a distributed plant: from the conventional centralized controller to the flexible distributed controllers. ....	39
Figure 3-3. A summarized flowchart of the Sparsity-Promoting optimal control algorithm. ....	44
Figure 3-4. 100 unstable integrator nodes with exponentially decay coupling [59].....	46

Figure 3-5. (a) Performance versus sparsity as increasing sparsity level. (b) Performance versus sparsity level compared to the optimal centralized controller [59].	46
Figure 3-6. Identified localized communication topologies of distributed controllers using Sparsity-Promoting approach with different desired level of sparsity [59].	47
Figure 4-1. Droop-controlled based primary control of DG inverter [93].	49
Figure 4-2. Power controller block diagram [93].	50
Figure 4-3. Equivalent d-axis and q-axis circuits of each DG [93].	52
Figure 4-4. Achieving a balance between performance and sparsity in microgrid's secondary controller via sparsity-promoting optimal control approach.	63
Figure 4-5. Microgrid test configuration.	68
Figure 4-6. $V_{od}$ , $Q$ , and $P$ in homogeneous system with identical line impedances before and after using secondary control under: no load, resistive load, and a large inductive load.	72
Figure 4-7. Suggested state-feedback matrix $K$ based on SP method with the corresponding communication links, for voltage regulation and power correction in homogenous system with identical line impedances.	73
Figure 4-8. $V_{od}$ responses in homogenous system with the distributed secondary voltage control (DSVC) compared to PID control and centralized optimal control.	74
Figure 4-9. $V_{od}$ , $Q$ , and $P$ responses in heterogeneous system with different line impedances, before and after adding the distributed secondary voltage control (DSVC), under: no load, resistive load, and a large inductive load.	76
Figure 4-10. Suggested state-feedback matrix $K$ based on SP method with the corresponding communication links, for voltage regulation and reactive power sharing in heterogeneous system with different line impedances.	77
Figure 4-11. $Q$ & $P$ responses with the distributed secondary voltage control (DSVC) compared with PID control.	79
Figure 4-12. $Q$ & $P$ responses with the distributed secondary voltage control (DSVC) compared with optimal centralized secondary control.	80
Figure 4-13. $V_{od}$ , $Q$ , and $P$ responses after DG4 disconnection at 2.5 sec, before and after using distributed secondary voltage control (DSVC).	83

## **PREFACE**

I would like to express my deepest appreciation to my advisor Dr. Zhi-Hong Mao, who has given me so much help in research as well as in life; I am extremely glad to have him as my advisor. His inspiration, assistance, and motivation has empowered me to achieve this dissertation. I might likewise want to acknowledge the committee members, Dr. Gregory Reed, Dr. Brandon Grainger, Dr. Ervin Sejdic, and Dr. Mingui Sun, for their guidance and help.

Also, I would like to express my most profound gratitude to my dear wife Mrs. Sumayah Alharbi for her encouragement and kind support, and to my children, Sattam and Talal. Lastly, my deep gratefulness goes abroad back home to my Father (Zeed) and Mother (Azizah), for their boundless love and support.

## 1.0 INTRODUCTION

To meet the rapid growth on the electric demand and to increase the overall system efficiency and sustainability, the challenge of integrating various forms of resources into the grid, particularly renewable resources, draws the attention of researchers worldwide. However, the conventional centralized architecture of current power grid with long transmission links is extremely large and complex, and adding further resources that are heterogeneous and distributed in nature, such as wind, photovoltaic, micro-turbines, etc., would cause the operation reliability and efficiency a difficult task to realize. Alternatively, microgrid is proposed as a different architecture that has the ability to prevent the existing grid from expanding while facilitating smooth integration of mixed distributed generators in order to address environmental and economic concerns in a reliable and sustainable manner [1].

In order to reach a reliable and efficient operation for the microgrid and to overcome the stability issues, lack of inertia, resistive nature of low voltage power-electronic based microgrids, uncertainty of produced energy and unbalanced conditions of system; a prosperous control design is required [11]. Due to the difference in timescales between the control objectives in microgrid, the control problem can be decoupled into different control levels with specific goals at each level; namely, primary control, secondary control, and tertiary control [7]- [9]. While the objectives of primary control are stabilizing the system and maintaining a proper load sharing between the DG's, which can be achieved via droop-controlled techniques; the objective of the voltage secondary

control level is to regulate any deviations in voltage magnitude of each DG with minimum impact in the established power sharing property in the primary level; preferably, at minimum communication links to have more reliable, secure and efficient system, which still a challenging task to realize.

## **1.1 RESEARCH OBJECTIVES**

The key objective of this research is to design a distributed voltage secondary control for small/medium scale AC inverter-based droop-controlled microgrids that is able to successfully achieve the standard secondary control objectives, as defined in hierarchal control structure of microgrid [7]- [9], as listed below:

- Compensating for the deviation in voltage (magnitude) caused by the primary control level.
- Maintaining proper active power sharing as established by the primary controllers.
- Maintaining proper reactive power sharing as established by the primary controllers.
- Achieving the desired level of sparsity; preferably, using only unidirectional links.
- Fast response with stable operation.
- Robustness against generator disturbances.

## **1.2 PREVIOUS WORK**

Secondary control of electronically coupled DG's in Hierarchical Control of Droop-Controlled AC microgrids has been discussed broadly in the technical literature with different proposed

communication structures; namely, centralized methods where a centralized controller is used with a dense of communication links [4], [7], [9], [32]- [34], fully decentralized methods without any communications between the distributed generators [27], [44]- [46], and localized methods using local (i.e. neighboring) communication links only [36], [48]- [55]. Each of these structures has its drawbacks and limitations.

The centralized structure control has reliability concerns, as the system is costly and susceptible to single point of failure. Moreover, such dense bidirectional communication architecture is less secure, as it needs to send unencrypted data over large areas, and less robust against communication delays and failures [43], [91]. Likewise, the decentralized techniques have raised stability concerns and deteriorated power sharing property of the MG, due to lack of coordination between the DG's [32]. To overcome the drawbacks of the previous two methods a localized structure has been proposed in several papers [36], [48]- [55]; meaning each agent (DG) will exchange information with other agents (typically, local agents (DG's)) to have more coordinated actions; however, each method has its own weaknesses and limitations.

In Chapter 2, a detailed review is presented about previous works in solving the highlighted design problem of a secondary control system in AC microgrids, stressing the drawbacks and limitations of each method.

### **1.3 SUMMARY OF CONTRIBUTION**

The problem of designing a distributed secondary controller in microgrid system can be formulated as an optimal control problem that is driven by a stochastic exogenous disturbance, where an

additional term is added to the standard objective function ( $H_2$  norm of the closed-loop system) to include sparsity structure. The solution of this optimization problem is a candidate  $K$  (state-feedback matrix) for the state-feedback controller  $u=-Kx$  that minimizes the objective function, i.e. able to optimize performance (as a regulator), lower the control effort, and eliminate insignificant elements (in the structured controller) to achieve the desired level of sparsity, while maintaining closed-loop stability of the system.

Using the approach of Sparsity-Promoting proposed in [59], the above-mentioned optimization problem can be iteratively solved by gradually increasing the desired level of sparsity (with zero initial condition, i.e. centralized controller) and tracing the homotopic path from the known optimal centralized solution to the desired distributed architecture. Along the solution path, the previous feedback gain  $K$  is repeatedly taken as initial condition for the current iteration until the desired sparsity is achieved. In this framework, the optimization tool recommended for each iteration of solving the optimization problem is the alternating direction method of multipliers (ADMM). As a final step, the conventional structured design problem will be solved (polishing), but with stabilizing “near-optimal” initial conditions suggested by the ADMM solution. Polishing is well known in compressing sensing application, which usually resulted in a slight improvement to the final solution.

Chapter 3 reviews the adopted approach (Sparsity-Promoting) that is suggested for solving the secondary control design problem with an illustrated example that shows the effectiveness of the proposed design approach in similar framework. Finally, Chapter 4 presents a design guides to formulate and solve the secondary control design problem as introduced in Chapter 2, using a customized algorithm based on the adopted approach.

## 1.4 IMPACT

Using Sparsity-Promoting approach in designing distributed (structured) secondary voltage controller for droop-controlled (inverter-based) AC microgrid is a systematic flexible framework that's trying to reach a balance between performance (voltage regulation "Consensus" and active/reactive power sharing property), Cost (control effort needed and number of communication links), and sparsity (Communication links needed). Moreover, it can be used to identify the communication topology based on a prescribed level of performance (acceptable level of performance compared with a central controller case) and based on need-to-know or availability/accessibility (not based on predetermined topology or neighboring basis), and it's able to recognize critical links.

In comparison to the existing methods highlighted in Chapter 2, Sparsity-Promoting method would require much lower gain that is tunable based on the choice of the control weight matrix  $R$ . Furthermore, this proposed method is also considering power-sharing property not only the regulation problems as seen in [49]- [51]. Also, because the communication topology is extracted from the state-feedback matrix  $K$ , the communication links does not have to be a bidirectional type in all links; this would higher the system's reliability, as unidirectional communication links is less susceptible to failures and delays. Furthermore, the resulted distributed (structured) regulator can be used to further enhance system stability (stabilizer), as sensitivity analysis in [29] and [83] has identified the states related to the low frequency oscillatory modes that has lower damping ratios (Higher frequency oscillatory modes improved their damping with larger  $R_d$  [83]), so it can help to regulate these states within acceptable limits. Further, as this method seems to provide encouraging results in homogenous scenarios, it has been evaluated in

heterogeneous scenarios (of multiple DGs with very dissimilar lines impedances) with satisfactory results, which is a challenging operating condition for most existing techniques [52]- [55].

## 2.0 MICROGRID: STATE OF THE ART

Current power grid is facing a critical challenge of integrating various forms of resources, which are distributed by their nature, into the grid to answer the rapid growth on the electric demand and to increase the overall system efficiency and sustainability. Due to the adopted centralized architecture of power grid with long transmission links, the system has become extremely large and complex; and with the added heterogeneous distributed resources, such as wind, photovoltaic, micro-turbines, etc., the operation reliability and efficiency would be a difficult task to realize. Therefore, existing power grid is no longer the best solution for such integration and development. This urged the need for a different architecture that has the ability to prevent the existing grid from expanding while facilitating smooth integration of such mixed distributed generators in order to address environmental and economic concerns in a reliable and sustainable manner. Microgrid is proposed for this reason, and it would allow for efficient, flexible, and reliable utilization and integration of various distributed energy generators [1].

As defined by the US Department of Energy (DOE); similarly, in Electric Power Research Institute (EPRI) and the Institute of Electrical and Electronic Engineers (IEEE), “a microgrid is a group of interconnected loads and distributed energy resources within clearly defined electrical boundaries that acts as a single controllable entity with respect to the grid” [2]. The locality feature of this architecture has added other advantageous, such as reducing transmission loss and quick

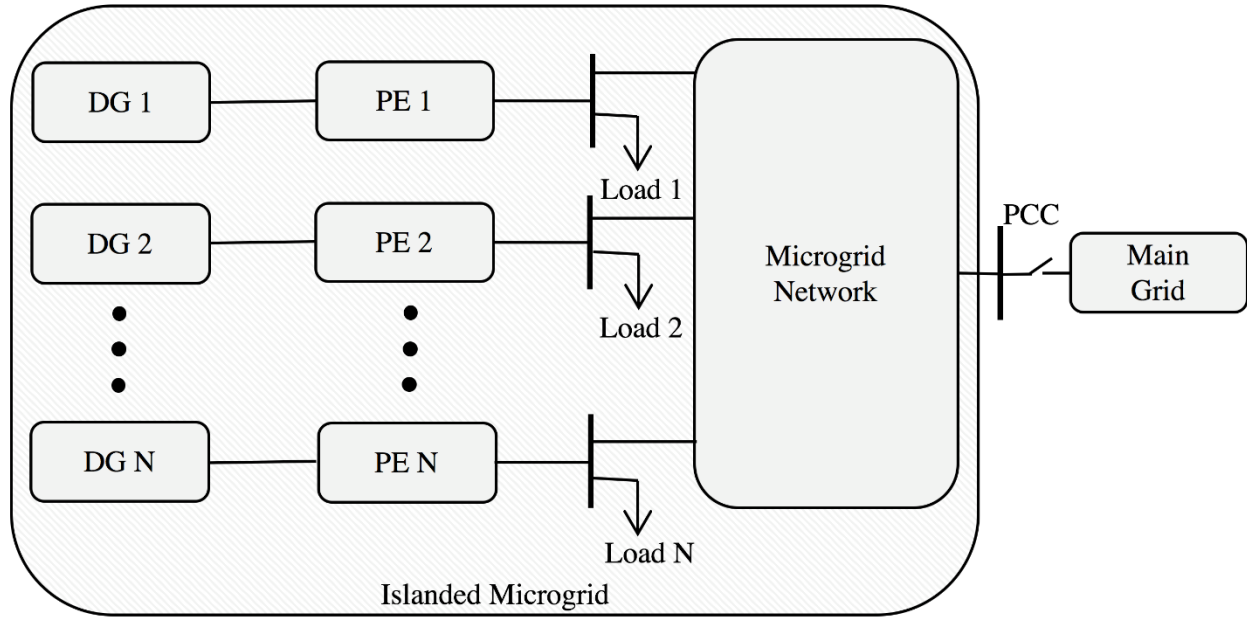


Figure 2-1. Schematic diagram of a typical islanded microgrid.

restoration in case of system blackouts [3]. Due to the heterogeneity among the system, power converters, such as VSI (voltage source inverter) or CSI (current source inverter), are necessary interfaces between distributed energy resources and the MG system, and control algorithms can be implemented through these converters. For flexibility, microgrid aimed to be able to work in two different operating modes depending on system's requirements: grid-connected mode, where it's connected to the grid at the point of common coupling (PCC), and islanded mode, which could be planned, or triggered by a fault in the main grid [2]- [5].

This new architecture has drawn lot of attention worldwide in the last 10 years, as more and more countries realized the necessity of integrating more renewable energy resources in their power grid, and various national polices are issued in order to encourage this movement to more renewable and sustainable resources. In US for instance, number of active current projects in microgrid has exceeded 200 projects; some of them are already in service [6], and this trend is expected to continue as many states plan to have more renewable share in the near future [11].

Same trend is observed in EU, D. E. Olivares et al. in their study about microgrid trends, they indicated that UK target is to have 15% of their produced energy to be from renewable sources by the end of 2016, and; on the other hand, Germany with more ambitious plan their targeted is to reach 50% of renewable sources by 2030 [11].

In the following sections/subsections a review for the hierarchical control structure in microgrids will be introduced with more focus on the secondary control level as the research problem. In Chapter 4, the overall system modeling with further details about the primary control will be presented.

## **2.1 HIERARCHICAL CONTROL OF DROOP-CONTROLLED AC MICROGRIDS**

In order to reach a reliable and efficient operation for the microgrid and being able to overcome several challenges such as; stability issues, lack of inertia, resistive nature of low voltage power-electronic based microgrids, uncertainty of produced energy and unbalanced conditions of system, having a successful control design is an essential requirement [11]. The overall control system of a microgrid is desired to achieve the following objectives [7] – [9]:

- Regulating output voltages or currents of all DG's to their reference values with appropriate damping to maintain system stability.
- Proper sharing of active/reactive power according to desired ratios, based on rated values of each DG in the microgrid, while keeping frequency and voltage agreement within acceptable limits.

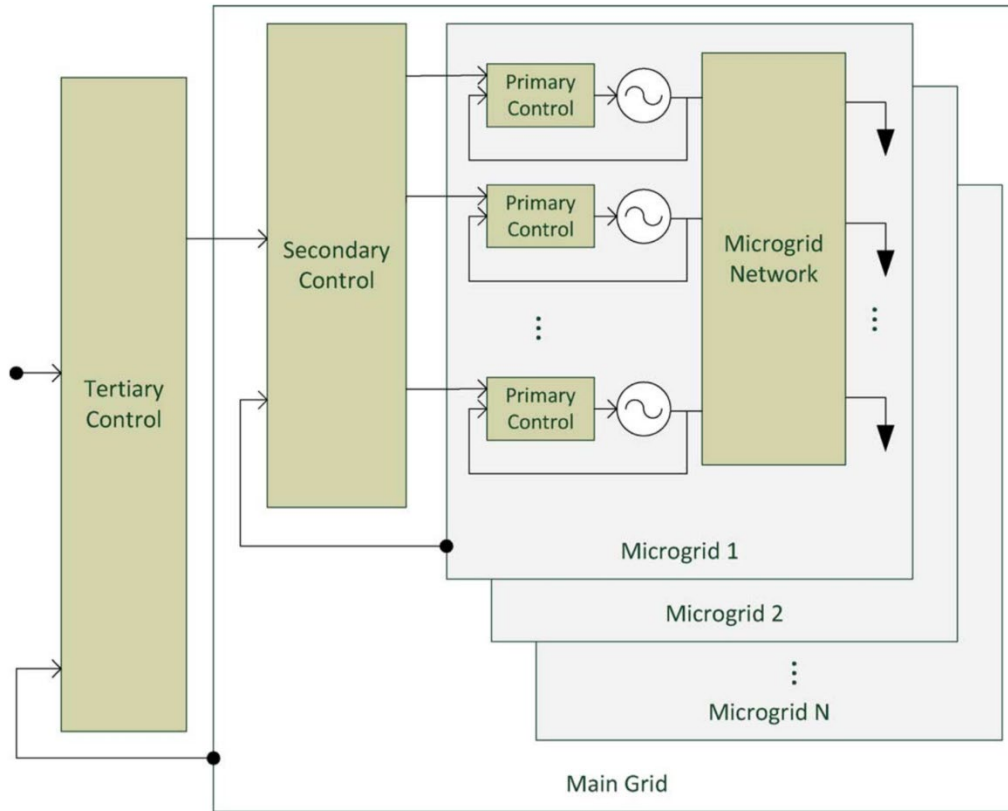


Figure 2-2. Hierarchical levels of controlling a microgrid [11].

- Flexible switching between the two modes of operation; namely grid-connected and stand-alone modes of operation, using a fast-response islanding detection procedure [10], [11].
- Optimizing the economical aspect of microgrid operating by having a proper power dispatching protocol.
- Plug and play feature when adding new distributed energy resources to the microgrid, without a continuous changing of controllers' settings when connecting a new DG.

Due to the difference in timescales between these objectives, the control problem can be decoupled in different control level, each level dealing with particular goals that are sharing the same timescale. Unlike other proposed methods of microgrid operation [12]- [16], the suggested

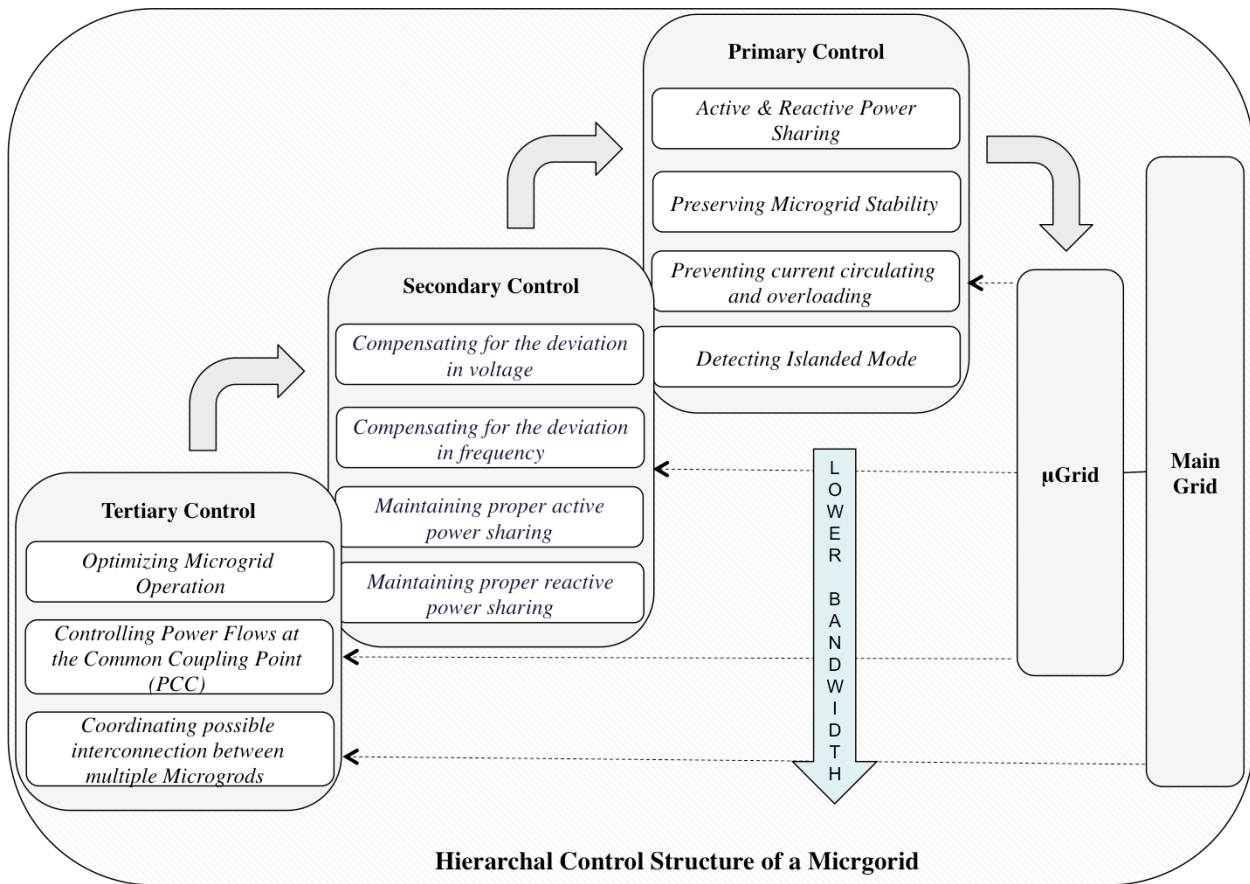


Figure 2-3. Objectives of each control’s level in the hierarchal control structure of a microgrid.

hierarchical control in [7] has considered the different control levels, and dealt with the controlling problem of microgrid as one problem with several layers. These control layers are: primary control, secondary control, and tertiary control. In the following sections, an overview and state of the art of each control level will be presented.

### 2.1.1 Primary Control

Primary control level has the fastest response and its main objectives are stabilizing the system by controlling the output voltage (amplitude and frequency) of each DG, and maintaining a proper load sharing between the DG’s. By achieving these goals, current circulating issue between the

DG's and overloaded conditions would be avoided in the microgrid operation. Moreover, in this primary layer, a suitable algorithm should be implemented to detect islanding mode to ensure faster reaction and smooth transition between different operating modes [17], [18], [19].

As explained earlier, microgrid consists of various form of distributed generator; thus, power converters, such as VSI (voltage source inverter) or CSI (current source inverter), are necessary interfaces. In VSI configuration there are two loops, known as inner loops; internal loop to control the current and outer loop to control the voltage. On the other hand, CSI has the same configuration but with outer loop that is a phase-locked (PLL) for grid synchronization [7]. In microgrid application, VSI is preferable inverter as it has the ability to stay synchronized without an external reference. Still, CSI inverters are required for energy resources that needs a maximum power point tracker; however, CSI can act as VSI when needed. Therefore, microgrid can be formed as several VSI's that are connected in parallel [7].

To realize the primary control level objectives, VSI inverter should have two phases of control: 1) one to regulate the output (output controller), and 2) another phase for power sharing control (power controller). While the inner loops of VSI considered as an output controllers that can regulate current and voltage, a power controller is added as an additional loop to feed reference voltage and current signals to the output controllers [[17], [18], [4], [20], [21], [22]- [26]]. The power controller in this configuration is implemented using active/reactive power and frequency/voltage droop controllers that imitate the droop characteristics of conventional synchronous generators where machine's inertia is used [27]. These droop controller methods are preferable since it depends only on local measurements without any communication links, unlike active power sharing methods that require dense communication links that is affecting the system

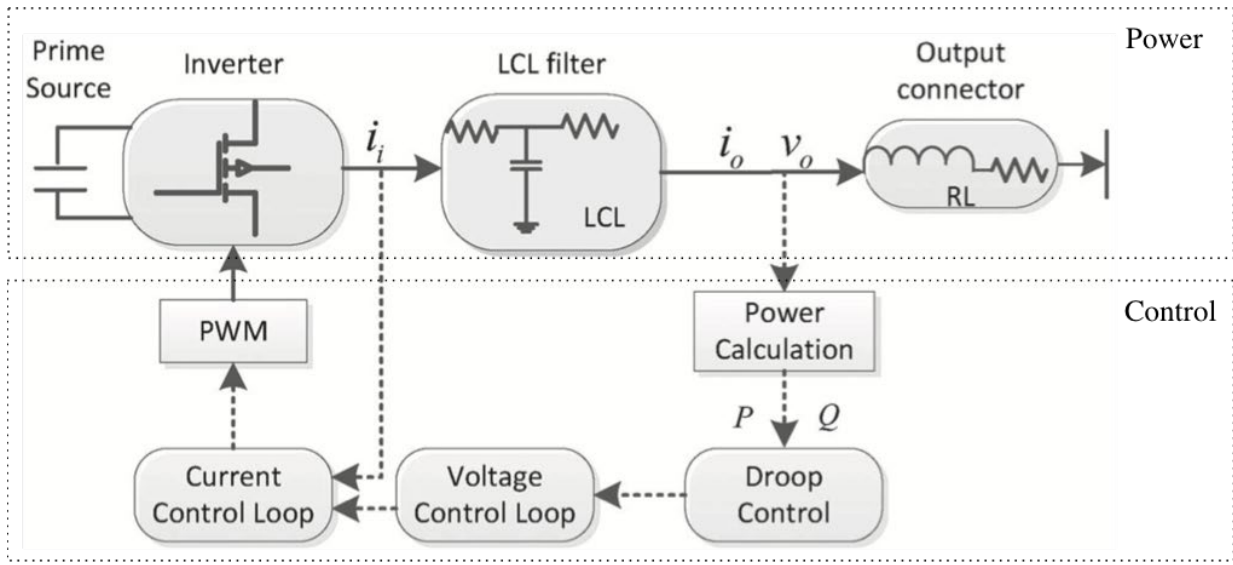


Figure 2-4. Droop-controlled based primary control of DG inverter [58].

reliability [29, 30, 4, 28, 31]. Further discussion and details is presented in Section 4.1 covering the small-signal modeling of “droop-controlled” inverter-based microgrids.

### 2.1.2 Secondary Control

Secondary control level has a slower response than primary level which facilitating separable design [8]. As added advantages, this decoupling will also decrease the required communication bandwidth, as only sampled measurements of system’s parameters are acquired, and will offer a sufficient time for computations [11]. The key objective of this level of control is to mitigate and regulate any deviations in voltage magnitude or frequency. These deviations are resulted from the primary controller responses on load disturbances that requiring adjustments in active/reactive power. This level of control, for electronically coupled DG’s in Hierarchical Control of Droop-Controlled AC microgrids, has been discussed broadly in the technical literature with different

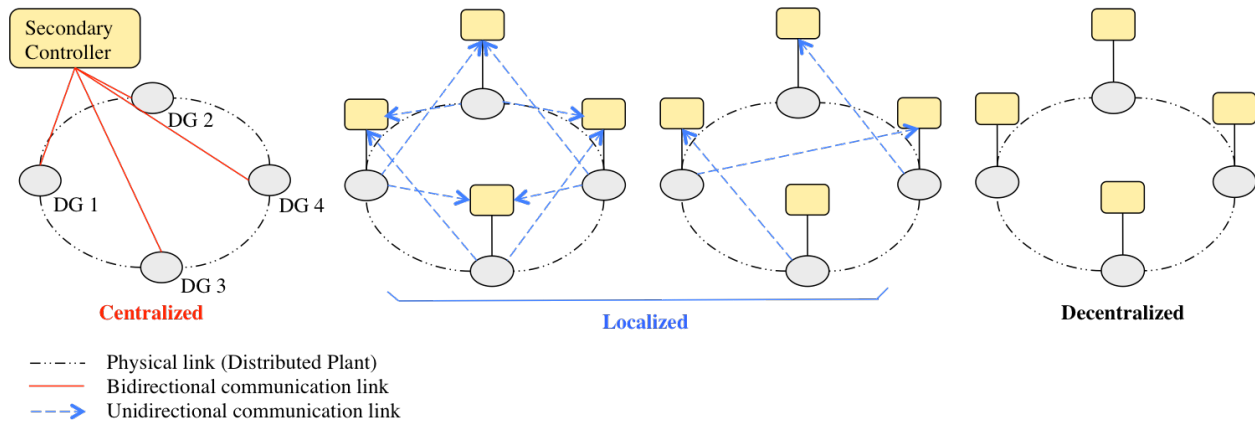


Figure 2-5. Communication structures in secondary control of a microgrid.

proposed structures; namely, centralized methods [4], [7], [9], [32]-[34], where a centralized controller is used with a dens of communication links, fully decentralized methods [27], [44]-[46], without any communications between the distributed generates, and localized methods [36], [48]-[55], using local (i.e. neighboring) communication links only.

**2.1.2.1 Centralized methods** Centralized secondary control has been applied widely in large interconnected power systems with acceptable results [35]. The idea has been extended to microgrids secondary control as well. However, in microgrid, secondary control is used not only for voltage and frequency levels regulations, but also for other objectives such as: maintaining adequate sharing of reactive power since it is an expected issue in small/medium scale microgrid due to the low  $r/x$  ratio [36], satisfying power quality requirements, such as voltage balancing for critical loads; and decreasing harmonic level in the microgrid.

In the centralized structure, all distributed generators are connected to a central processor (Microgrid Central Controller “MGCC”) through bidirectional (from the remote sensory to MGCC, then from MGCC to all distributed generators and vice versa) low bandwidth (slower time scale) communication links to acquire sample measurements of systems’ variables periodically.

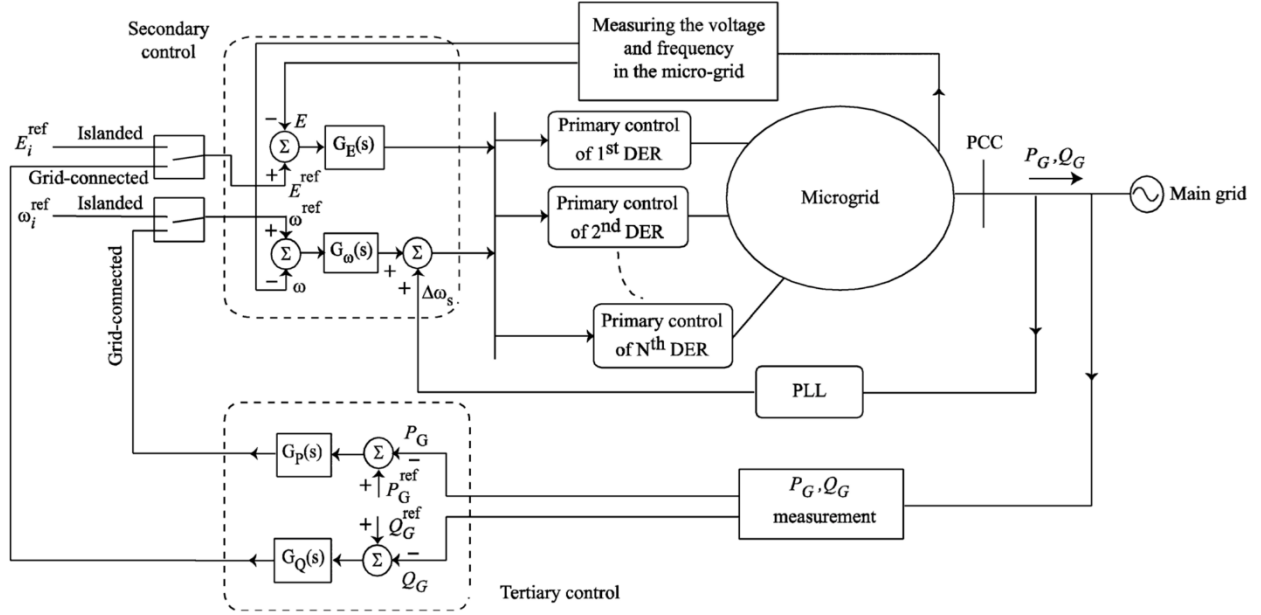


Figure 2-6. Centralized structure of secondary and tertiary controls in a microgrid [7].

At the central controller (MGCC), the measured frequency and terminal voltage, at a given bus or DG, of the microgrid,  $w_{MG}$ ,  $E_{MG}$ , are compared with reference values,  $w_{ref}$ ,  $E_{ref}$ . The resulting error is processed by the MGCC then correction signals,  $\delta\omega$  and  $\delta E$ , are send back to the distributed generators so the microgrid will be restored to its reference level. Theses references levels  $w_{ref}$ ,  $E_{ref}$  can be chosen differently based on the operating mode. In grid-connected mode, references are selected by the tertiary control according to the economic aspects of the hosting grid, while in the islanded mode; the secondary control becomes the highest level of hierarchal control with references set to nominal values 50/60 Hz,  $E_{nominal}$ , or it can be chosen to maintain a critical bus voltage at its nominal value [37].

As implemented in [7], frequency regulator at MGCC can be obtained as follows:

$$\delta\omega = k_{p\omega}(\omega_{ref} - \omega_{MG}) + k_{i\omega} \int (\omega_{ref} - \omega_{MG}) dt + \Delta\omega_s \quad (2.1)$$

where  $k_{p\omega}$  &  $k_{i\omega}$  are the PI controller parameters,  $\Delta\omega_s$  is the PLL (phase-locked loop) output signal to facilitate synchronization with the main grid in grid-connected mode, and it is set to zero during islanded mode [38]- [42]. Same procedure is used to derive the MGCC voltage regulator as below:

$$\delta E = k_{pE}(E_{ref} - E_{MG}) + k_{iE} \int (E_{ref} - E_{MG}) dt \quad (2.2)$$

The control protocols mentioned above for secondary centralized controller can be furthered enhanced to encounter for other power quality concerns such as voltage balancing for critical loads [37], decreasing harmonic level in the microgrid [33], and maintaining adequate power sharing [32].

In [37], the voltage unbalance factor VUF, at a given bus in the microgrid, is computed (in the dq reference frame) in order to compare it with the reference  $VUF_{ref}$ . The resulted error signal is fed to a PI-compensator to generate a correction signal that multiplied by the negative sequences before it sent back to the local (primary) controllers of the DG's as a correction values to the reference value  $E_{ref}$ , as illustrated in Figure 2-7. The calculation of VUB is according to the following equation:

$$VUF = 100 \frac{\sqrt{(E_d^-)^2 + (E_q^-)^2}}{\sqrt{(E_d^+)^2 + (E_q^+)^2}} \quad (2.3)$$

where  $E_d^-$ ,  $E_q^-$ ,  $E_d^+$  and  $E_q^+$  are the negative and positive sequence voltages of a give bus in dq reference frame. Similar procedure can be implemented to compensate for the unbalanced harmonic distortion of nonlinear unbalanced loads [33]. The proposed method has the ability to

share the compensation effort between heterogeneous generators through some modification at primary control level.

To improve reactive power sharing in centralized secondary control, recently the authors in [32] has proposed a modified algorithm implemented at MGCC to enhance reactive power sharing through the distributed generators. The algorithm is based on reassigning reactive power demand of each DG based on the total demand and the DG's Q-E droop gain as follows:

$$Q_x^* = \frac{Q_{total}}{n_x \sum_{i=1}^k \frac{1}{n_i}} \quad (2.4)$$

where  $Q_{total}$  is the total reactive power demand of the microgrid,  $Q_x^*$  is the calculated reactive power share of the  $x^{\text{th}}$  DG, and  $n$  is Q-E droop gain of each generator. The resulted  $Q_x^*$  is, then, passed through a PI-controller to compute the change of voltage ( $\Delta E_x$ ) needed at each generator to generate the assigned reactive power as below:

$$\Delta E_x = k_{pQ}(Q_x^* - Q_x) + k_{iQ} \int (Q_x^* - Q_x) dt \quad (2.5)$$

where  $k_{pQ}$  &  $k_{iQ}$  are the PI regulator parameters,  $Q_x^*$  &  $Q_x$  are assigned reactive power (as calculated in (4)) and current reactive power of the  $x^{\text{th}}$  generator, respectively.

For frequency regulation, the same regulator as implemented in (2.1) is used here. However, voltage regulation task has been incorporated in slightly different way than the conventional regulator in (2.2). In this method, because of the strong coupling between voltage and reactive power, voltage deviation in the microgrid is interpreted as additional reactive power

demand  $\Delta Q_{rest}$  added to the total reactive power  $Q_{total}$ . Thus, the resulted  $\Delta E_x$  is not only controlling reactive power sharing, but also regulating the deviations as well. The  $\Delta Q_{rest}$  is obtained as follows:

$$\Delta Q_{rest} = k_{pE}(E_{ref} - E_{MG}) + k_{iE} \int (E_{ref} - E_{MG}) dt \quad (2.6)$$

where  $k_{pE}$  &  $k_{iE}$  are the PI controller parameters,  $E_{ref}$  &  $E_{MG}$  are reference and current (measured) voltage level of microgrid, respectively.

As an alternative approach to the mentioned methods above, the MGCC algorithm can also be implemented based on minimizing potential functions that assigned for each controller, using gradient decent method, to achieve secondary controller objectives [34]. However, the method is requiring bidirectional communication links between the MGCC and the distributed units, which is limiting its practicality/reliability in higher scale of microgrid.

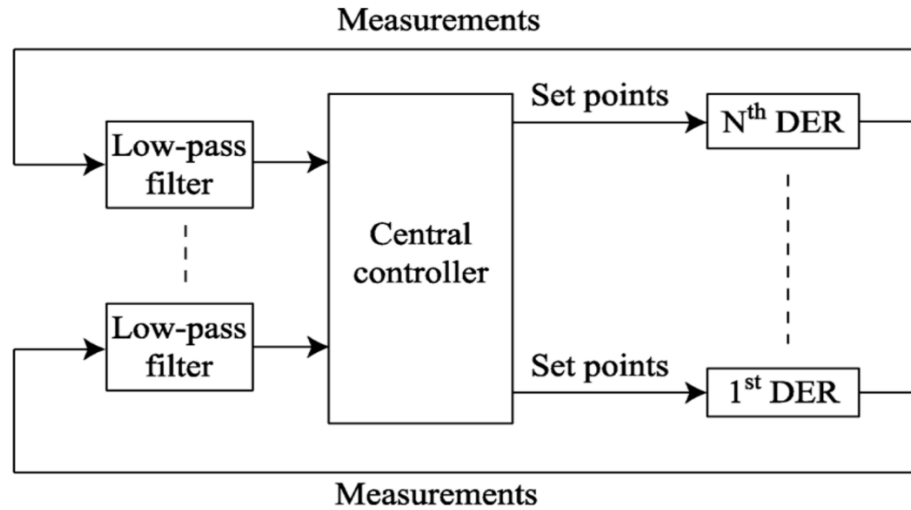


Figure 2-7. Potential Function Method (PFM) based secondary control of a microgrid [34].

In general, centralized structure control methods are costly and have lower reliability, as the system is susceptible to single point of failure. Moreover, such dense bidirectional communication links are insecure, as it needs to send unencrypted data over large areas. Also, centralized control methods are less robust against communication delays and failures [43], [36].

**2.1.2.2 Decentralized methods** Due to the disadvantages of the centralized structure, several decentralized methods were proposed to overcome the concerns and limitations of centralized techniques. In general, there are two ways of implementing such a decentralized structure: 1) using local measurements with no coordination with other DGs, 2) using estimation techniques to acquire global variables to react in a more coordinated way.

The first technique, to design a fully decentralized controller, is by locally implementing similar regulators to the centralized case, as obtained in (1) and (2), at each generator to maintain DG's reference levels. However, no communication links are needed [27]. In fact, this attempt will cause, in most cases, stability problems since there is no coordination and agreement with other DGs in the microgrid while sharing the same demand; and it will sacrifice power sharing causing the whole system to be susceptible to stability collapse [32]. Moreover, even though the decentralized seems to be having a fast response and very competitive performance with centralized one in a local perspective, it would be much slower in global sense (i.e. restoring MG, as a system, to its reference values/levels, if possible, would require longer time).

Another way of designing secondary control, in decentralized structure, is by using estimation techniques of system's variables [44]- [46]. Hence, each DG is locally estimating the necessary system's measurements for local computation, instead of acquiring them directly through communication links. As presented in [44], a voltage-predictive control based on system's variables estimation (MG's voltages level) is proposed. As illustrated in Figure 2-8, a local

estimator is used at each DG to obtain the global voltage levels of the MG. Then, to accomplish voltage regulation at each DG, a voltage-predictive regulator is used locally to produce a corrective action to the DG's voltage value, by minimizing the following cost function:

$$\begin{aligned}
& \min_{\Delta u(k|k), \dots, \Delta u(m-1+k|k)} J \\
& = \left\{ \sum_{i=1}^{p-1} \left( \sum_{j=1}^{n_b} (w_{bj} (V_{busj}(k+i+1|k) - V_{refj}))^2 \right. \right. \\
& \quad \left. \left. + \sum_{j=1}^{n_c} (w_{cj} \Delta u_{cj}(k+i|k))^2 \right) \right\} \tag{2.7}
\end{aligned}$$

where  $w_{bj}$ ,  $w_{cj}$  are weights of buses and control increments network voltages, respectively;  $p$  is prediction limit;  $n_b$  is number of buses;  $n_c$  is number of voltage control inputs;  $(k+i+1|k)$  represents information predicted at time  $k$  for time  $k+i+1$ .  $V_{refj}$  is set to zero initially.

The abovementioned proposed method is tested under uncertainties of system's parameters and shows the ability to overcome such robustness concerns [44]. However, still stability analysis needs to be further investigated, as such decentralized estimation-based techniques tend to be rather complicated and sensitive [47]. Moreover, the proposed control design does not consider reactive power-sharing problem that may cause one or more DGs to be overloaded.

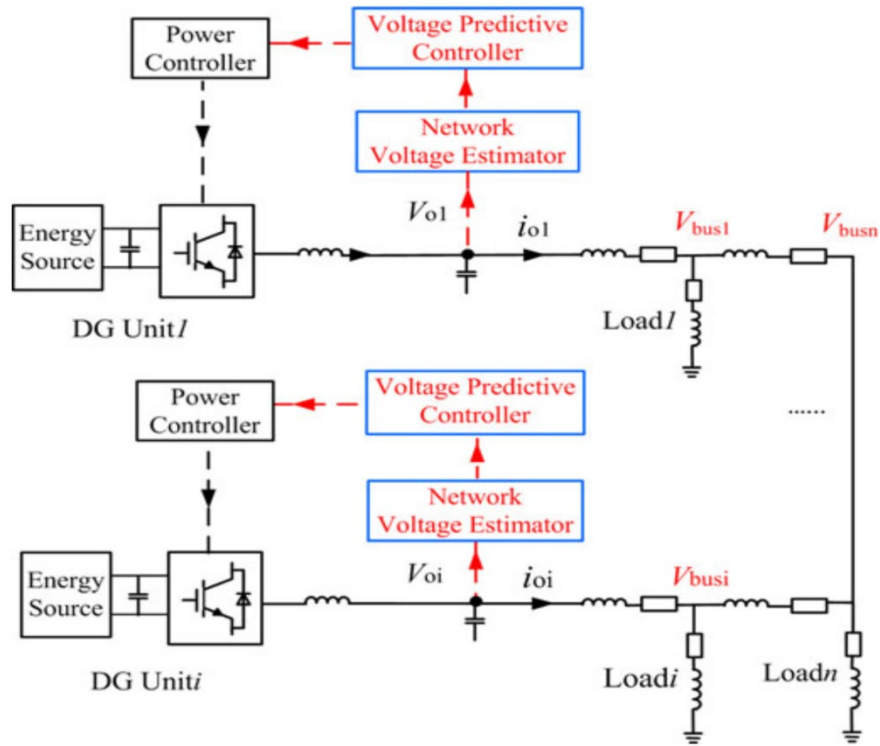


Figure 2-8. Decentralized structure of Estimator-based secondary control of a microgrid [44].

**2.1.2.3 Localized methods** As discussed in the previous subsection, the main motivation of the decentralized design was to avoid the central computation node (MGCC), that requires dense communication links between agents (distributed generators) to have more reliable, flexible and secure system [43]. However, decentralized techniques have raised stability concerns and deteriorated power-sharing property of the MG, due to the lack of coordination between the DG's [32]. Therefore, an alternative structure of implementing the secondary control, for droop controlled AC MG, is needed.

Various methods have been proposed in the technical literature to provide a reliable secondary control design that can overcome the drawbacks of the previous two methods [36], [48]-[55]. All of these alternative methods are implemented in a localized structure; meaning each

agent (DG) will exchange information with other agents (typically, local agents (DG's)) to have more coordinated actions, unlike the decentralized way; and no centralized control unit is needed, as each agent will act based on local controller (with help of the collected measurements).

In [36] and [48], a strongly connected communication topology is proposed in order to regulate the voltage and frequency and maintain power-sharing property based on averaging approach within the maximum limit of each DG. For frequency regulation, each DG will communicate its frequency measurement to all other DGs in the MG system, then a local controller will regulate the deviation of the average value from the reference value as follows:

$$\delta\omega = k_{p\omega}(\omega_{ref} - \bar{\omega}_{MG}) + k_{i\omega} \int (\omega_{ref} - \bar{\omega}_{MG}) dt \quad (2.8)$$

$$\bar{\omega}_{MG} = \frac{\sum_{i=1}^N \omega_{MGi}}{N} \quad (2.9)$$

where  $k_{p\omega}$  &  $k_{i\omega}$  are the PI controller parameters,  $N$  is number of connected DGs in the system,  $\bar{\omega}_{MG}$  is the average frequency value. A small signal model has been developed in to tune PI controller parameters.

To maintain the nominal voltage across all distributed generators (DGs), same procedure is used to derive a local voltage regulator as below:

$$\delta E = k_{pE}(E_{ref} - \bar{E}_{MG}) + k_{iE} \int (E_{ref} - \bar{E}_{MG}) dt \quad (2.10)$$

$$\bar{E}_{MG} = \frac{\sum_{i=1}^N E_{MGi}}{N} \quad (2.11)$$

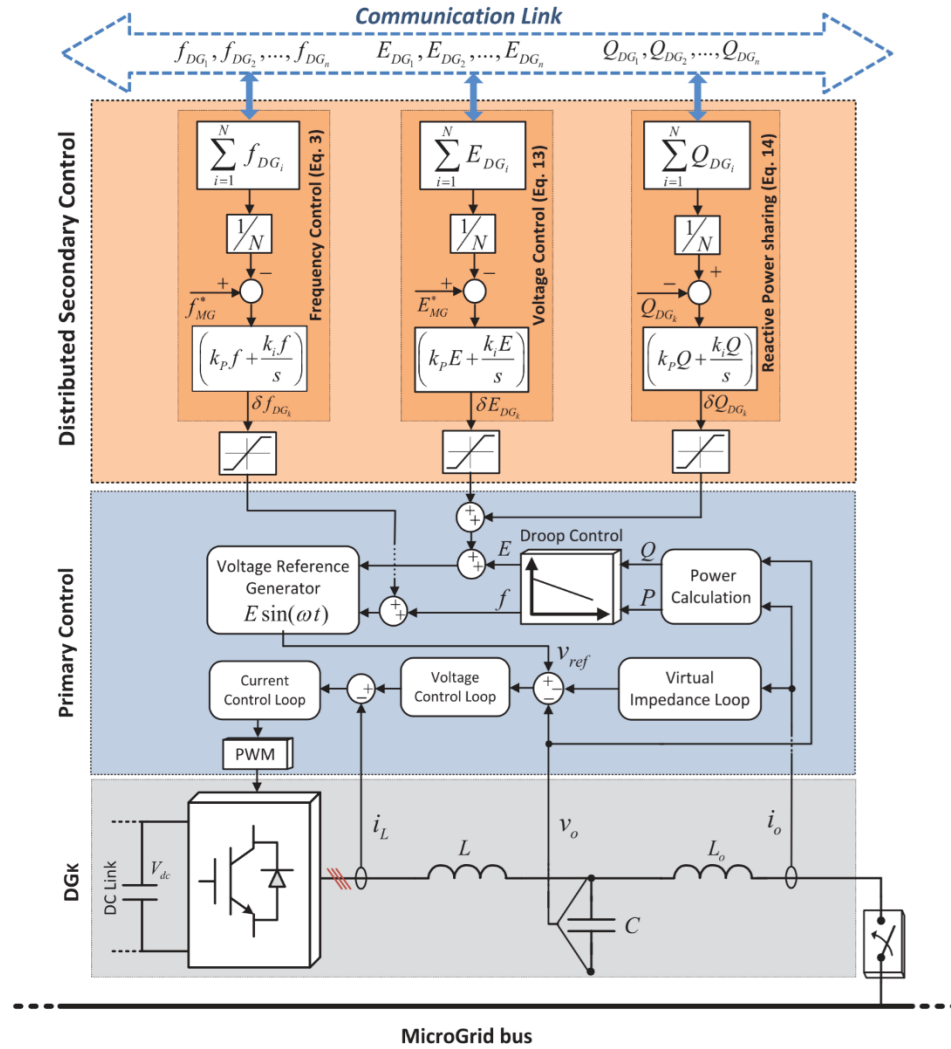


Figure 2-9. Distributed secondary control of a microgrid: strongly connected communication topology [36].

where  $k_{pE}$  &  $k_{iE}$  are the PI controller parameters,  $N$  is number of connected DGs in the system,  $\bar{E}_{MG}$  is the average voltage value.

Furthermore, to maintain a proper reactive power sharing, through communicating reactive power measurements between the DGs, similar averaging approach is used to keep  $Q$  of each DG at average value as shown below:

$$\delta Q = k_{pQ}(\bar{Q}_{MG} - Q) + k_{iQ} \int (\bar{Q}_{MG} - Q) dt \quad (2.12)$$

$$\bar{Q}_{MG} = \frac{\sum_{i=1}^N Q_{MGi}}{N} \quad (2.13)$$

where  $k_{pQ}$  &  $k_{iQ}$  are the PI controller parameters,  $N$  is number of connected DGs in the system,  $\bar{Q}_{MG}$  is the average reactive power value.

Despite that this method was able to remove the risk of having a central processing unit that is vulnerable to single-point failures, it requires high communication links and reactive power sharing is only possible with a very careful tuning of the controller parameters with identical DGs [52], [55].

In [49]- [51], a cooperative secondary control of AC microgrid is proposed by applying optimal design approach of multi-agent system [56]. The secondary control objectives, namely, regulating frequency/ voltage values of the microgrid to their reference levels, are achieved by employing input-output feedback linearization that transformed the nonlinear microgrid model of dissimilar DGs into a homogenous and linear model. This transformation has enabled the Riccati design of local cooperative tracker, as presented in [56], to be applied using one node (an agent “DG”) as a leader with either fixed reference value or varying reference value according to voltage’s variation of a critical bus. The linearized model of each agent ( $DG_i$ ) has yield to a double integrator model, as follows:

$$\dot{y}_i = Ay_i + Bv_i \quad (2.14)$$

$$\text{where, } y_i = [y_i \dot{y}_i]^T, A = \begin{bmatrix} 0 & 1 \\ 0 & 0 \end{bmatrix}, v_i = \ddot{y}_i, \text{ and } B = \begin{bmatrix} 0 \\ 1 \end{bmatrix}$$

And the linearized model of the leader ( $DG_o$ ) is defined as bellow:

$$\dot{y}_o = Ay_o \quad (2.15)$$

where  $y_o = [y_{ref} \ 0]^T$ . For voltage regulation problem, the auxiliary control  $v_i$  is implemented as below:

$$v_i = -cke_i \quad (2.16)$$

where  $c$  is the coupling gain,  $k$  is local feedback gain, and  $e_i$  (tracking error) is expressed as:

$$e_i = \sum_{j=1}^N a_{ij}(y_i - y_j) + b_i(y_i - y_o) \quad (2.17)$$

where  $a_{ij}$  is the corresponding value in A matrix (adjacency matrix) that capturing the communication topology, and  $b_i$  is a nonzero value for only one node (DG).

According to Riccati design of local cooperative tracker in [56], the diagraph should have a spanning tree,  $k$  is designed as standard feedback gain of local LQR, and coupling gain ( $c$ ) should be chosen as:

$$c \geq \frac{1}{2\lambda_{min}} \quad (2.18)$$

where  $\lambda_{min}$  is min eigenvalue of the matrix  $(L + B)$ ,  $L$  is Lablacian matrix of the communication graph. Finally, the control signal  $u_i$  ( $= E_i^*$  "primary control reference in droop control equation") is realized in term of  $v_i$  as shown in Figure 2.10 [51].

A similar formula is used for frequency regulation and the control signal  $u_{fi}$  is proposed as bellow:

$$u_{fi} = -c_f \left( \sum_{j=1}^N a_{ij}(\omega_i - \omega_j) + b_i(\omega_i - \omega_{ref}) + \sum_{j=1}^N a_{ij}(m_i P_i - m_j P_j) \right) \quad (2.19)$$

where  $m$  is the active power droop coefficient of each DG. If the digraph is having a spanning tree and  $b$  is nonzero for only one DG (with relatively high gain  $c_f$ ); then, a frequency consensus to  $\omega_{ref}$  will be achieved while maintaining accurate active power sharing.

The above-proposed method was able to accurately regulate the voltage and frequency quickly and with very low communication links (only limited to spanning tree formation), and it would also facilitate plug-and-play operating of the microgrid [51]. However, the authors have assumed the stability of the internal dynamics of each DG and the system is worked in a lossless transmission network, and consequently, did not account for reactive power sharing problem, which could cause one or more DGs to be overloaded. Moreover, such a model-based approach that relying in classical input-output feedback linearization is highly susceptible to uncertainties since the resulted dynamics is very different from the original one [57], resulted in such a high gain controllers [55]. Also, it did not consider the inherent coupling between the frequency and the voltage in such application [58].

Alternatively, as proposed in [52]- [55], a Distributed Averaging Proportional Integral(DAPI) is adopted for implementing the secondary control, aimed at accurate frequency regulation & active power sharing, while trying to achieve the best trade-off between two conflicting objectives: voltage regulation & reactive power sharing [55]. The method has integrated the droop and integral control with consensus algorithms of multi agent system. So, this proposed method is considering the secondary controller design problem as a consensus problem, as seen in the previous method [51], but it takes into account the resistive nature of the network and trying to simultaneously solve reactive power sharing challenge.

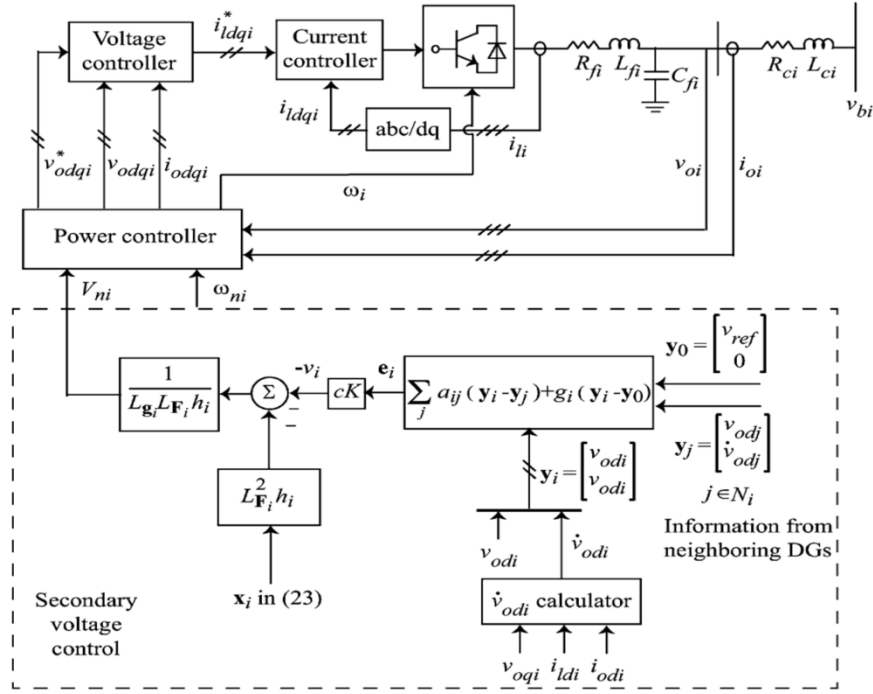


Figure 2-10. Distributed cooperative secondary control of a microgrid: pre-specified topology with a spanning tree [51].

For frequency regulation, the following controller is applied:

$$\omega_i = \omega^* - m_i P_i + \Omega_i \quad (2.20)$$

$$k_{i\omega} \frac{d\Omega_i}{dt} = -(\omega_i - \omega^*) - \sum_{j=1}^n a_{ij} (\Omega_i - \Omega_j) \quad (2.21)$$

where  $\Omega_i$  is the additional adjustment to the frequency (frequency control input),  $k_{i\omega}$  is integral variable, and  $a_{ij}$  is the corresponding value in A matrix (adjacency matrix) that capturing the communication topology. To achieve accurate power sharing and frequency regulation, communication topology must be connected [55].

For voltage regulation & reactive power sharing, as mentioned earlier these two objectives are conflicting for droop controlled AC microgrid, with low r/x ratio, and no precise solution can be achieved. Therefore, the following tunable controller is proposed to set best compromise between voltage regulation/ reactive power sharing, per designer's priorities:

$$E_i = E^* - n_i Q_i + e_i \quad (2.22)$$

$$k_{iE} \frac{de_i}{dt} = -\beta_i (E_i - E^*) - \sum_{j=1}^n b_{ij} \left( \frac{Q_i}{Q_i^*} - \frac{Q_j}{Q_j^*} \right) \quad (2.23)$$

where  $e_i$  is the additional adjustment to the voltage (voltage control input),  $k_{iE}$  and  $\beta_i$  are integral and weighting variables; respectively,  $b_{ij}$  is the corresponding value in B matrix (adjacency matrix) that capturing the communication topology, and  $Q_i^*$  is the reactive power rating. Different settings of  $b_{ij}$  &  $\beta_i$  are used to illustrate different compromises; suggesting that voltage tracking of a selected leader agent would yield to the best trade-off.

This “model-free” method has a lower controller gains in comparison with [51], and lower communication links compared to [36], and it's using communication arrangements as one of the design variables. Moreover, it has taken into consideration reactive power sharing property and facilitate plug-and-play feature. Though, the method has assumed homogeneity of the microgrid, that network impedances and connected DGs are having relatively comparable values. Also, the method needs a systematic procedure for tuning design variables in more practical/ complicated scenarios, as leader-follower setting would raise again the single-point failure problem in centralized architecture.

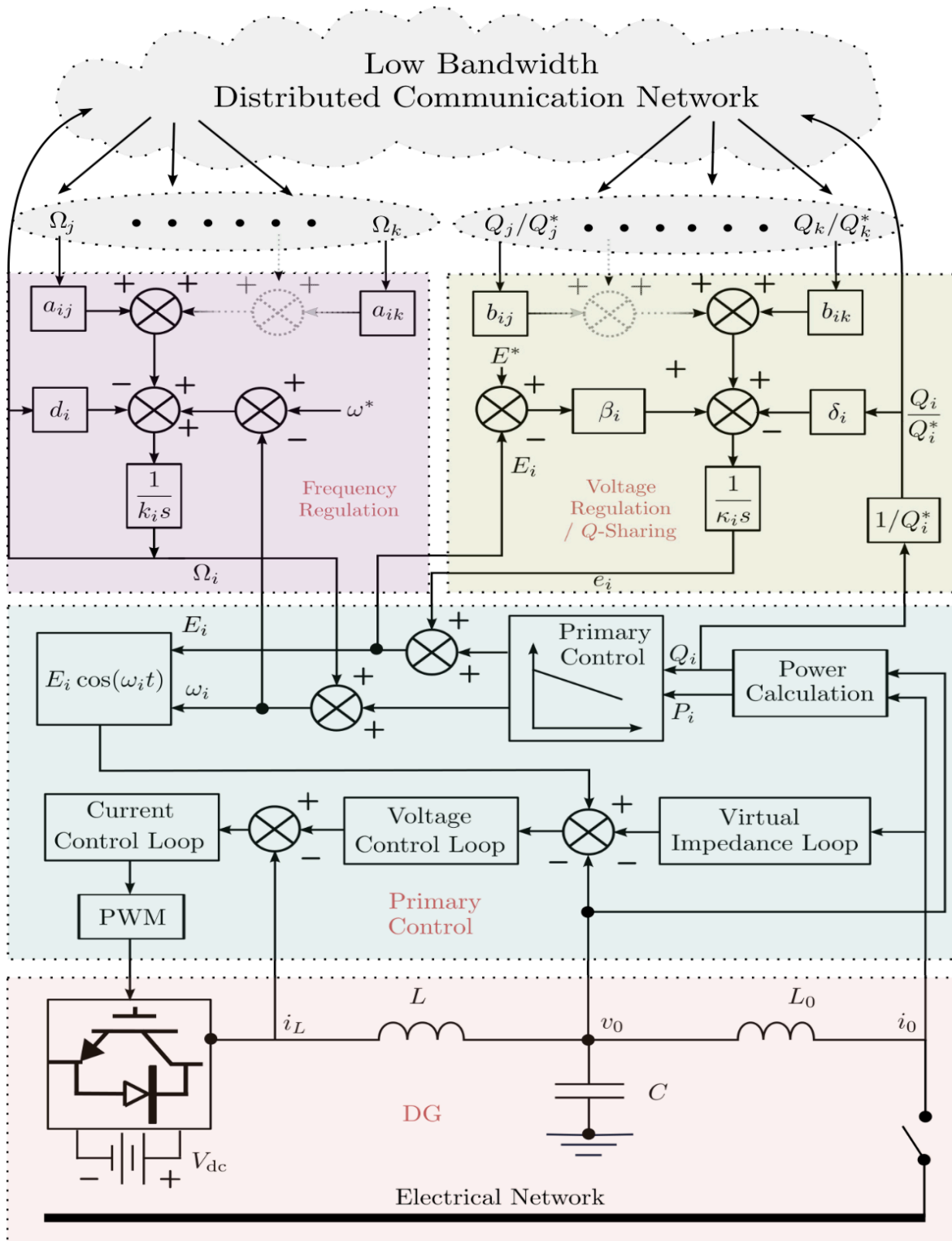


Figure 2-11. Distributed secondary control of a microgrid via distributed averaging: neighboring-basis communication topology [55].

### 2.1.3 Tertiary Control

The tertiary control is the higher and slowest control level in the hierarchal control structure of the microgrid, and its main objective is to set voltage amplitude and frequency references to the microgrid based on power requirements of the hosting grid [7], based on the following equations:

$$\omega_{MG}^* = k_{pP}(P_G^* - P_G) + k_{iP} \int (P_G^* - P_G) dt \quad (2.24)$$

$$E_{MG}^* = k_{pQ}(Q_G^* - Q_G) + k_{iQ} \int (Q_G^* - Q_G) dt \quad (2.25)$$

where,  $k_{iQ}, k_{iP}, k_{pQ}, k_{pP}$  are the controller parameters and  $P_G^*, Q_G^*$  are the desired active and reactive power that are compared with the measured powers  $P_G, Q_G$ .

Additionally, the tertiary control can be used also for coordinating possible interconnection between multiple microgrids, and in this case, this level of control will work as a primary control that is coordinating multiple microgrids, just as multiple DGs in a single microgrid, by eliminating the integral control part from the above equations [11]. The settings of this tertiary control is designed based on economic optimization of the hosting grid and it's not part of the microgrid, and won't be discussed further in this study.

### **3.0 SPARSITY-PROMOTING OPTIMAL CONTROL VIA ALTERNATING DIRECTION METHOD OF MULTIPLIERS**

In this chapter, the designing approach of a sparse feedback control system using alternating direction method of multipliers, [59], is presented, which will be extended in the next chapter as a solution for distributed secondary voltage control design in microgrids.

In the past few decades, more attention has been drawn to the problem of controlling a distributed plant, where the entities of the plant are dynamically coupled, using a distributed control system, instead of the conventional centralized approach. This distributed control architecture is more efficient, reliable, and flexible; and it has its application not only in engineering context, such as electric power system, and computer science, but also in many other fields, including economics, biology, and social studies. As highlighted in [60], the problem of designing a distributed control system can be categorized based on the overall purpose of the control system. The targeted goals of such distributed controlled/coordinated system can be generally classified as: consensus, formation, optimization, task assignment, distributed estimation and control, and intelligent coordination.

Optimization problems in distributed control system, as one of the above-mentioned categories, can be formulated to achieve various goals in optimal manner such as consensus, coordination, and designing a structured controller [60]. Recently, the consensus problem of a homogenous system (i.e. identical agents) has been investigated as optimization problem based on

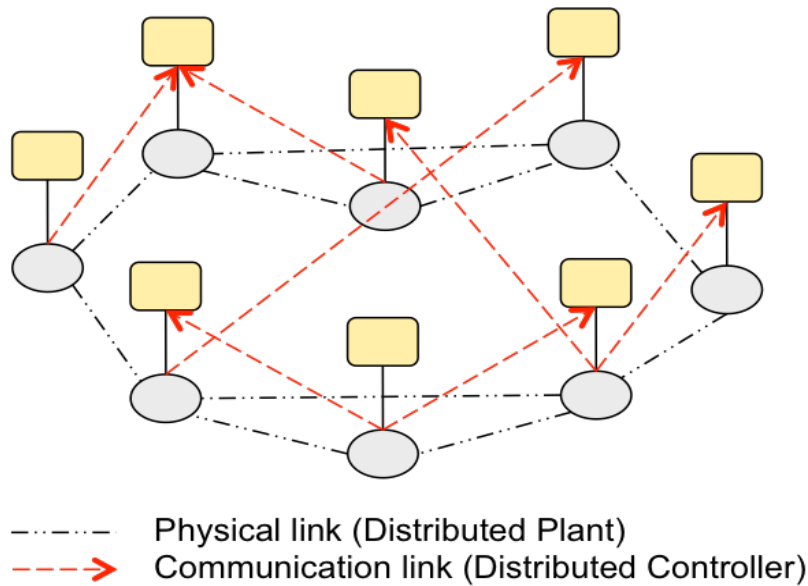


Figure 3-1. A generic distributed plant controlled by a distributed controller with sparse communication structure.

local [56] and global objectives [56], [61]. While local optimal design in [56] is based on the well-defined optimal solution of standard LQR design for local agents in order to reach consensus (synchronization/tracking) task in a stable manner, the resulted control protocols is by no means optimal in term of standard LQR objective function. Furthermore, for global optimality in the same framework, the local objective function was modified to form a global one, taking into account the communication topology as a global quantity, to achieve faster consensus, but optimization measure is still nonstandard, and it's primarily focusing on convergence speed. This will result in high gain controllers as the proposed coupling gain, in the distributed control protocol, is destroying the accomplished minimized control effort gains suggested by local or global LQR solutions.

Moreover, designing a structured optimal controller using usual performance measures (closed-loop norm of a feedback system, such as  $H_2$ ,  $H_\infty$ , LQR) is another problem that can be formulated as optimization problem, which is recognized as a hard problem [62], [63]. Note that,

even though this problem is considered as a structured optimal controller design problem, it can be used as well to design a consensus network as suggested in [64]. Earlier research efforts in solving this problem were aiming at finding special classes of structured control problems, with certain communication structure, that are tractable by convex optimization tools [65]- [68]. However; these methods have imposed prior restrictions in the communication topology.

Recently, as proposed in latest publications [59], [69]- [74]; the focus in solving the design problem of a structured optimal controller has shifted from identifying classes, which are optimally solvable, towards finding computationally efficient algorithms that is able to provide a non-exact, yet satisfactory, solutions with no prior restrictions in the communication topology. As proposed in [73], an algorithm is developed using weighted  $l_1$  norm as a relaxation of the sparsity optimization cost function to design a sparse “distributed” control system that guarantee a certain level of  $H_\infty$  measure. Further improvement is suggested to this method in [74], by modifying the performance constraint to maintain  $H_\infty$  level of the resulted distributed control system to be within a prescribed margin from the optimal centralized controller, which verifies applicability of the algorithm. Alternatively, the authors in [59] applied the alternating direction method of multipliers (ADMM) algorithm, along with other structured/ unstructured  $H_2$  optimization algorithms, to directly solve the distributed nonconvex optimization problem. Thus, the proposed method allows for simultaneously identifying the communication topology, according to desired level of sparsity, and optimizing the  $H_2$  performance of the resulted sparse controller. This chapter is meant to summarize this approach and to present its recent applications as published in technical literatures.

This chapter is organized as follows. Firstly, in Section 3.1, the formulation of the sparsity-promoting optimal control design problem is presented, where the objective function is including

two separated terms: performance cost (closed loop  $H_2$ ) and sparsity cost. Then, in Section 3.2, the alternating direction method of multipliers (ADMM) optimization tool is used to solve the optimization problem employing the separability of the penalty functions, and provide analytical solutions to the sub-problems for both sparse and block sparse minimization problems and numerical one for performance optimizing. In Section 3.3, a summarized flowchart of the Sparsity-Promoting optimal control algorithm is given to showing the major role of ADMM optimization tool in forming the overall algorithm of solving the optimization problem, which is in this case sparse controller with comparable performance to the standard centralized optimal control (i.e. the standard Linear Quadratic Regulator “LQR”). Finally, to demonstrate the effectiveness of the developed approach, an example of controlling a system that has 100 unstable integrator nodes, that are spatially distributed (randomly & uniformly) in a square region of 10 units and coupled with other nodes through exponentially decay coupling, is introduced [78], [59].

### **3.1 PROBLEM FORMULATION OF DESIGNING A DISTRIBUTED STATE-FEEDBACK CONTROLLER**

First, let's consider the standard state-feedback  $H_2$  norm problem as following;

$$\begin{aligned}
 \dot{x} &= Ax + B_w w + B_u u \\
 z &= Cx + Du \\
 u &= -Kx
 \end{aligned}
 \tag{3.1}$$

where;  $w$  is an exogenous disturbance input (reference, noise, etc.),  $u$  is a control input,  $z$  is the performance output, and  $K$  is the state-feedback matrix. For standard formulation of the problem, we consider  $C = [\sqrt{Q} \ 0]^T$  and  $D = [0 \ \sqrt{R}]^T$  with the following assumptions:

- $(A, B_u)$  is stabilizable.
- $(A, \sqrt{Q})$  is detectable.
- $Q$  is a positive definite.
- $R$  is a positive semi-definite.

Our objective is to find a state-feedback controller  $K$  that minimizes  $J(K)$ , which is the  $H_2^2$  norm of the closed-loop system. The objective function  $J(K)$ , for stabilizing  $K$ , can be calculated as below:

$$\begin{aligned} \text{Minimize } J(K) &= \text{trace}(B_w^T P(K) B_w) \quad (3.2) \\ \text{(Or equivalently " } J(K) &= \text{trace}(C_{cl} S(K) C_{cl}^T \text{")"} \end{aligned}$$

where,  $P(K)$  is the closed-loop observability Gramian (resp.  $S(K)$  is the closed-loop reachability Gramian) that is defined as follow:

$$\begin{aligned} P(K) &= \int_0^\infty e^{(A-B_u K)^T t} (Q + K^T R K) e^{(A-B_u K) t} dt \\ \text{(Or " } S(K) &= \int_0^\infty e^{(A-B_u K)^T t} B_w B_w^T e^{(A-B_u K) t} dt \text{ ")} \end{aligned} \quad (3.3)$$

The above observability (and reachability) Gramian can be obtained by solving the following Lyapunov equation:

$$\begin{aligned} (A - B_u K)^T P + P(A - B_u K) &= -(Q + K^T R K) \\ \text{(Or " } (A - B_u K)^T S + S(A - B_u K) &= -B_w B_w^T \text{")"} \end{aligned} \quad (3.4)$$

For centralized controller case (i.e. single node with full access), even though the objective function  $J(K)$  in (3.2) is considered as a non-convex function of the optimization variable  $K$  (the state-feedback matrix) [75], a global optimal solution can be obtained analytically using Algebraic Riccati equation (ARE) as bellow:

$$K = R^{-1}B_u^T P \quad (3.5)$$

where  $P$  can be obtained by solving the below Algebraic Riccati equation (ARE),

$$A^T P + PA - PB_u R^{-1} B_u^T P + Q = 0 \quad (3.6)$$

The centralized problem can also be formulated as a convex optimization problem using change of variables technique, and can be solved via linear programming, yielding very close solutions to the analytical one [75].

For distributed structure of the feedback controller, there will be a structural constraint  $G$  on the feedback matrix  $K$  and the problem is redefined as below:

$$\begin{aligned} \text{Minimize} \quad & J(K) = \text{trace}(B_w^T P(K) B_w) \\ \text{Subject to} \quad & K \in G \end{aligned} \quad (3.7)$$

In this case, change of variables method won't be able to formulate the problem in a convex format; therefore, the alternative proposed approach by [59] suggests to find a non-exact, yet satisfactory performance, solutions using tools from control theory, optimization, and compressive sensing to simultaneously identify the spares structure (no prior restrictions), according to a desired level of

sparsity ( $d$ ), and optimize the  $H_2$  performance of the resulted sparse controller. To realize this goal, first, the objective function should be modified to include sparsity structure, and the problem is reformulated as following:

$$\begin{aligned} \text{Minimize} \quad & J(K) + d g(G) \\ \text{Subject to} \quad & K - G = 0 \end{aligned} \tag{3.8}$$

where  $J(K)$  is the standard objective function defined in (3.2),  $d$  desired level of sparsity, and  $g(G)$  is structure optimization cost function of  $K$ , which is relaxed to  $l_1$  norm, weighted  $l_1$  norm, or sum of logs function [59]. Note that, the equality constraint here will allow the separation between the sparsity optimization term and the performance optimization term.

Accordingly, the design goal is to find  $K$  that minimizes (3.8), i.e. optimize performance (as a regulator), lower control effort, and eliminate insignificant elements (in the structured controller) to achieve the desired level of sparsity by tracing the optimal trade-off curve [77].

## 3.2 SOLVING THE DESIGN PROBLEM USING ADMM OPTIMIZATION

### ALGORITHM

As proposed in [59], the optimization problem in (3.8) can be iteratively solved by gradually increasing  $d$  desired level of sparsity (with zero initial condition, i.e. centralized controller) and tracing the homotopic path from the known optimal centralized solution to the desired distributed controller. Along the solution path, the previous feedback gain  $K$  is repeatedly taken as initial condition for the current iteration until the desired sparsity is achieved. In general, the resulted

structure of the controller depends on interconnection topology of the original plant (physical model of the distributed plant), and performance index, which in our case is  $H_2^2$  norm of the closed-loop system  $J(K)$ . As highlighted earlier, this approach would provide applicable solutions with satisfactory performance, but not exact one due to the non-convexity characteristic of the objective function. The original structured design problem (3.7) will be solved as a final step (polishing), but this time with a stabilizing “near-optimal” initial condition suggested by the ADMM solution. Polishing is well known in compressing sensing application, which usually resulted in a slight improvement to the final solution.

In this framework, the optimization tool recommended for each iteration of solving (3.8) is the alternating direction method of multipliers (ADMM), which is used offline to compute  $K$  with specific  $d$ , not as usual case where ADMM is used as an online distributed optimization tool. This optimization tool has the good robustness of method of multipliers and can support decomposition [76]. Because of the decomposability feature, the optimization problem in (3.8) can be decomposed into simpler minimization sub problems.

The augmented Lagrangian for (3.8) is formed as a standard Lagrangian with added quadratic penalty on the deviation between  $F$  and  $G$  as following:

$$L_\rho(K, G, \Lambda) = J(K) + d g(G) + \text{trace}(\Lambda^T(K - G)) + \left(\frac{\rho}{2}\right) \|K - G\|_F^2 \quad (3.9)$$

where  $\Lambda$  is Lagrange multiplier,  $\rho > 0$  is penalty parameter, and  $\| \cdot \|_F$  is the Forbenius norm. Then, ADMM will minimize the augmented Lagrangian (3.9) iteratively, at given  $d$ , using the following iterations:

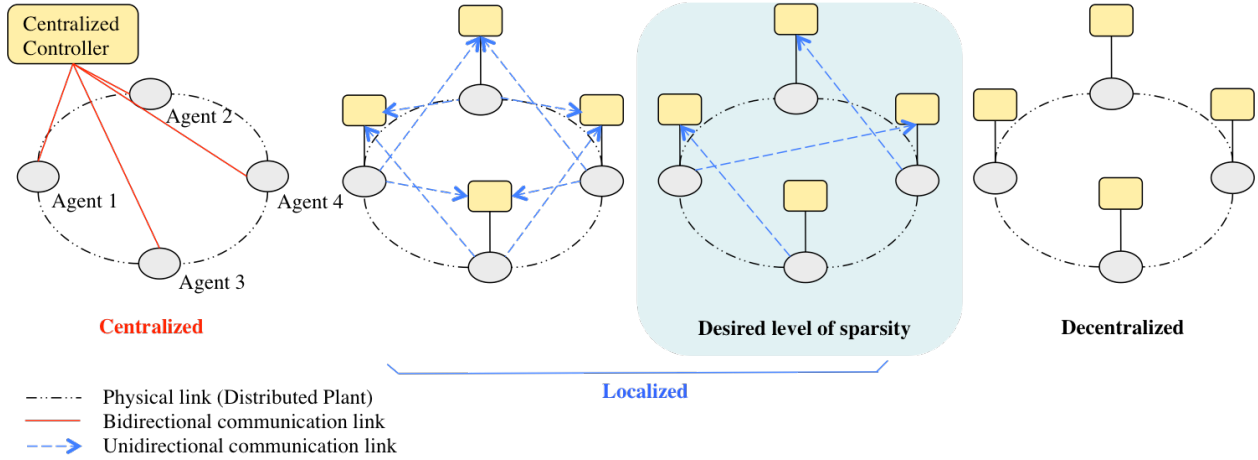


Figure 3-2. Communication structures for controlling a distributed plant: from the conventional centralized controller to the flexible distributed controllers.

$$K^{k+1} := \arg \min_K L_\rho(K, G^k, \Lambda^k) \quad (3.10)$$

$$G^{k+1} := \arg \min_G L_\rho(K^{k+1}, G, \Lambda^k) \quad (3.11)$$

$$\Lambda^{k+1} := \Lambda^k + \rho(K^{k+1} - G^{k+1}) \quad (3.12)$$

The Lagrangian (3.9) will be minimized in the first iteration (3.10) with respect to  $K$  using previous optimized values of  $G$  and  $\Lambda$ . Then, in second iteration (3.11), using updated value of  $K$  and previous  $\Lambda$ , the Lagrangian is minimized with respect to  $G$ . Finally, (3.12) is updating the Lagrange multiplier  $\Lambda$  into the direction of constraint violation, with  $\rho$  as a step size [76]. These iterations will continue till the first iteration, which optimize performance  $K$ , and second iteration, which optimize sparsity  $G$ , reach certain agreement (i.e. quadratic cost of the deviation between  $F$  and  $G$  is below stopping criteria tolerance [76]).

### 3.2.1 Performance Optimization Iteration

For the minimization problem in the first iteration (3.11), Anderson & Moore algorithm is used to optimize the Lagrangian with respect to  $K$  [59]. Considering  $K$  as an optimization variable, while fixing other variables, the Lagrangian in (3.9) is reformed as following:

$$\min_K \varphi(K) = J(K) + \left(\frac{\rho}{2}\right) \|K - U^k\|_F^2 \quad (3.13)$$

where,  $U^k = G^k - \left(\frac{1}{\rho}\right) \Lambda^k$ . The initial condition for  $K$  (at  $k=0$ ) is the solution of (3.8) of previous value of  $d$  (desired level of sparsity), with no structure constraint on  $K$ . The gradient of the above objective function is:

$$\nabla \varphi(K) := \nabla J(K) + \rho(K - U^k) \quad (3.14)$$

where,  $\nabla J(K) = 2(RK - B_u^T P)S$ . The necessary conditions for optimality are obtained as two Lyapunov equations of reachability and observability Gramian (3.3), and the below Sylvester equation that updates  $K$  in each optimization iteration:

$$KS + \rho(2R)^{-1}K = R^{-1}B_u^T P S + \rho(2R)^{-1}U^k \quad (3.15)$$

### 3.2.2 Sparsity Optimization Iteration

For the second minimization problem (3.11), the optimized  $G$  (as relaxed in weighted  $l_1$  norm) can be obtained analytically and element-wise using soft-thresholding (proximal mapping of the  $l_1$ -norm) as following [76]:

$$G_{ij}^* = \begin{cases} \left(1 - \frac{\varepsilon}{|V_{ij}|}\right) V_{ij}, & \text{for } |V_{ij}| > \varepsilon \\ 0, & \text{for } |V_{ij}| < \varepsilon \end{cases} \quad (3.16)$$

where,  $V^k = \left(\frac{1}{\rho}\right) \Lambda^k + F^{k+1}$ , and  $\varepsilon = \left(\frac{d}{\rho}\right) w_{ij}$  with the weighted value  $w_{ij}$  chosen as  $(1/|K_{ij}|)$ . So,  $\varepsilon$  (thresholding operator) is linearly dependent on the desired sparsity  $d$  and inversely dependent on the significant of the gain/contribution of each element, resulted in dropping more insignificant elements as  $d$  is increased. Note that it's possible to assign zero values to some  $G$  elements whenever it's desirable.

### 3.3 FURTHER ENHANCEMENT FOR FINAL HEURISTIC SOLUTION

The resulted distributed (structured) controller from the previous subsections is an approximation solution due to that the mentioned approach of solving the problem formulated in (3.8) by gradually changing  $d$ , with the suggested approximation cost functions such as  $l_1$ -norm, is itself a heuristic approach of tracing the optimal trade-off curve between performance and sparsity [77]. Moreover, the objective function is not a convex function of feedback gain matrix  $K$  resulted in

non-exact solutions. Therefore, resolving the optimization problem using the identified sparsity pattern can further enhanced the results to obtain a final approximation solution [59].

In this case, the problem turned back to its original format in (3.7), as  $H_2$  optimal controller design problem with structural constraints, which can be solved using Newton's method with conjugate gradient. Similar necessary conditions for optimality to the case of performance optimization in Subsection 3.2.1 are obtained as two Lyapunov equations of reachability and observability Gramian (3.3), and the below equation that updates K, but with structural constraint as follows:

$$[(RK - B_u^T P)S] \circ I_s = 0 \quad (3.17)$$

where  $I_s$  is representing the sparsity pattern identified through solving the optimization problem (3.8).

### 3.4 SUMMARIES AND OVERALL FLOWCHART OF THE ALGORITHM

To summarize the previous sections / subsections, a simplified flowchart of the overall algorithm is presented, which reveals the relationships between various steps in the algorithm. It shows the major role of ADMM optimization tool in forming the overall algorithm. As explained earlier, the algorithm is intended for solving the design problem of finding a state-feedback matrix K that can minimize (3.8), i.e. traces optimal trade-off curve between optimizing the performance ( $H_2^2$ -norm measure of the closed-loop system), lowering the control effort, and eliminating insignificant gains in the state-feedback matrix K to achieve the desired level of sparsity.

As depicted in Figure 3.3, the algorithm starts with calculating the state-feedback matrix ( $K$ ) of the standard central LQR, and setting the resulted  $K$  matrix as initial condition for the algorithm. Also, as initialization step, the range for the values that could be taken by the level of sparsity ( $d$ ) until reaching the desired one should be specified, a suggested way is based on logarithmic scale [59]. Then, the algorithm will run ADMM iterations for solving (3.8) as  $d$  varies over  $[\alpha_0, d]$ , as discussed in Sections 3.2.1, 3.2.2, and eq. (3.12) with specific stopping criterion, until reaching the desired level of sparsity. Finally, the resulted distributed (structured) controller is further enhanced based on the method discussed in Section 3.3, to obtain a final approximated solution.

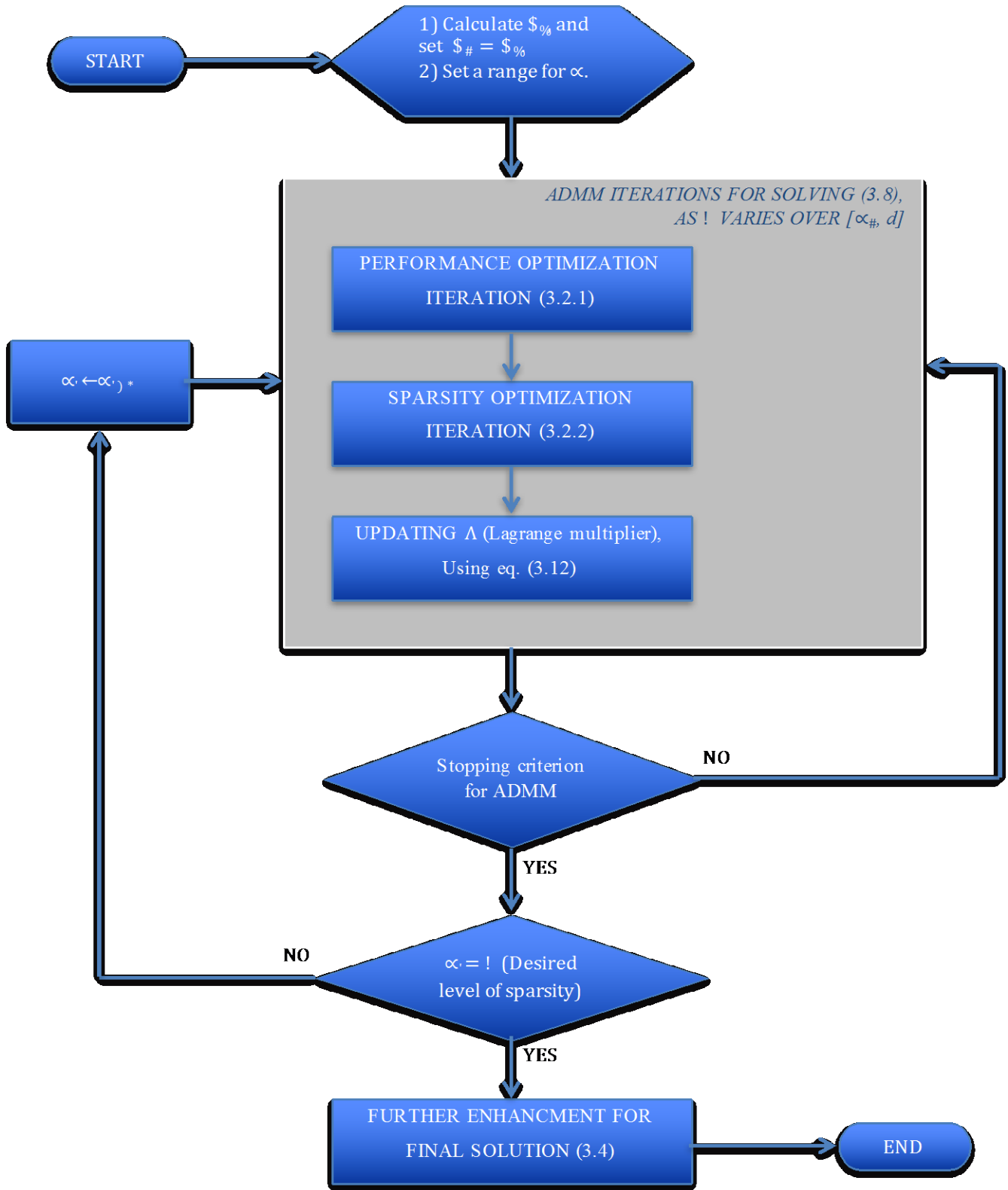


Figure 3-3. A summarized flowchart of the Sparsity-Promoting optimal control algorithm.

### 3.5 AN ILLUSTRATED EXAMPLE

To illustrate the effectiveness of the Sparsity-Promoting approach, an example of controlling a system that has 100 unstable integrator nodes that are spatially distributed (randomly & uniformly) in a square region of 10 units and coupled with other nodes through exponentially decay coupling [78], [59]. The goal is to minimize the state variance via a distributed state-feedback controller under stochastic disturbance. The dynamics of each node (including the coupling part) is as follow:

$$\begin{bmatrix} \dot{p}_i \\ \dot{v}_i \end{bmatrix} = \begin{bmatrix} 1 & 1 \\ 1 & 2 \end{bmatrix} \begin{bmatrix} p_i \\ v_i \end{bmatrix} + \sum_{j \neq i} e^{-\alpha(i,j)} \begin{bmatrix} p_i \\ v_i \end{bmatrix} + \begin{bmatrix} 0 \\ 1 \end{bmatrix} (d_i + u_i) \quad (3.18)$$

where,  $p$  &  $v$  are state variables,  $\alpha$  is distance between node  $i$  and  $j$ ,  $d$  stochastic disturbance input, and  $u$  is the control input.

Using the Sparsity-Promoting approach, with  $Q$  &  $R$  are identity matrices and the desired  $d$  is set to 100, the design approach is able to come up with a distributed controller at various level of sparsity that is has very comparable performance to the centralized feedback gain, and able to maintain closed-loop stability while increasing the sparsity to desired  $d$ , which is only 2.4% non-zero elements relative to the centralized controller.

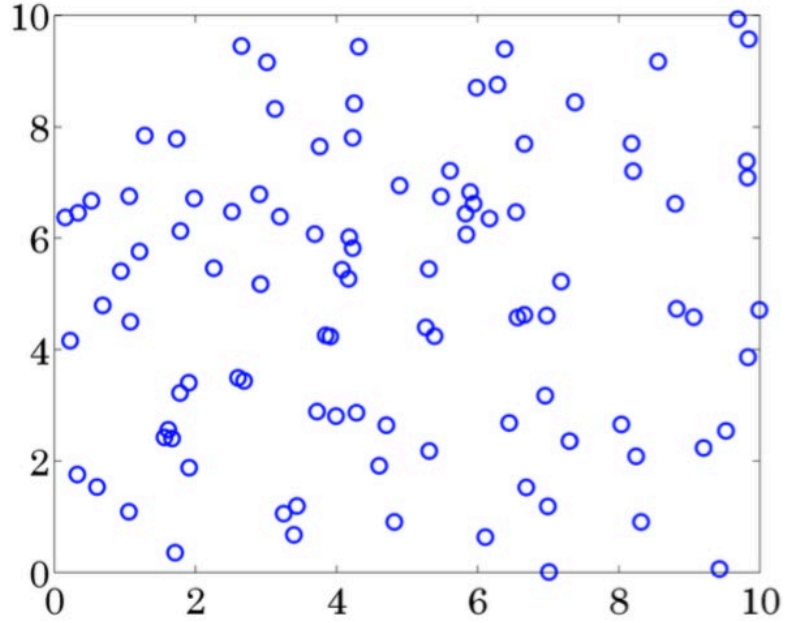


Figure 3-4. 100 unstable integrator nodes with exponentially decay coupling [59].

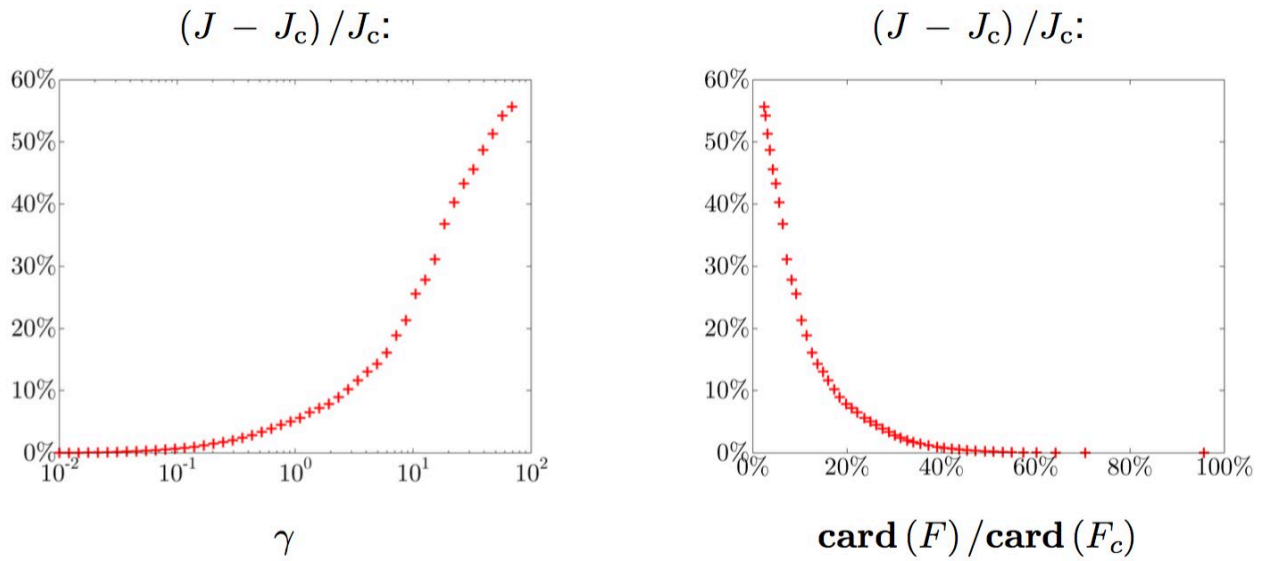


Figure 3-5. (a) Performance versus sparsity as increasing sparsity level. (b) Performance versus sparsity level compared to the optimal centralized controller [59].

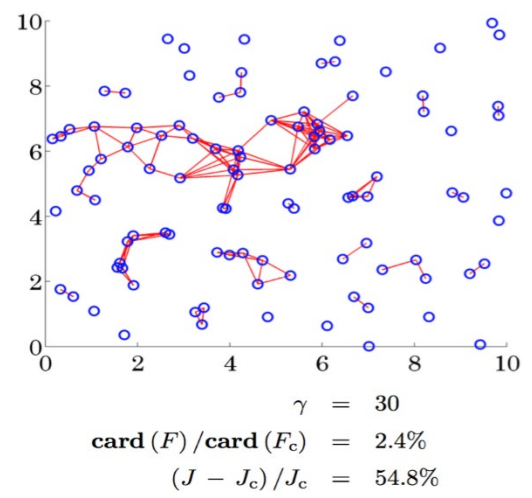
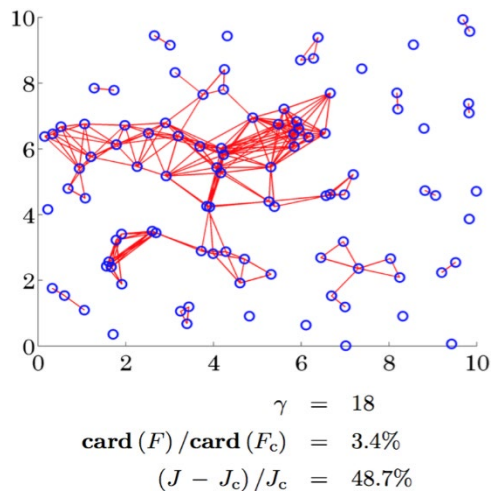
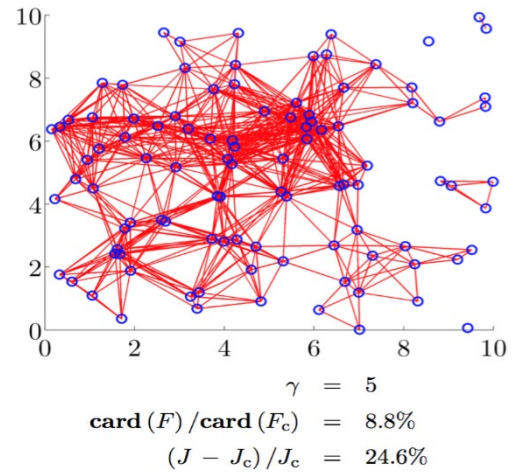
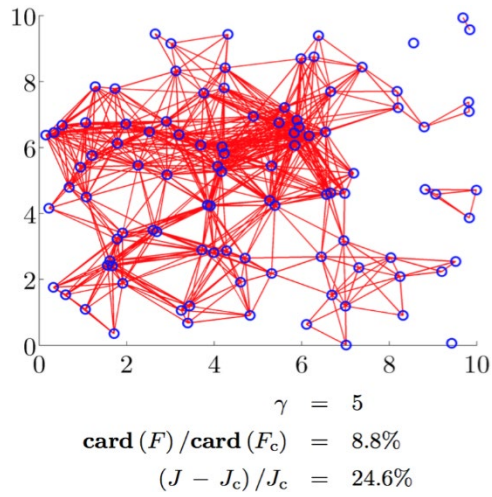


Figure 3-6. Identified localized communication topologies of distributed controllers using Sparsity-Promoting approach with different desired level of sparsity [59].

## **4.0 DISTRIBUTED SECONDARY VOLTAGE CONTROL (DSVC) FOR AC MICROGRID USING SPARSITY-PROMOTING APPROACH**

### **4.1 REDUCED SMALL-SIGNAL STATE-SPACE MODEL OF INVERTER-BASED MICROGRID**

In full order model, to avoid neglecting relatively important dynamics during extreme operation modes and large load disturbances for stability study, the assumption of an ideal inverter and disregarding network dynamics in [82] is avoided in [29]. Therefore, the full order model in [29] is intended to capture the dynamics of the whole system, all represented in a common reference frame, including high frequency dynamics; namely, network & load dynamics, voltage & current controllers. Matrices representing this model is shown in Appendix A. However, such an oversized model is intended for stability studies and not suitable for designing a secondary control system in a microgrid that may have multiple DGs.

Therefore, to decrease dimensionality for less burden computations and to reduce the order of resulted secondary control, a feasible reduced order model is considered thru identifying dominant modes (modes of interest) and eliminating states associated with modes that are less significant to the secondary control level. This identification process is based on the dynamic analysis of a simulated prototype microgrid to detect various modes of the system, which has reveals the two time-scale nature of the system. Therefore, as reported in [93], the model is

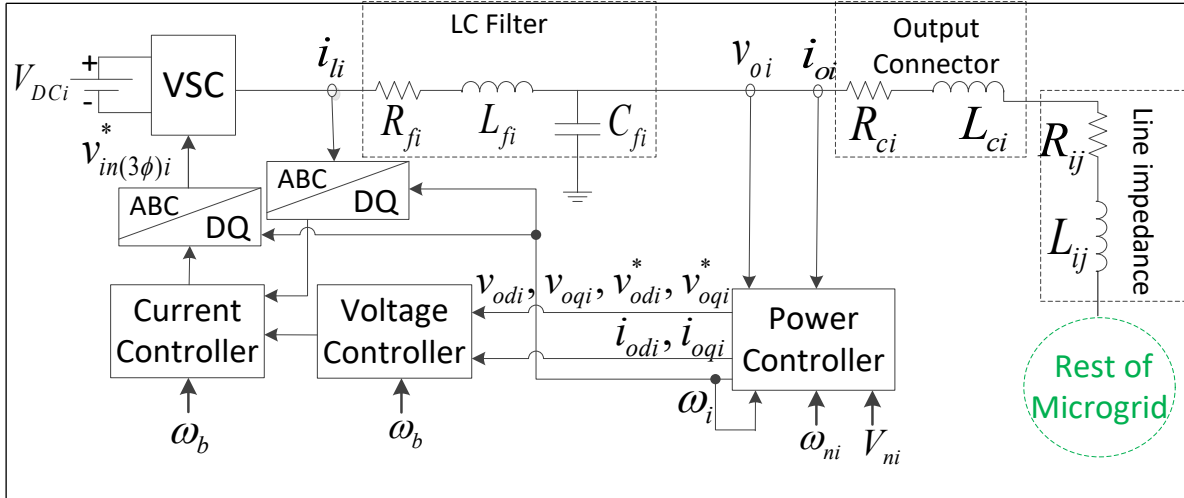


Figure 4-1. Droop-controlled based primary control of DG inverter [93].

reconstructed considering only relevant states for the secondary control design along with the steady states solutions of the fast modes. Hence, the model presented in [93] is adopted in this study.

As shown in Figure 4-1, the one DG unit includes four parts: power controller, current controller, voltage controller, and the LCL filter. The role of power controller is maintaining a proper load sharing between the DG's, and it is implemented using active/reactive power - frequency/voltage droop controllers that imitate the droop characteristics of conventional synchronous generators where machine's inertia is used. These droop controller methods are preferable since it depends only on local measurements without any communication links, unlike active power sharing methods that require dense communication links that is affecting system reliability [29, 30, 4, 28, 31]. Then, a voltage controller is used to compensate for changing in the output voltage based on the reference voltage value that is obtained from the droop controller. An additional internal control loop is used following the outer one to compensate for changing in the inductor current based on a reference current value that is attained from the voltage controller.

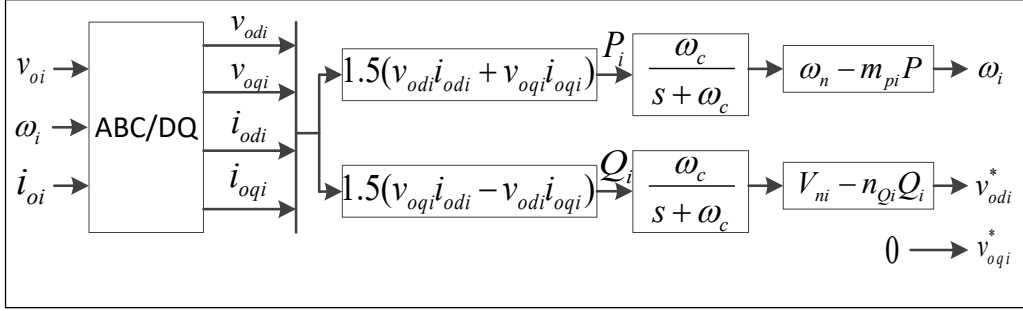


Figure 4-2. Power controller block diagram [93].

Finally, the output of the current control loop generates a reference signal that is used to generate PWM pulses to control switching states of the converter. As shown in Figure 4-2, the droop controller equations are as follows:

$$v_{oi}^* = V_{ni} - n_{qi} Q_i \quad (4.a)$$

$$\omega_i = \omega_{ni} - m_{pi} P_i \quad (4.b)$$

where  $V_{ni}$  is the reference voltage,  $n_{qi}$  is the reactive power droop gain,  $Q_i$  is the reactive power,  $v_{oi}^*$  is the reference value of the inner current controllers. Similarly,  $\omega_{ni}$  is the reference angular frequency,  $m_{pi}$  is the real power droop gain,  $P_i$  is the real power, and the resulted  $\omega_i$  is the resulted angular frequency of the DG. Assuming  $v_{oqi}^* = 0$ , in case of complete alignment of phase A voltage to the d-axis, equation (4.b) can be rewritten as

$$v_{odi}^* = V_{ni} - n_{qi} Q_i \quad (4.c)$$

In Figure 4-2, the active and reactive power are the output of the LPF, that is filtering the fundamental elements from the instantaneous active and reactive powers, as follows:

$$P = \frac{\omega_c}{s + \omega_c} \tilde{p} \quad (4.1)$$

$$Q = \frac{\omega_c}{s + \omega_c} \tilde{q} \quad (4.2)$$

where  $\omega_c$  is the cut-off frequency of the LPF, and  $\tilde{p}$  and  $\tilde{q}$  are instantaneous active/reactive power obtained from:

$$\tilde{p} = v_{od}i_{od} + v_{oq}i_{oq} \quad (4.3)$$

$$\tilde{q} = v_{od}i_{oq} - v_{oq}i_{od} \quad (4.4)$$

From (4.1) and (4.2), the dynamic of real and reactive power is then given by

$$\dot{P}_i = -\omega_c P_i + \frac{3}{2} \omega_c (v_{odi}i_{odi} + v_{oqi}i_{oqi}) \quad (4.5)$$

$$\dot{Q}_i = -\omega_c P_i + \frac{3}{2} \omega_c (v_{oqi}i_{odi} - v_{odi}i_{oqi}) \quad (4.6)$$

With a high bandwidth of the internal inner controllers, usually about 500 Hz for the voltage controller with a current controller that is at least 5 times higher (about 1.5 kHz), and a perfect alignment for the dq-transformation resulted in  $v_{oqi} = 0$ , real and reactive power will have the following form:

$$\dot{P}_i = -\omega_c P_i + \frac{3}{2} \omega_c v_{odi}i_{odi} \quad (4.7)$$

$$\dot{Q}_i = -\omega_c P_i - \frac{3}{2} \omega_c v_{odi}i_{oqi} \quad (4.8)$$

Applying Kirchhoff's voltage law (KVL) to the circuits on the Figure 4-3, we reach the following expression that is representing the current dynamic of both dq-components as,

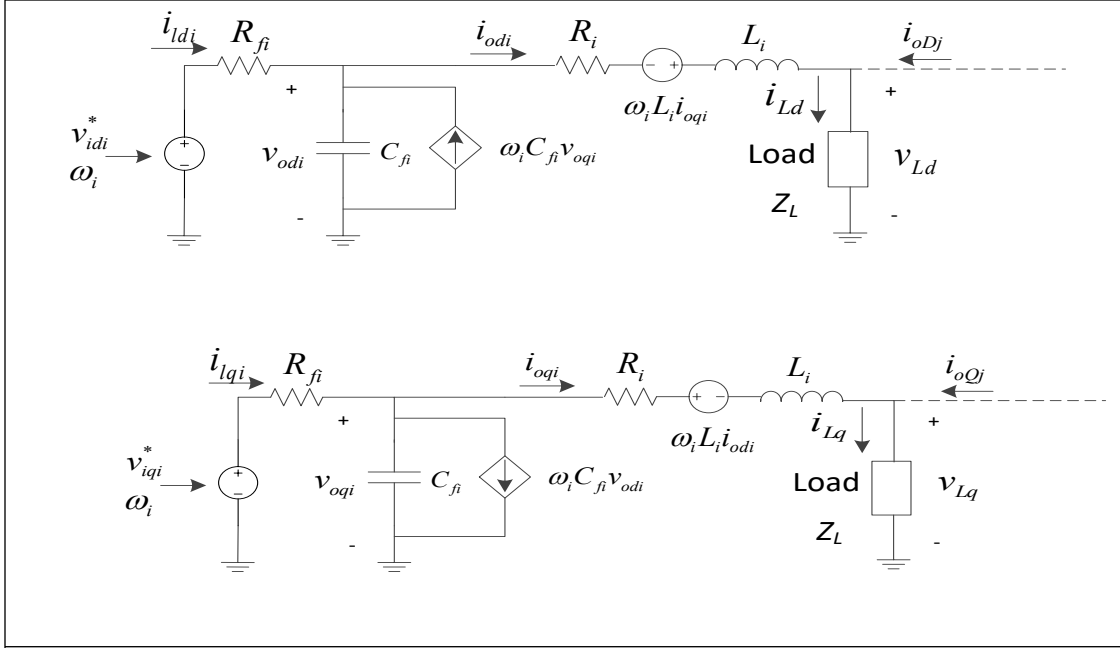


Figure 4-3. Equivalent d-axis and q-axis circuits of each DG [93].

$$i_{di} = \frac{1}{L_i} v_{odi} - \frac{R_i}{L_i} i_{odi} + \omega_i i_{oqi} - \frac{1}{L_i} v_{Ld} \quad (4.9)$$

$$i_{qi} = \frac{1}{L_i} v_{oqi} - \frac{R_i}{L_i} i_{oqi} + \omega_i i_{odi} - \frac{1}{L_i} v_{Lq} \quad (4.10)$$

where  $L_i$  and  $R_i$  are the inductance and resistance of the sum of the cable and connector for each DG. Similarly, by Applying Kirchhoff's current law (KCL), we reach

$$i_{Ld} = i_{odi} + i_{odj} \quad (4.11)$$

$$i_{Lq} = i_{oqi} + i_{oqj}. \quad (4.12)$$

By redefining the voltage at the load by its own state along with the DG neighboring states, we arrive at

$$v_{Ld} = Z_L (i_{odi} + i_{odj}) \quad (4.13)$$

$$v_{Lq} = Z_L (i_{oqi} + i_{oqj}) \quad (4.14)$$

where  $Z_L$  is the impedance value of the load. Now, (4.9) and (4.10) can be rewritten using (4.13) and (4.14) while keep the assumption of having  $v_{oqi} = 0$ , we reach

$$\dot{i}_{odi} = \frac{1}{L_i} v_{odi} - \left( \frac{R_i}{L_i} + \frac{Z_L}{L_i} \right) i_{odi} + \omega_i i_{oqi} - \frac{Z_L}{L_i} i_{oDj} \quad (4.15)$$

$$\dot{i}_{oqi} = - \left( \frac{R_i}{L_i} + \frac{Z_L}{L_i} \right) i_{oqi} - \omega_i i_{odi} - \frac{Z_L}{L_i} i_{oQj} \quad (4.16)$$

Again, substitute (4.b) into (4.15) and (4.16), we obtain the following expressions for the d-component and q-component of the output current

$$\begin{aligned} \dot{i}_{odi} &= \frac{1}{L_i} v_{odi} - \left( \frac{R_i}{L_i} + \frac{Z_L}{L_i} \right) i_{odi} + \omega_{ni} i_{oqi} \\ &\quad - m_{pi} P_i i_{oqi} - \frac{Z_L}{L_i} i_{oDj} \end{aligned} \quad (4.17)$$

$$\begin{aligned} \dot{i}_{oqi} &= - \left( \frac{R_i}{L_i} + \frac{Z_L}{L_i} \right) i_{oqi} + \omega_{ni} i_{odi} \\ &\quad + m_{pi} P_i i_{odi} - \frac{Z_L}{L_i} i_{oQj} \end{aligned} \quad (4.18)$$

Before proceeding to combine the previous modeling parts in a single form, synchronizing between inverters in the system should be carefully considered. For synchronizing the inverters, the reference frequency ( $\Delta\omega_{com}$ ) should be available to all connected inverters. For synchronizing each inverter with the whole system, its input  $\Delta v_{bdq}$  (from system's network) and output  $\Delta i_{odq}$  should be transformed to the common reference frame as follows [84]:

$$\begin{bmatrix} i_{oDj} \\ i_{oQj} \end{bmatrix} = \begin{bmatrix} \cos \delta_j & -\sin \delta_j \\ \sin \delta_j & \cos \delta_j \end{bmatrix} \begin{bmatrix} i_{odj} \\ i_{oqj} \end{bmatrix}. \quad (4.19)$$

Using the previous transformation in (4.19), into (4.17), and (4.18) converted them into

$$\begin{aligned} \dot{i}_{odi} &= \frac{1}{L_i} v_{odi} - \left( \frac{R_i}{L_i} + \frac{Z_L}{L_i} \right) i_{odi} + \omega_{ni} i_{oqi} \\ &\quad - m_{pi} P_i i_{oqi} - \frac{Z_L}{L_i} \cos(\delta_{ij}) i_{odj} + \frac{Z_L}{L_i} \sin(\delta_{ij}) i_{oqj} \end{aligned} \quad (4.20)$$

$$\begin{aligned} \dot{i}_{oqi} &= -\left( \frac{R_i}{L_i} + \frac{Z_L}{L_i} \right) i_{oqi} + \omega_{ni} i_{odi} \\ &\quad - m_{pi} P_i i_{odi} - \frac{Z_L}{L_i} \sin(\delta_{ij}) i_{odj} - \frac{Z_L}{L_i} \cos(\delta_{ij}) i_{oqj} \end{aligned} \quad (4.21)$$

Now, by applying KCL again at the filter node for the d-axis and q-axis circuits, we obtain the following expressions for the d-component and q-component of the output voltage

$$C_{fi} \dot{v}_{odi} = C_{fi} \omega v_{oqi} + i_{ldi} - i_{odi} \quad (4.22)$$

$$C_{fi} \dot{v}_{oqi} = -C_{fi} \omega v_{odi} + i_{lqi} - i_{oqi} \quad (4.23)$$

where the current entering the LC filter is as follows,

$$i_{ldi} = \frac{v_{idi}^* - v_{odi}}{R_{fi}} \quad (4.24)$$

Using equation (4.c) into (4.24), we reach the following expression that is describing the same dynamic (i.e. system's state) but using previously defined states, as follows

$$i_{ldi} = \frac{V_{ni} - n_{qi}Q_i - v_{odi}}{R_{fi}}. \quad (4.25)$$

And again, use the above equation in (4.22), we arrive at

$$v_{odi} = \frac{V_{ni}}{C_{fi}R_{fi}} - \frac{n_{qi}}{C_{fi}R_{fi}}Q_i - \frac{1}{C_{fi}R_{fi}}v_{odi} - \frac{1}{C_{fi}}i_{odi} \quad (4.26)$$

Finally, the angle between each DG and the common reference frame is expressed as

$$\dot{\delta} = \omega_i - \omega_{com} \quad (4.27)$$

where  $\omega_{com}$  is the angular frequency of the common reference frame, which usually is chosen to be the angular frequency of DG1 ( $\omega_1 = \omega_{com}$ ). Using the droop equation in (4.b) into (4.27), we get

$$\dot{\delta}_i = \omega_{mi} - m_{pi}P_i - \omega_{n1} + m_{p1}P_1 \quad (4.28)$$

With the states for a 2 DG system defined as follows: (Note that the state  $\delta_1=0$ )

$$x \equiv [P_1 \ Q_1 \ i_{od1} \ i_{ioq1} \ v_{od1} \ P_2 \ Q_2 \ i_{od2} \ i_{ioq2} \ v_{od2} \ \delta_2]^T \quad (4.29)$$

A small-signal linearized model is obtained as follows:

$$\begin{aligned} \dot{x} &= A\bar{x} + B\bar{u} \\ \bar{y} &= C\bar{x} + D\bar{u} \end{aligned} \quad (4.30)$$

where, the input and output of the system can be chosen as:

$$u = [V_{n1} \quad V_{n2}]^T$$

$$y = [v_{od1} \quad v_{od2}]^T$$
(4.31)

Hence, based on the introduced model above and the procedure followed in [93], the linearized state space model of a simplified microgrid system consisting of two distributed generators connected to a common bus, through inductive transmission lines, and supplying power to a common load is as follows:

For a simplified microgrid with two distributed generators (DG)

(i) State Matrix:

$$A = \begin{bmatrix} A_{11} & A_{12} \\ A_{21} & A_{22} \end{bmatrix}$$

where the above matrices are defined as follows:

$$A_{11} = \begin{bmatrix} -\omega_c & 0 & d_1 & 0 & \frac{3}{2}\omega_c i_{od10} \\ 0 & -\omega_c & 0 & -d_1 & -\frac{3}{2}\omega_c i_{oq10} \\ -m_{p1} i_{oq10} & 0 & b_1 & a_1 & \frac{1}{L_1} \\ m_{p1} i_{od10} & 0 & m_1 & b_1 & 0 \\ 0 & n_{q1} c_1 & \frac{-1}{C_{f1}} & 0 & c_1 \end{bmatrix}$$

$$A_{22} = \begin{bmatrix} -\omega_c & 0 & d_2 & 0 & \frac{3}{2}\omega_c i_{od20} & 0 \\ 0 & -\omega_c & 0 & -d_2 & -\frac{3}{2}\omega_c i_{oq20} & 0 \\ -m_{p2} i_{oq20} & 0 & b_2 & a_2 & \frac{1}{L_2} & 0 \\ m_{p2} i_{od20} & 0 & m_2 & b_2 & 0 & 0 \\ 0 & n_{q2} c_2 & \frac{-1}{C_{f2}} & 0 & c_1 & 0 \\ -m_{p2} & 0 & 0 & 0 & 0 & 0 \end{bmatrix}$$

$$A_{12} =$$

$$\begin{bmatrix} 0 & 0 & 0 & 0 & 0 & 0 \\ 0 & 0 & 0 & 0 & 0 & 0 \\ 0 & 0 & \frac{-Z_L}{L_1} & \frac{Z_L}{L_1} \delta_{20} & 0 & \frac{Z_L}{L_1} i_{oq20} \\ 0 & 0 & \frac{-Z_L}{L_1} \delta_{20} & \frac{-Z_L}{L_1} & 0 & -\frac{Z_L}{L_1} i_{od20} \\ 0 & 0 & 0 & 0 & 0 & 0 \end{bmatrix}$$

$$A_{21} =$$

$$\begin{bmatrix} 0 & 0 & 0 & 0 & 0 \\ 0 & 0 & 0 & 0 & 0 \\ 0 & 0 & \frac{-Z_L}{L_2} & 0 & 0 \\ 0 & 0 & 0 & \frac{-Z_L}{L_2} & 0 \\ 0 & 0 & 0 & 0 & 0 \\ m_{p1} & 0 & 0 & 0 & 0 \end{bmatrix}$$

And  $b_i$  and  $d_i$  are defined as follows;

$$b_i = \frac{-R_i - Z_L}{L_i}, \quad c_i = -\frac{1}{C_{fi} R_{fi}}$$

$$d_i = \omega_c v_{odi0}, \quad m_i = m_{pi} P_{i0} - \omega_{ni}$$

(ii) Input Matrix:

$$B = \begin{bmatrix} 0 & 0 & 0 & 0 & -c_1 & 0 & 0 & 0 & 0 & 0 & 0 \\ 0 & 0 & 0 & 0 & 0 & 0 & 0 & 0 & 0 & -c_2 & 0 \end{bmatrix}^T$$

(iii) Output Matrix:

$$C = \begin{bmatrix} 0 & 0 & 0 & 0 & 1 & 0 & 0 & 0 & 0 & 0 & 0 \\ 0 & 0 & 0 & 0 & 0 & 0 & 0 & 0 & 0 & 0 & 1 \end{bmatrix}$$

For more generalized representation in case of a larger microgrid, that is consisting of multiple distributed generators (with number of generators “n”), the following model is used:

$$A = \begin{bmatrix} A_{11} & A_{12} & L & A_{1n} \\ A_{21} & A_{22} & L & A_{2n} \\ M & M & O & M \\ A_{n1} & A_{n2} & L & A_{nn} \end{bmatrix}$$

where the above matrices are defined as follows:

$$A_{1n} = \begin{bmatrix} 0 & 0 & 0 & 0 & 0 & 0 \\ 0 & 0 & 0 & 0 & 0 & 0 \\ 0 & 0 & \frac{-Z_L}{L_1} & \frac{Z_L}{L_1} \delta_{n0} & 0 & \frac{Z_L}{L_1} i_{oqn0} \\ 0 & 0 & \frac{-Z_L}{L_1} \delta_{n0} & \frac{-Z_L}{L_1} & 0 & -\frac{Z_L}{L_1} i_{iodn0} \\ 0 & 0 & 0 & 0 & 0 & 0 \end{bmatrix} \quad A_{n1} = \begin{bmatrix} 0 & 0 & 0 & 0 & 0 \\ 0 & 0 & 0 & 0 & 0 \\ 0 & 0 & \frac{-Z_L}{L_n} & 0 & 0 \\ 0 & 0 & 0 & \frac{-Z_L}{L_n} & 0 \\ 0 & 0 & 0 & 0 & 0 \\ m_{p1} & 0 & 0 & 0 & 0 \end{bmatrix}$$

$$A_{nk} = \begin{bmatrix} 0 & 0 & 0 & 0 & 0 & 0 \\ 0 & 0 & 0 & 0 & 0 & 0 \\ 0 & 0 & \frac{-Z_L}{L_n} & \frac{Z_L}{L_n} \delta_{k0} & 0 & \frac{Z_L}{L_n} I_{oqk0} \\ 0 & 0 & \frac{-Z_L}{L_n} \delta_{k0} & \frac{-Z_L}{L_n} & 0 & -\frac{Z_L}{L_n} I_{odk0} \\ 0 & 0 & 0 & 0 & 0 & 0 \\ m_{pk} & 0 & 0 & 0 & 0 & 0 \end{bmatrix}$$

and  $n \neq k$ ,  $n \neq 1$ , and  $k \neq 1$ .

The sensitivity analysis of a full order model and a reduced order model, which has been developed in a similar method, are reported in [29] and [83]. In [83], a simplified system of two equally rated inverters supplying two different loads and connected through a distribution line is used as a test system. The modeling method adopted is similar to the full order model presented in the Appendix, except that in this model LCL filter damping resistor  $R_d$  is added and the dynamics of the PLL (phase locked loop) is included. Based on the sensitivity analysis, there are two groups of modes that are not well damped and may cause stability problems some belongs to fast decaying modes with high oscillatory frequency, and the others are slow decaying modes with low oscillatory frequency. Using participation factor analysis, states associated with these modes are identified. Even though the states associated with fast decaying modes can be neglected later in

the model reduction process, their poor damping suggested that to increase system's stability margin a larger damping resistor  $R_d$  can be added (however, this would impact the efficiency of the system), or maintain these states to be included in the regulator design procedure. A similar sensitivity analysis is conducted in [29] indicated similar sensitivity behavior.

## 4.2 OPTIMIZATION PROBLEM OF DISTRIBUTED STATE-FEEDBACK SECONDARY CONTROLLER

As discussed in Chapter 3, the problem of designing a distributed secondary voltage controller (DSVC) in microgrid system can be also formulated as an optimal control problem that is driven by a stochastic exogenous disturbance, where an additional term is added to the standard objective function (2.2) ( $H_2^2$  norm of the closed-loop system) to include the sparsity structure. The solution of this optimization problem is a candidate  $K$  (state-feedback matrix) for the state-feedback controller  $u = -Kx$  that minimizes the objective function, i.e. able to optimize performance (as a regulator), lower the control effort, and eliminate insignificant elements (in the structured controller) to achieve the desired level of sparsity, while maintaining closed-loop stability of the system. A similar optimization problem to (3.8) can be used here:

$$\begin{aligned}
 & \text{Minimize} \quad \text{trace}(B_w^T P(K) B_w) + d g(G) \\
 & \text{Subject to} \quad \begin{cases} K - G = 0 \\ (A_{mg} - B_u K)^T P + P(A_{mg} - B_u K) = -(Q + K^T R K) \end{cases} \quad (4.32)
 \end{aligned}$$

where  $P(K)$  is the closed-loop observability Gramian,  $d$  desired level of sparsity,  $A_{mg}$  is the overall microgrid system's state matrix,  $B_w$  disturbance input matrix,  $B_u$  control input matrix, where the control input is chosen to be  $v_{od}$  of each controller, and  $g(G)$  is structure optimization cost function of  $G$ , which can be relaxed to  $l_1$  norm, weighted  $l_1$  norm, or sum of logs function [59], with the following standard assumptions:

- $(A, B_u)$  is stabilizable.
- $(A, Q)$  is detectable.
- $Q$  is a positive definite.
- $R$  is a positive semi-definite.

The resulted distributed (structured) secondary controller (regulator) is desired to be able to regulate the voltage and the frequency of each DG, maintain active/reactive power sharing properties established in the primary control level (absorbed into the plant model), maintain the closed-loop system stability, and reach the desired level of sparsity. In the next section, the design framework of solving this problem based on Sparsity-Promoting approach will be discussed in further details.

### **4.3 SPARSITY PROMOTING VIA ADMM**

Using the approach of Sparsity-Promoting presented in [59], as reviewed in Chapter 3, the optimization problem in (3.8), can be iteratively solved by gradually increasing  $d$  desired level of sparsity (with zero initial condition, i.e. centralized controller) and tracing the homotopic path from the known optimal centralized solution to the desired distributed controller. Along the solution

path, the previous feedback gain  $K$  is repeatedly taken as initial condition for the current iteration until the desired sparsity is achieved. In this framework, the optimization tool recommended for each iteration of solving (3.8) is the alternating direction method of multipliers (ADMM). As a final step, the original structured design problem, as presented in Section 3.3, will be solved (polishing), but this time with a very suitable initial condition suggested by the ADMM solution. Polishing is well known in compressing sensing application, which usually resulted in a slight improvement to the final solution. The overall algorithm is summarized in Section 3.4, and the algorithms used for each minimization step is presented in Subsections 3.2.1 and 3.2.2.

For the second minimization problem (3.11), the optimized  $G$  (as relaxed in weighted  $l_1$  norm) can be obtained analytically and element-wise using soft-thresholding (proximal mapping of the  $l_1$ -norm) as following:

$$G_{ij}^* = \begin{cases} \left(1 - \frac{\varepsilon}{|V_{ij}|}\right) V_{ij}, & \text{for } |V_{ij}| > \varepsilon \\ 0, & \text{for } |V_{ij}| < \varepsilon \end{cases} \quad (4.33)$$

where,  $V^k = \left(\frac{1}{\rho}\right) \Lambda^k + F^{k+1}$ , and  $\varepsilon = \left(\frac{d}{\rho}\right) w_{ij}$  with the weighted value  $w_{ij}$  chosen as  $(1/|K_{ij}|)$ . So,  $\varepsilon$  (thresholding operator) is linearly dependent on the desired sparsity  $d$  and inversely dependent on the significant of the gain/contribution of each element, resulted in dropping more insignificant elements as  $d$  is increased. Note that, it's possible to assign zero values to some  $G$  elements whenever it's desirable.

## 4.4 CHOOSING THE DESIGN PARAMETERS

As mentioned in the previous sections, the goal of the desired distributed (structured) secondary controller (regulator) is to regulate the voltage and the frequency of each DG, maintain active/reactive power sharing properties established in the primary control level (absorbed into the plant model), maintain the system closed-loop stability, and reach the desired level of sparsity. In order to realize these objectives, which have some contradicting to some degree (e.g. the highlighted conflict between voltage regulation & reactive power sharing in a typical low r/x ratio microgrid), the design parameters; namely, 1) state weight matrix Q, 2) control weight matrix R, 3) disturbance matrix  $B_w$ , and 4) the desired level of sparsity d, should be carefully chosen to achieve the desired performance. In this section a discussion about different possible settings of these design parameters is presented in order to realize the design objectives. The possible settings of the design parameters can be summarized as following:

### 4.4.1 Augmented tunable error states for nominal voltage tracking and improved reactive power sharing ( $e_i$ )

As stated in [94] and detailed in [95], instead of tracking a reference input, it is preferable to track the integration of the error between the targeted state and its reference value, which resulted in an LQR control that's able to achieve zero steady-state error in this tracking mode. These additional error states are used for correcting the deviation in the output voltage of each DG, as follows:

$$e_i = \int (v_{odi} - v_{nominal}) dt \quad (4.34)$$

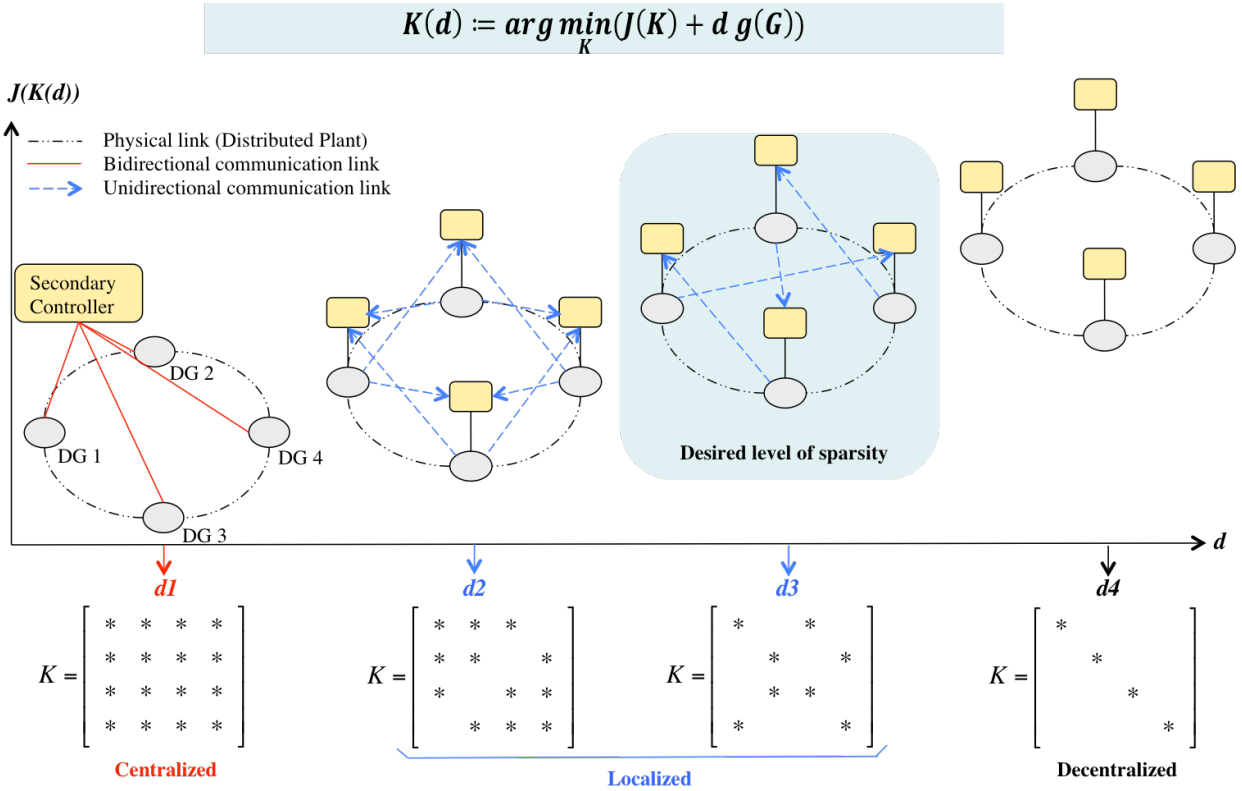


Figure 4-4. Achieving a balance between performance and sparsity in microgrid's secondary controller via sparsity-promoting optimal control approach.

where,  $v_{odi}$  is the output voltage of  $i^{th}$  DG,  $v_{odj}$  is the output voltage power of  $j^{th}$  DG,  $v_{nominal}$  is the nominal in the microgrid.

The lines impedances used for the microgrid connections can have very dissimilar values. Therefore, in order to maintain acceptable level of reactive power sharing between the DGs, the formulation of the above tracking states needs to be implemented in a tunable way that's considering its effect of on the reactive power sharing as well between all DGs. Therefore, the optimal corrective control action is the one that can reach the best tradeoff between:

- Correcting the voltage deviation of each DG from its nominal value, to avoid lower quality of the power system (as the connected loads will be working at lower values than its nominals),

- Correcting the voltage deviations between DGs to avoid current circulating issue between the connected DGs,
- And maintaining a fair share of the produced power between all DGs based on their capability, to avoid overloading conditions.

Based on this understating, the below expression is used for each error state dynamic. This tunable control protocol allows multiple options for the designers based on their preferences for the microgrid, as follows:

$$e_i = \int \left[ l(Q_i - Q_j) + m \left( v_{odi} - \frac{n}{m} v_{odj} - \frac{p}{m} v_{nominal} \right) \right] dt \quad (4.35)$$

where,

$Q_i$  is the reactive power of  $i^{th}$  DG,

$Q_j$  is the reactive power of  $j^{th}$  DG,

$v_{odi}$  is the output voltage of  $i^{th}$  DG,

$v_{odj}$  is the output voltage power of  $j^{th}$  DG,

$v_{nominal}$  is the nominal in the microgrid,

$l$  is reactive power sharing weight of  $i^{th}$  DG,

$m$  overall voltage deviation correction weight of  $i^{th}$  DG,

$n$  is voltage deviation from the  $j^{th}$  DGs correction weight of  $i^{th}$  DG,

$p$  is voltage deviation from nominal correction weight of  $i^{th}$  DG.

Note that  $m = n + p$ . As shown in the above equations, the formulation of these additional states can be realized with only few additional low-bandwidth communication links between neighboring DGs or as suggested by the sparsity promoting procedure.

#### 4.4.2 State Weight Matrix (Q)

In microgrid secondary control problem, based on the design objective of regulating the voltage of each DG, and maintaining acceptable level of reactive power sharing between all DGs, the targeted states, of the state matrix  $A_{mg}$ , that desired to be regulated within optimal transient response are the error states of each DG that was introduced in the previous section. Therefore, a reasonable choice of the state weight matrix  $Q$  is to be a diagonal matrix with nonzero diagonal elements (weights) for these targeted states. To unify the states weights with different units, all weights are identical and normalized according to the rating values of their DG. Note that other controllable states such as local currents and reactive power, can be targeted as well to improve their transient response during load changes. However, to focus our attention to the voltage correction problem, these states are not considered in the regulation problem.

#### 4.4.3 Control Weight Matrix (R)

Similar to the adopted method in unifying states' weights, the control weight (effort) are also follows the same arrangement. Therefore, assuming all DGs are having comparable ranges of control effort ( $\rho$ ), the control weight matrix can be chosen simply as  $R = \frac{1}{\rho^2}I$ , where  $I$  (identity matrix)  $\in \mathbb{R}^{s \times s}$  ( $s$ : number of inverters in the system). However, one needs to consider that the system model is a linearized one around a stable operating point; therefore, should avoid high gains

that may derive the system away from its linear region where the approximated linearized model is no longer valid. Moreover, lower gains guarantee a lower bandwidth secondary controller to provide the necessary decoupling between the primary control level and the secondary level to avoid conflicts over disturbances.

#### **4.4.4 Disturbance Matrix ( $B_w$ )**

It's important here to consider the choice of  $B_w$  as a part of the design parameters since the Reachability Gramian  $S(K)$ , as discussed in Chapter 3, is highly depending on the disturbance matrix  $B_w$  for evaluating the optimal gain  $K$  for distributed controller. For simplicity, the disturbance matrix can be chosen to model a noisy channel of the control signal ( $B_w = B_u$ ).

#### **4.4.5 Desired Level of Sparsity ( $d$ )**

As shown in Section 3.2,  $d$  is a design parameter that reflects the level of sparsity that the designer would like to reach (i.e. number of communication links in the system). Higher value of this positive variable will place farther weight to the additional term in the cost function of the optimization problem (3.8). As suggested in [59], the desired level of sparsity is reached by solving the optimal problem (3.8) iteratively starting with smaller value of  $d$  until reaching the desired  $d^*$ , preferably in logarithmic scale.

## 4.5 SIMULATION AND RESULTS

### 4.5.1 Test System Description

In order to verify the ability of the introduced distributed secondary voltage controller (DSVC), presented in the previous sections, to achieve its objectives with satisfactory results, a simulated model of a typical microgrid system has been implemented accordingly, and tested under various operation conditions. The selected test system in Figure 4-5, with system parameters as shown in Table 4.1, has been implemented in MATLAB/SIMULINK. The DC side of each DG is represented by a voltage source (ideal source) that is limited by a rating value of 10 kVA, such assumption is safe and has no effect on the analysis [29]. This DC power source is connected to the VSC converter and then to the common bus through a transmission line. As shown, the system is operated on the islanded mode where the point of common coupling (PCC), which connected the microgrid to the main grid, was kept open throughout the test. The suggested size of the microgrid in this study was selected based on its capability to proof the effectiveness of the control method, while avoiding unnecessary additional complexity to the system.

### 4.5.2 Design Guides

- 1) Obtaining the steady-state initial conditions (stable operating point) by applying a stable load condition (within rating values of the microgrid) and use a general power-flow (load-flow) solvers, that typically used in conventional power grid to obtain the corresponding stable operating point. Alternately, these steady-state initial conditions can be obtained by using a simulated model in MATLAB/SIMULINK environment that emulate the real

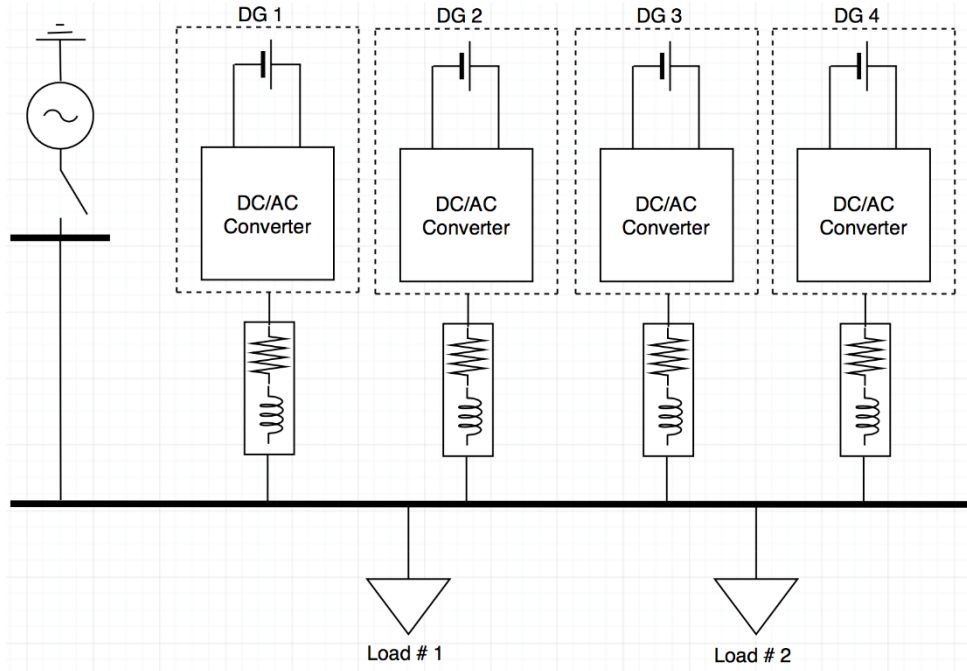


Figure 4-5. Microgrid test configuration.

system. It's recommended to choose an operating point that is in a moderate range of operation. For sanity check, one can obtain multiple operating points, especially those that are in the extreme end of the operation, and check their stability in the mathematical model. In this case the stability of these operating points would confirm the validity of the mathematical model.

- 2) Using the attained steady-state operating point from step one along with the test system's parameters, the system's mathematical model can be calculated; namely, the state matrix  $A_{mg}$  of the system. Since the model is linearized around a stable operating point, the parameters in the system are needed to obtain the state matrix of the reduced order model that's developed in the previous section. A simulated mathematical model was build in MATLAB/SIMULINK environment as well to compare the resulted dynamic represented

Table 4-1 System parameters.

DGs parameters (10 kVA rating)			
Parameter	Value	Parameter	Value
$V_{DC}$	650 V	$R_f$	0.1 $\Omega$
$V_n$	381.0512 V	$L_f$	1.35 mH
$m_p$	0.000094	$C_f$	50 $\mu$ F
$n_Q$	0.0013	$R_c$	0.03 $\Omega$
$f$	50 Hz	$L_c$	0.35 mH
$K_{pv}$	0.05	$K_{pc}$	10.5
$K_{iv}$	390	$K_{ic}$	16k
Lines parameters			
$R_{l1}$	0.23 $\Omega$	$R_{l2}$	0.5 $\Omega$
$L_{l1}$	2.9 mH	$L_{l2}$	318 $\mu$ H
$R_{l3}$	0.23 $\Omega$	$R_{l4}$	0.6 $\Omega$
$L_{l3}$	1.8 mH	$L_{l4}$	1.9 mH
Loads parameters			
$P_{load1}$	5.8 kW	$P_{load2}$	33 kW
$Q_{load1}$	0	$Q_{load2}$	18.7 kVAR

by this reduced order system with the full order nonlinear representation of the system. The finding of this comparison was reported in [93], which indicate a high accuracy of the model.

- 3) Then, directed by the recommendations on Section 4.4, the design parameters of the distributed (structured) secondary controller (regulator) are obtained accordingly, which are state weight matrix Q, control weight matrix R, disturbance matrix  $B_w$ , and the desired level of sparsity  $d$ . Note that the tunable error states in the Q matrix ( $e_i$ ) are defined with the flexibility to accommodate designer preferences in case of mismatch line impedances. For homogenous scenario, where line impedances are identical, these error states do not need to be tunable and would follow the general definition as presented in (4.34).

- 4) Now, solve the design problem of distributed (structured) optimal regulator using the suggested Sparsity-Promoting approach, as highlighted in Section 3.4 and as detailed in Chapter 3, to find the state-feedback matrix  $K$  that can achieve the desired performance and sparsity of the controller. Note that the optimization problem is solved offline to calculate the recommended static gains of the state-feedback matrix  $K$ ; then, this set of gains is uploaded to the system for real time implementation.

### 4.5.3 Test Procedure and Results

Using the design steps highlighted in the previous section, the expected outcome is to have a memoryless “Sparse” secondary controller (regulator), which is capable of the microgrid voltage levels restoration, providing needed active/reactive power, maintaining both active/reactive power sharing and the system’s closed-loop stability, with low communication links, preferably unidirectional. To verify these capabilities of the controller using the simulated model of the test system in MATLAB/SIMULINK environment, the simulated model was tested under homogenous setup (identical line impedances), heterogeneous setup (different line impedances), and Generators Disturbances, as follows:

#### 4.5.3.1 Voltage Levels Restoration and Power Correction in homogenous Setup (identical

**line impedances)** To test the controller’s ability for voltage restoration, the system will be initially running at no load condition followed by two load interruptions. Firstly, with a relatively small resistive load of 5.8 kW ( $25 \Omega$  per phase) at  $t = 1$  sec. Then, by a large inductive (RL) load of 38 kVA with power factor of 0.87 at  $t = 3$  sec. Transmission lines in this test has identical values ( $Z = 0.23 + j 0.91$ ). As shown in Figure 4-7, during resistive load (from  $t = 1$  sec to  $t = 3$  sec) primary

control loops were able to provide the needed active power (P), which is shared equally between the DGs. This control action produced by the primary control level has no effect on the output voltage ( $v_{od}$ ), as all DGs has maintained their nominal values. However, applying the inductive load at  $t = 3$  sec have caused consistent deviations in voltage magnitude in all DGs in order to produce the required reactive power (Q), as shown in Figure 4-6. This deviation has the same value for all DGs (output error = 3%, bus error = 7%) since transmission lines are identical, with an equal share of the reactive load between DGs. However, as a result of working away from system nominal voltage value, the total produced active power (P) has a deficiency of 2 kW.

Following the design guides highlighted in 4.5.2, a distributed secondary voltage control was integrated into the system. Figure 4-7 shows the suggested state-feedback matrix K based on sparsity-promoting method with the corresponding communication links, and Table. 4.2 illustrates the number of nonzero elements and performance degradation compared to the equivalent centralized controller. The same load conditions were applied again while using the DSVC control to verify the ability of the controller to correct the deviations resulted from the primary control loops. As shown in Figure 4-6, the DSVC controller was able to restore nominal voltage to all DGs with a settling time of 10 msec (resulted bandwidth < 100 Hz, much lower than the primary control bandwidth). It also showed that the controller didn't disturb the operation of the primary control level under no-load and the resistive load periods. Moreover, as the controller was able to correct the voltage deviation in all DGs, the total produced active power was corrected as well with no deviations, as depicted in Figure 4-6. Finally, the voltage correction response of the DSVC controller was compared with a centralized controller, and a decentralized PID controller. Since both secondary controlling methods reached the same steady-state value in this homogenous test,

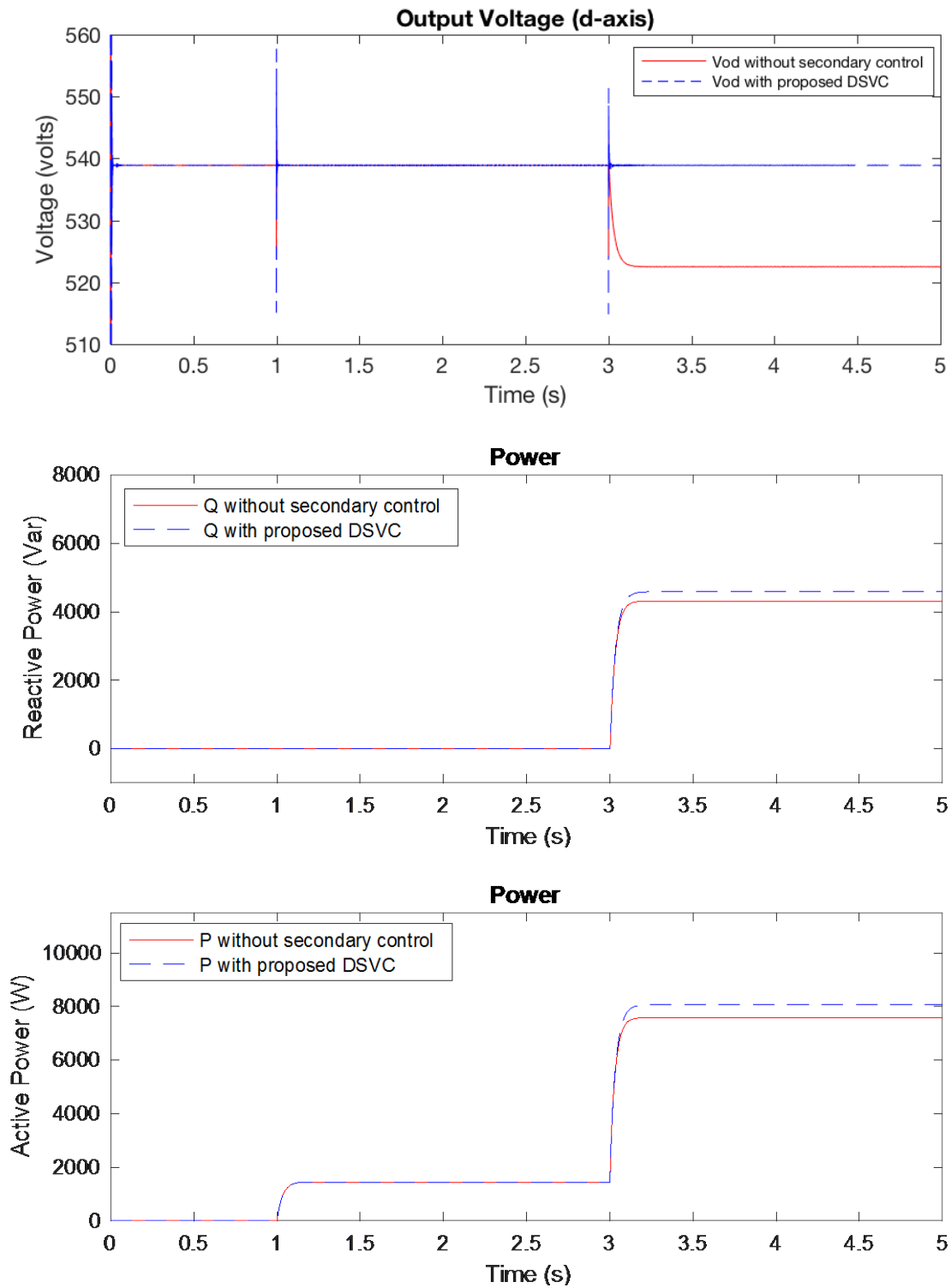


Figure 4-6.  $V_{od}$ ,  $Q$ , and  $P$  in homogeneous system with identical line impedances before and after using secondary control under: no load, resistive load, and a large inductive load.

comparing the transient responses is more accurate in this case. As illustrated in Figure 4-8, the DSVC controller demonstrates its superiority over the PID controller (tuned using classical Ziegler-Nichols method) in term of overshooting (PID has relatively higher value 1.2%) and time constants (50 times faster than PID). Moreover, the DSVC controller indicates a very comparative step response characteristics compared to the centralized controller.

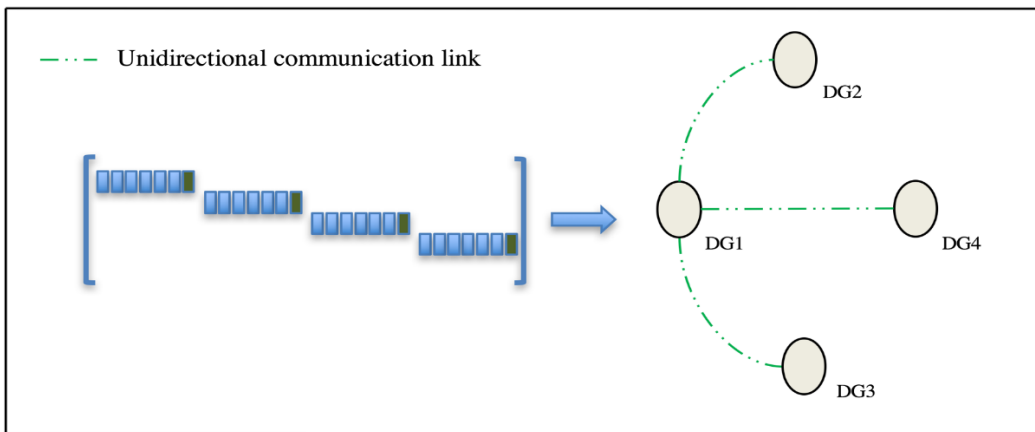


Figure 4-7. Suggested state-feedback matrix  $K$  based on SP method with the corresponding communication links, for voltage regulation and power correction in homogenous system with identical line impedances.

Table 4-2. Number of nonzero elements and performance degradation compared to the equivalent centralized controller, case (1).

	Level of sparsity (d)	Number of nonzero elements (K)	Degradation in performance
Centralized Optimal Control	0	108	0%
Distributed Optimal Control (case 1)	1.6	27	0.82%

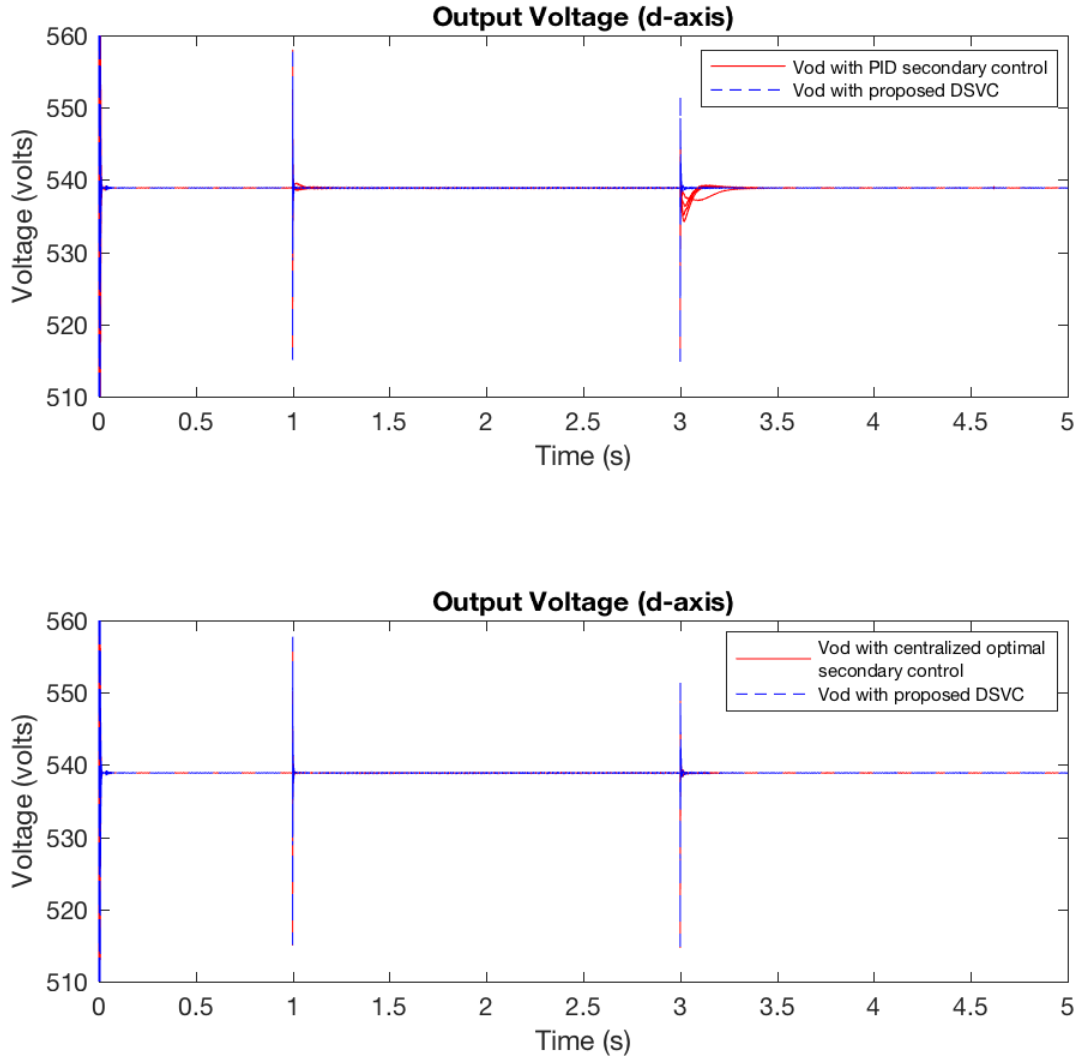


Figure 4-8. Vod responses in homogenous system with the distributed secondary voltage control (DSVC) compared to PID control and centralized optimal control.

**4.5.3.2 Voltage Levels Restoration, Power Correction, and Reactive Power Sharing in**

**Heterogeneous Setup (different line impedances)** Similar test will be repeated, but with different

line impedances, to verify the controller ability for both voltage/ power corrections and active/ reactive power sharing property. The same load disturbances were applied within the same time

periods; however, the line impedances in this setup have very dissimilar values as illustrated in

table. 1. As shown in Figure 4-9, during resistive load (from  $t = 1$  sec to  $t = 3$  sec), primary control

loops were able to provide the required active power (P), which is shared equally between the DGs. This control action produced by the primary control level has no effect on the output voltage ( $v_{od}$ ) as all DGs have maintained their nominal values. However, applying a large inductive load at  $t = 3$  sec have caused diverse deviations in voltage magnitude for all DGs to produce the required reactive power (Q), as shown in Figure 4-9. These voltage deviations have different values, due to the dissimilarity in transmission lines, with max output voltage error of 3.6% and bus voltage error of 7.22%. However, reactive power sharing between DGs was at acceptable level (normalized standard deviation between DGs = 0.8459). The total produced active power (P) during this large inductive load was distributed equally, but with a deficiency of 3.2 kW as a result of working away from system nominal values.

Again, following the design guides highlighted in 4.5.2, a distributed optimal secondary voltage control was integrated into the system. However, in this heterogeneous setup, further communication links are needed to promote reactive power sharing while preserving an acceptable level of output voltage for all DGs. These additional links can be chosen as suggested by sparsity-promoting method, after decreases the level of sparsity (lower value of (d)), or can be arbitrary selected based on geographical restrictions or economic factors; the earlier method is adopted in this study. These selected communication links are considered with zero weights during sparsity promoting optimization iteration, and will slightly improve the performance index, as the state-feedback (K) been dragged toward more centralization structure (number of nonzero elements increases). The final step of designing the distributed secondary voltage control in heterogeneous condition is to use the added links in formulating the tunable error states as presented in 4.4.1 (with the following weight values:  $l = \frac{1}{100}$ ,  $m = 3$ ,  $n = 1$ ,  $p = 2$ ).

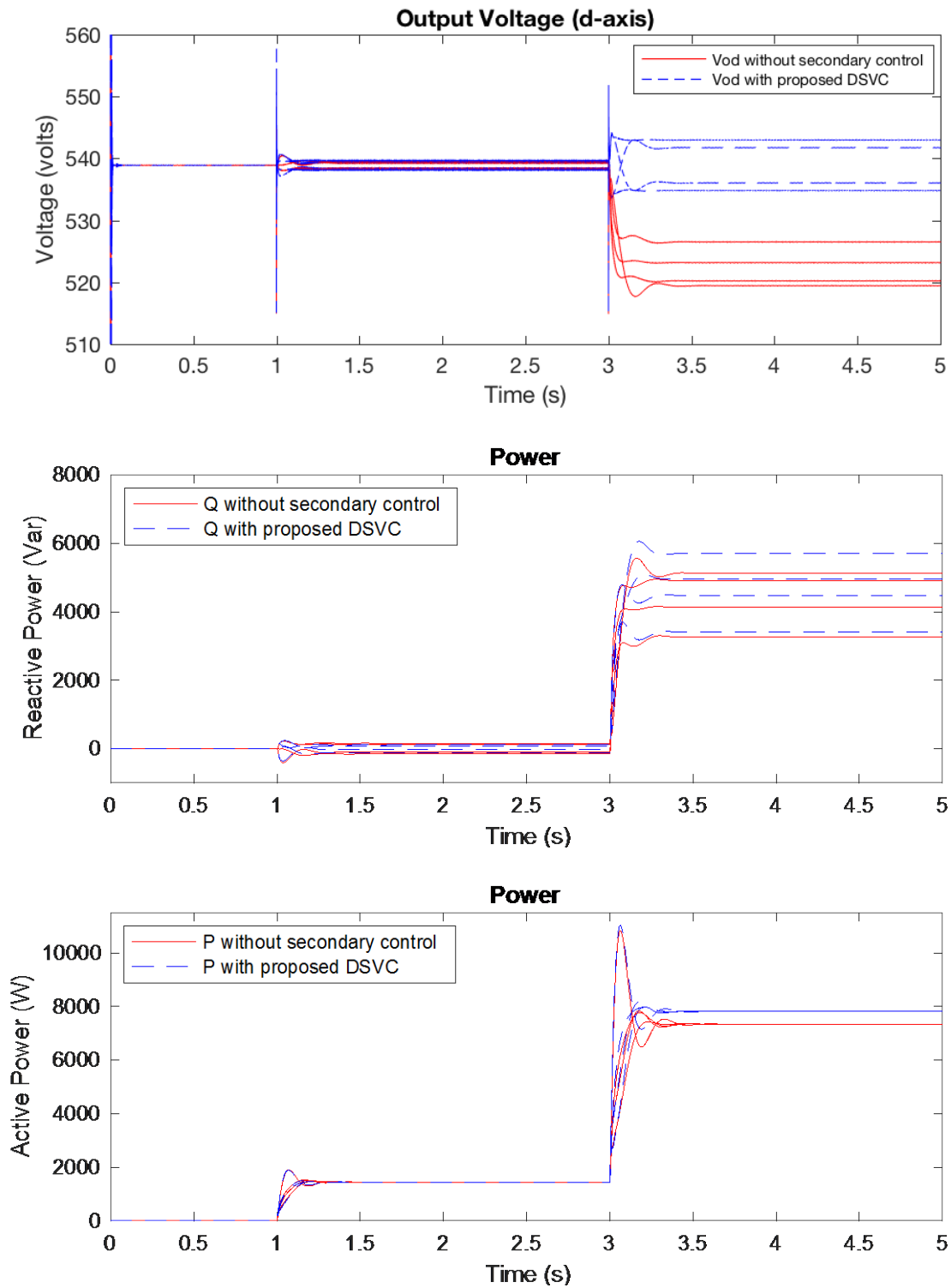


Figure 4-9.  $V_{od}$ ,  $Q$ , and  $P$  responses in heterogeneous system with different line impedances, before and after adding the distributed secondary voltage control (DSVC), under: no load, resistive load, and a large inductive load.

Figure 4-10 shows the suggested state-feedback matrix  $K$  based on sparsity-promoting method with the corresponding communication links, and Table 4-3 illustrates the number of nonzero elements and performance degradation compared to the equivalent centralized controller. The same test was conducted while using the DSVC controller to verify the ability of the controller to correct the deviations resulted from the primary control loops and preserve acceptable level of power sharing. As shown in Figure 4-9, the DSVC controller was able to restore acceptable level

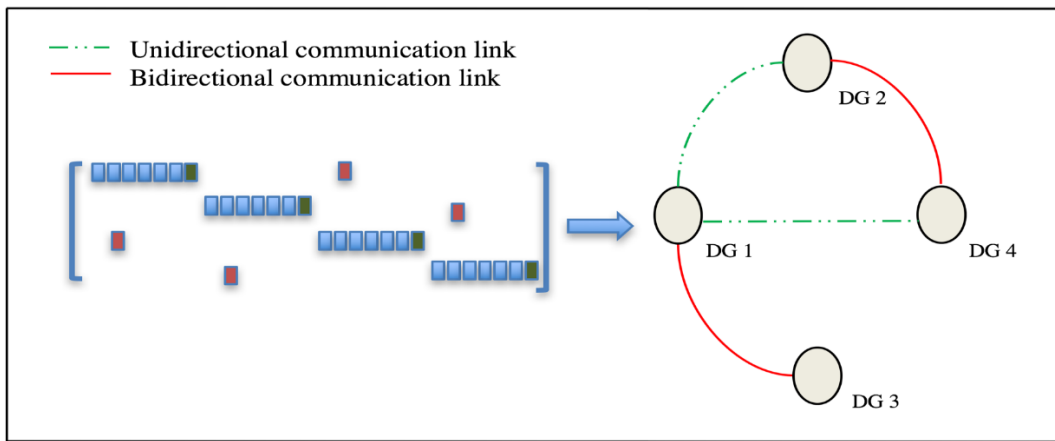


Figure 4-10. Suggested state-feedback matrix  $K$  based on SP method with the corresponding communication links, for voltage regulation and reactive power sharing in heterogeneous system with different line impedances.

Table 4-3. Number of nonzero elements and performance degradation compared to the equivalent centralized controller, case (2).

	Level of sparsity (d)	Number of nonzero elements (K)	Degradation in performance
Centralized Optimal Control	0	108	0%
Distributed Optimal Control (case 2)	0.9	31	0.6%

of deviation from nominal voltage of all DGs (max output error = 0.7%, bus error = 4.06%) with a settling time of 0.3 sec. It also showed that the controller didn't disturb the operation of the primary control level under no-load and resistive load periods. Moreover, as the controller was able to reduce voltage deviations in all DGs, the total produced active power was also corrected with a minimal deviation (200 W), as depicted in Figure 4-9. Also, as shown in the same figure, the controller was able to preserve tolerable level of reactive power sharing between the DGs (normalized standard deviation between DGs = 0.9687).

Finally, the reactive power sharing results of the DSVC controller was compared with the decentralized PID controller and the centralized controller. As illustrated in Figure 4-11, the DSVC controller achieved tolerable level of reactive power sharing between the DGs (normalized standard deviation between DGs = 0.9687), compared to the PID controller which has an overloaded DG with normalized standard deviation between DGs of 2.7743. Moreover, as shown in Figure 4-12, the centralized controller has established reactive power sharing values that has much lower normalized standard deviation of 0.3792 compared to the primary controller. Furthermore, the DSVC controller indicates very comparative results to the other controllers in term of total active power correction, approximately 200 W lower than the PID controller with very marginal difference compared to the centralized controller.

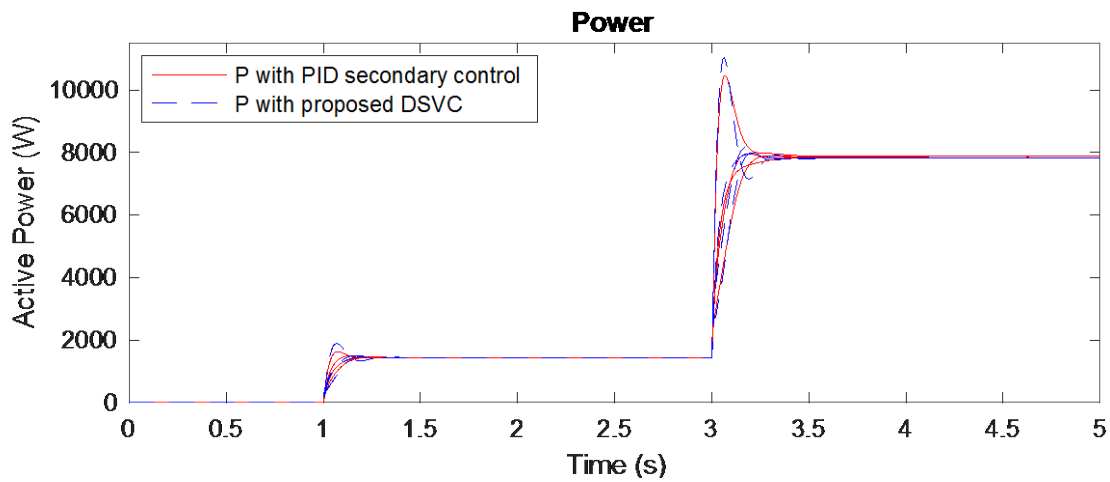
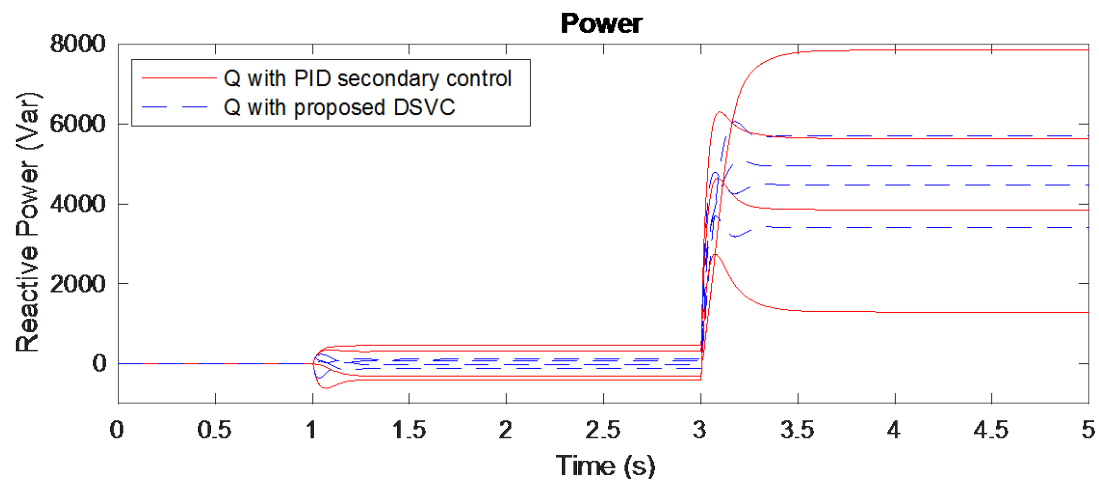


Figure 4-11. Q & P responses with the distributed secondary voltage control (DSVC) compared with PID control.

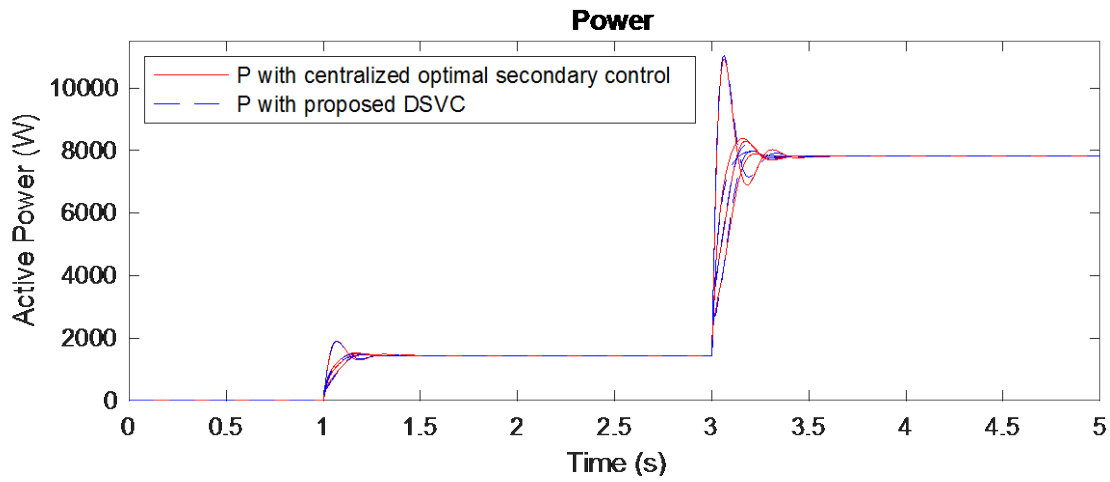
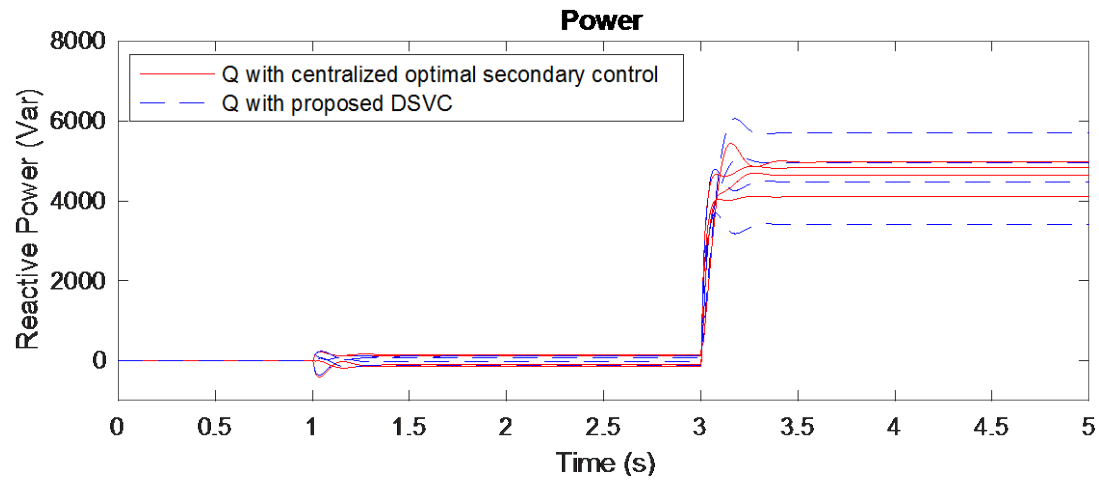


Figure 4-12. Q & P responses with the distributed secondary voltage control (DSVC) compared with optimal centralized secondary control.

**4.5.3.3 Reliability Against Generators Interruptions** Large signal stability analysis of the overall system is highly complex and beyond the scope of this dissertation; instead, the DSVC controller was tested under various challenging conditions to verify its reliability. In the previous two tests, the distributed secondary voltage controller was tested under the whole spectrum of the microgrid operation range, namely: no load, low resistive load, large inductive load; with satisfactory results. In this section, the controlled system is tested under generators disconnections as these disturbances are often expected in microgrids.

To test the controller's ability under generator interruptions, the system will be initially running at large inductive load condition followed by a generator interruption. Firstly, the connected load is shared by the 4 DGs; then, DG-4 was disconnected from the system at  $t = 2.5$  sec. The transmission line impedances in this test are on the homogenous setup as presented in the initial test. As shown in Figure 4.13, during the initial period where all 4 DGs are connected (from  $t = 0$  sec to  $t = 2.5$  sec), the primary and secondary control levels showed same level of performance as presented in previous sections in term of output voltage, power correction, and load sharing between generators. In the second period, where DG 4 is disconnected from the system ( $t = 2.5$  sec to  $t = 5$  sec), the distributed secondary controller was able to uphold stable operation and maintain nominal values of the output voltages, compared to the system response without adding the secondary layer with output voltage error of 3.06%, and bus voltage error of 7.14%. Moreover, the total produced active and reactive power before adding the secondary control has a deficiency of 2 kW and 1.2 kVar, respectively. This has been successfully corrected after adding the distributed secondary control layer. It has been observed, as shown in Figure 4.13, that DG 4 has a lower reactive power contribution compared to the other DGs. Such unequal share of the reactive power is unexpected in homogenous condition where all transmission lines have similar values. In

fact, this reactive power deviation of DG 4 was due to the additional impedance of the circuit breaker that was placed at the connection point of the generator, causing again dissimilar values of the transmission lines. After disconnecting DG 4, reactive power was equally shared between the connected DGs, which confirms the above analysis.

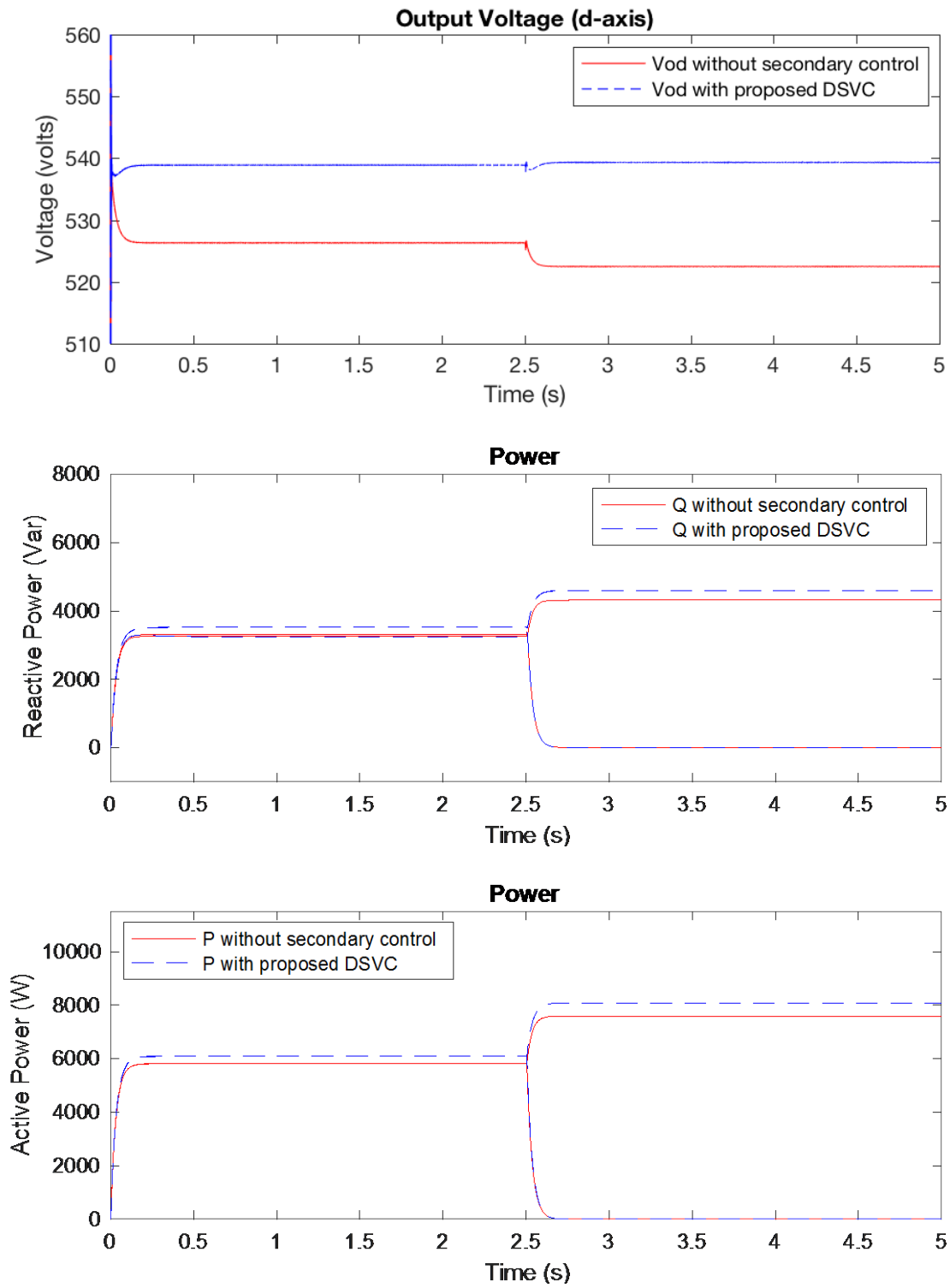


Figure 4-13. Vod, Q, and P responses after DG4 disconnection at 2.5 sec, before and after using distributed secondary voltage control (DSVC).

## **5.0 CONCLUSION AND FUTURE WORK**

### **5.1 CONCLUSION**

In conclusion, this research study successfully achieves its objective of designing a distributed secondary voltage controller for small/medium scale AC microgrids (inverter-based and droop-controlled) that is able to realize the standard secondary control goals, as defined in hierarchical control structure of microgrid [7]- [9]. Firstly, the ability of the introduced distributed voltage controller (DSVC) to restore the output voltage of all connected DGs to their nominal values, or to tolerable levels of deviation in case of heterogeneous conditions. Attaining this task enables the connected DGs to produce a total power that matches the demand at higher accuracy. Secondly, the developed distributed secondary voltage controller demonstrates its capability to maintaining a proper level of active and reactive power sharing as established by the primary controllers, even during very dissimilar impedances in line transmissions. Moreover, the established structure of the suggested controller accomplishes a desired level of sparsity using only unidirectional links in homogenous condition, and limited bidirectional links in heterogeneous setups. In term of performance, the resulted controlled system shows superior response compared to the conventional PID controllers, and very similar resulted to the optimal centralized secondary controller, with stable operation under the full spectrum of operations. Furthermore, a robustness test against

challenging operation conditions such as generator interruptions was conducted, and the obtained results concluded a satisfactory performance of the DSVC controller under such conditions.

The simulation results have showed that using Sparsity-Promoting approach in designing distributed (structured) secondary controller for droop-controlled (inverter-based) microgrid is a systematic flexible framework that's trying to reach a balance between performance (voltage and frequency regulation "Consensus" and active/reactive power sharing property), Cost (control effort needed and number of communication links), and sparsity (Communication links needed). Moreover, it provides the flexibility to choose communication links on need-to-know or availability/accessibility basis (not neighboring basis), and able to identify (recognize) critical links. In comparison to the existing methods, as highlighted in Chapter 2, Sparsity-Promoting method would require much lower gain that is tunable based on the choice of the control weight matrix  $R$ . These lower control gains are desirable for maintaining lower bandwidth to avoid possible instability effects caused by improper coupling between the primary and secondary control levels. Furthermore, this employed method has considered power-sharing property, not only the regulation problems as seen in [49]- [51]. Moreover, because the communication topology is extracted from the state-feedback matrix  $K$ , the communication links does not have to be a bidirectional type in all links; this would increase the system's reliability, as unidirectional communication links are less susceptible to failures and delays. Besides, as this control method was able to achieve encouraging results in homogenous scenarios, it was also able to provide satisfactory results in heterogeneous scenario, of multiple DGs with very dissimilar line impedances values, which is a challenge situation for most existing techniques [52]- [55]. To summarized these advantages, they are listed as follow:

- Systematic and flexible method providing a balance between performance (voltage regulation “Consensus” and active/reactive power sharing property), Cost (control effort needed and number of communication links), and level of sparsity (Communication links needed).
- Communication links can be identified based on a prescribed level of performance (acceptable level of performance compared with a central controller case) and based on need-to-know or availability/accessibility basis (not based on predetermined topology or neighboring basis).
- Capability of identifying (recognizing) critical links; this is a very helpful guidance for the system’s protection designer in the protection scheme.
- Requiring much lower control gains that is tunable based on the selection of control weight matrix  $R$  as a design parameter.
- Maintaining active/reactive power-sharing property, not only voltage magnitude regulation requirements.
- The unidirectional communication links would higher the system’s reliability, as they are less susceptible to failures and delays.
- Provide encouraging results in heterogeneous scenarios (very dissimilar line impedances values).

On the other hand, the Sparsity-Promoting approach would have some limitations. The major drawback of this approach is the limited scalability because of the cubic complexity nature of the algorithm. However, microgrid is meant to be in small or medium size, so the algorithm is well fitting for the application. Also, a reduced order model can be used to reduce dimensionality in

case of larger scales microgrid. The other limitation of this method is maintaining the plug and play property (i.e. the flexibility of plugging-in and plugging-out system's DGs, loads, or storages) when affecting a critical communication link. To allow such property, a moderate level of sparsity should be maintained.

## 5.2 FUTURE WORK

This dissertation provides very promising results for a distributed optimal control in appropriate flexible framework that allows tradeoffs in performance indexes for AC microgrid application. However, a set of important problems remain unconcluded, and opens avenues for further development and improvements, as follows:

- Firstly, the resulted distributed (structured) regulator can be used to further enhance system stability (stabilizer), as sensitivity analysis in [29] and [83] has identified states related to the low frequency oscillatory modes with lower damping ratios (Higher frequency oscillatory modes improved their damping with larger  $R_d$  [83]), so it can help to regulate these states within acceptable limits. However, to enable such stabilizing task, a full order model should be used that representing states of interest, instead of the reduced order model used in this study, with a modified set of control inputs (B matrix) that can control the targeted states, based on an appropriate controllability analysis.
- Moreover, in such network control systems, communications delay is a common problem that needs to be intensely studied to conclude time delay margins of the system where the system can work with a desired level of reliability. Such study is still an open problem in

secondary control level of AC microgrid application, and its findings would be a great contribution to the developed control system in this dissertation.

- Furthermore, even though small signal analysis showed a stable operation of the system, which have been confirmed under challenging simulation testes, an extensive large signal stability study is needed to be able to run the system with a proper level of stability margins for higher level of reliable operation.
- In more compact implementation of microgrid, single-phase generators might be preferable over the typical three-phase ones due to the small scale of the system (smaller units and shorter distances) and nature of the connected loads. In such a small microgrid, a similar control levels can still be used but in this case a centralized structure might be preferable as the communication cost and reliability would not be a big concern. However, a distributed structure can be still implemented in the same manner. The challenge task in this implementation is to find an effective way to convert the single-phase AC signal into the dqo-synchronous frame (with acceptable time delay) to maintain same level of performance as achieved in the three-phase implementation, such conversion can be done using all pass filter as suggested in [96].
- Additionally, to preserve stability in imbalance load conditions, an additional control loop could be added in the primary control level to compensate for the zero-component in the synchronous (dqo) frame. These additional loops will follow the same control settings in the dq-components and its additional voltage state can be neglected holding the similar assumption used for the q-component.
- Finally, similar analysis and design can be conducted and implemented for frequency control as well for more comprehensive solution.

## APPENDIX

### Full Order Model of AC Microgrid

Full Order Small-Signal State-Space Model of inverter-based (droop-controlled) AC microgrid, as reported in [29]:

Power Controller:

$$\begin{aligned}
 A_P &= \begin{bmatrix} 0 & -m_p & 0 \\ 0 & -\omega_c & 0 \\ 0 & 0 & -\omega_c \end{bmatrix}, B_{Pwcom} = \begin{bmatrix} -1 \\ 0 \\ 0 \end{bmatrix}, B_P = \begin{bmatrix} 0 & 0 & 0 & 0 & 0 & 0 \\ 0 & 0 & \omega_c I_{od} & \omega_c I_{oq} & \omega_c V_{od} & \omega_c V_{oq} \\ 0 & 0 & \omega_c I_{oq} & -\omega_c I_{od} & -\omega_c V_{oq} & \omega_c V_{od} \end{bmatrix} \\
 C_{P\omega} &= \begin{bmatrix} 0 & -m_p & 0 \end{bmatrix}, C_{Pv} = \begin{bmatrix} 0 & 0 & -n_q \\ 0 & 0 & 0 \end{bmatrix}
 \end{aligned}$$

Voltage Controller:

$$\begin{aligned}
 B_{V1} &= \begin{bmatrix} 1 & 0 \\ 0 & 1 \end{bmatrix}, B_{V2} = \begin{bmatrix} 0 & 0 & -1 & 0 & 0 & 0 \\ 0 & 0 & 0 & -1 & 0 & 0 \end{bmatrix}, C_V = \begin{bmatrix} K_{iv} & 0 \\ 0 & K_{iv} \end{bmatrix} \\
 D_{V1} &= \begin{bmatrix} K_{pv} & 0 \\ 0 & K_{pv} \end{bmatrix}, D_{V2} = \begin{bmatrix} 0 & 0 & -K_{pv} & -\omega_n C_f & F & 0 \\ 0 & 0 & \omega_n C_f & -K_{pv} & 0 & F \end{bmatrix}
 \end{aligned}$$

Current Controller:

$$B_{c1} = \begin{bmatrix} 1 & 0 \\ 0 & 1 \end{bmatrix}, B_{c2} = \begin{bmatrix} -1 & 0 & 0 & 0 & 0 & 0 \\ 0 & -1 & 0 & 0 & 0 & 0 \end{bmatrix}, C_c = \begin{bmatrix} K_{ic} & 0 \\ 0 & K_{ic} \end{bmatrix}$$

$$D_{c1} = \begin{bmatrix} K_{pc} & 0 \\ 0 & K_{pc} \end{bmatrix}, D_{c2} = \begin{bmatrix} -K_{pc} & -\omega_n L_f & 0 & 0 & 0 & 0 \\ \omega_n L_f & -K_{pc} & 0 & 0 & 0 & 0 \end{bmatrix}$$

LCL output filter:

$$A_{LCL} = \begin{bmatrix} \frac{-r_{L_f}}{L_f} & \omega_o & \frac{-1}{L_f} & 0 & 0 & 0 \\ -\omega_o & \frac{-r_{L_f}}{L_f} & \frac{-1}{L_f} & 0 & 0 & 0 \\ \frac{1}{C_f} & 0 & 0 & \omega_o & \frac{-1}{C_f} & 0 \\ 0 & \frac{1}{C_f} & -\omega_o & 0 & 0 & \frac{-1}{C_f} \\ 0 & 0 & \frac{1}{L_c} & 0 & \frac{-r_{L_c}}{L_c} & \omega_o \\ 0 & 0 & 0 & \frac{1}{L_c} & -\omega_o & \frac{-r_{L_c}}{L_c} \end{bmatrix}, B_{LCL1} = \begin{bmatrix} \frac{1}{L_f} & 0 \\ 0 & \frac{1}{L_f} \\ 0 & 0 \\ 0 & 0 \\ 0 & 0 \\ 0 & 0 \end{bmatrix}, B_{LCL3} = \begin{bmatrix} 0 & 0 \\ 0 & 0 \\ 0 & 0 \\ -\frac{1}{L_c} & 0 \\ 0 & -\frac{1}{L_c} \end{bmatrix}$$

$$B_{LCL3} = \begin{bmatrix} I_{iq} & -I_{id} & V_{oq} & -V_{od} & I_{oq} & -I_{od} \end{bmatrix}^T$$

Reference-frame Transformation matrices:

$$T_S = \begin{bmatrix} \cos(\delta_o) & -\sin(\delta_o) \\ \sin(\delta_o) & \cos(\delta_o) \end{bmatrix}, T_C = \begin{bmatrix} -I_{od} \sin(\delta_o) - I_{oq} \cos(\delta_o) \\ I_{od} \cos(\delta_o) - I_{oq} \sin(\delta_o) \end{bmatrix}$$

$$T_V^{-1} = \begin{bmatrix} -V_{bd} \sin(\delta_o) + V_{bq} \cos(\delta_o) \\ -V_{bd} \cos(\delta_o) - V_{bq} \sin(\delta_o) \end{bmatrix}$$

Single Inverter Model:

$$A_{INVi} = \begin{bmatrix} A_{Pi} & 0 & 0 & B_{Pi} \\ B_{V1i} C_{Pvi} & 0 & 0 & B_{V2i} \\ B_{C1i} D_{V1i} C_{Pvi} & B_{C1i} C_{Vi} & 0 & B_{C1i} D_{V2i} + B_{C2i} \\ B_{LCL1i} D_{C1i} D_{V1i} C_{Pvi} & & & A_{LCLi} \\ B_{LCL2i} [T_V^{-1} \ 0 \ 0] & B_{LCL1i} D_{C1i} C_{Vi} & B_{LCL1i} C_{Ci} & B_{LCL1i} (D_{C1i} D_{V2i} + D_{C2i}) \\ B_{LCL3i} C_{P\alpha i} & & & \end{bmatrix}_{13 \times 13}$$

$$B_{INVi} = \begin{bmatrix} 0 \\ 0 \\ 0 \\ B_{LCL2i} T_S^{-1} \end{bmatrix}_{13 \times 2}, B_{i\alpha\omega} = \begin{bmatrix} B_{P\alpha\omega} \\ 0 \\ 0 \\ 0 \end{bmatrix}_{13 \times 1}, C_{INV\alpha i} = \begin{cases} \begin{bmatrix} C_{P\omega} & 0 & 0 & 0 \end{bmatrix}_{1 \times 13} & i=1 \\ \begin{bmatrix} 0 & 0 & 0 & 0 \end{bmatrix}_{1 \times 13} & i \neq 1 \end{cases}$$

$$C_{INVci} = \begin{bmatrix} [T_C \ 0 \ 0] & 0 \ 0 & [0 \ 0 \ T_S] \end{bmatrix}_{2 \times 13}$$

Multiple Inverters Model:

$$A_{INV} = \begin{bmatrix} A_{INV1} + B_{1\omega com} C_{INV\omega 1} & 0 & 0 & \cdot \\ 0 & A_{INV2} + B_{2\omega com} C_{INV\omega 1} & 0 & \cdot \\ \cdot & \cdot & \cdot & \cdot \\ \cdot & \cdot & \cdot & A_{INVs} + B_{s\omega com} C_{INV\omega 1} \end{bmatrix}_{13s \times 13s}$$

$$B_{INV} = \begin{bmatrix} B_{INV1} \\ B_{INV2} \\ \cdot \\ \cdot \\ B_{INVs} \end{bmatrix}_{13s \times 2m}, C_{INVc} = \begin{bmatrix} [C_{INVc1}] & 0 & 0 & \cdot \\ 0 & [C_{INVc2}] & 0 & \cdot \\ \cdot & \cdot & \cdot & \cdot \\ \cdot & \cdot & \cdot & [C_{INVcs}] \end{bmatrix}$$

$$[\Delta v_{bDQ}] = [\Delta v_{bDQ1} \quad \Delta v_{bDQ2} \quad \dots \quad \Delta v_{bDQm}]$$

Network Model:

$$A_{NETi} = \begin{bmatrix} \frac{-r_{linei}}{L_{linei}} & \omega_o \\ -\omega_o & \frac{-r_{linei}}{L_{linei}} \end{bmatrix}, B_{2,NETi} = \begin{bmatrix} I_{lineQi} \\ -I_{lineDi} \end{bmatrix}$$

$$B_{1,NETi} = \begin{bmatrix} \dots & \frac{1}{L_{linei}} & 0 & \dots & \frac{-1}{L_{linei}} & 0 & \dots \\ \dots & 0 & \frac{1}{L_{linei}} & \dots & 0 & \frac{-1}{L_{linei}} & \dots \end{bmatrix}$$

$$A_{NET} = \begin{bmatrix} A_{NET1} & 0 & \dots & 0 \\ 0 & A_{NET2} & \dots & 0 \\ \dots & \dots & \dots & \dots \\ 0 & 0 & \dots & A_{NETn} \end{bmatrix}_{2n \times 2n}$$

$$B_{1NET} = \begin{bmatrix} B_{1NET1} \\ B_{1NET2} \\ \dots \\ B_{1NETn} \end{bmatrix}_{2n \times (2m)}$$

$$, B_{2NET} = \begin{bmatrix} B_{2NET1} \\ B_{2NET2} \\ \dots \\ B_{2NETn} \end{bmatrix}_{2n \times 1}$$

Individual Load Model:

$$A_{loadi} = \begin{bmatrix} \frac{-R_{loadi}}{L_{loadi}} & \omega_o \\ \omega_o & \frac{-R_{loadi}}{L_{loadi}} \end{bmatrix}, B_{2loadi} = \begin{bmatrix} I_{loadQi} \\ -I_{loadDi} \end{bmatrix}$$

$$B_{1loadi} = \begin{bmatrix} \dots & \frac{1}{L_{loadi}} & 0 & \dots \\ \dots & 0 & \frac{1}{L_{loadi}} & \dots \end{bmatrix}$$

Multiple Loads Model:

$$A_{load} = \begin{bmatrix} A_{load1} & 0 & \dots & 0 \\ 0 & A_{load2} & \dots & 0 \\ \dots & \dots & \dots & \dots \\ 0 & 0 & \dots & A_{loadp} \end{bmatrix}_{2p \times 2p}$$

$$B_{load} = \begin{bmatrix} B_{load1} \\ B_{load2} \\ \dots \\ B_{loadp} \end{bmatrix}_{2p \times (2m)}, \quad B_{2load} = \begin{bmatrix} B_{2load1} \\ B_{2load2} \\ \dots \\ B_{2loadp} \end{bmatrix}_{2p \times (1)}$$

microgrid Overall Model:

$$A_{mg} = \begin{bmatrix} A_{INV} + B_{INV}R_N M_{INV} C_{INVc} & B_{INV}R_N M_{NET} & B_{INV}R_N M_{load} \\ B_{1NET}R_N M_{INV} C_{INVc} + B_{2NET}C_{INV\omega} & A_{NET} + B_{1NET}R_N M_{NET} & B_{1NET}R_N M_{load} \\ B_{1load}R_N M_{INV} C_{INVc} + B_{2load}C_{INV\omega} & B_{1load}R_N M_{NET} & A_{load} + B_{1load}R_N M_{load} \end{bmatrix}$$

## BIBLIOGRAPHY

- [1] R. H. Lasseter, "MicroGrids," Power Engineering Society Winter Meeting, 2002. IEEE, 2002, pp. 305-308 vol.1.
- [2] IEEE Guide for Design, Operation, and Integration of Distributed Resource Island Systems with Electric Power Systems," in IEEE Std 1547.4-2011, vol., no., pp.1-54, July 20 2011.
- [3] LI, Qing, Zhao XU, and Li YANG. "Recent advancements on the development of microgrids." Journal of Modern Power Systems and Clean Energy, vol. 2, no. 3, 2014, pp. 206-211.
- [4] J. A. P. Lopes, C. L. Moreira and A. G. Madureira, "Defining control strategies for MicroGrids islanded operation," in IEEE Transactions on Power Systems, vol. 21, no. 2, pp. 916-924, May 2006.
- [5] M. Smith, D. Ton, "Key Connections: The U.S. Department of Energy's Microgrid Initiative," Power and Energy Magazine, IEEE, vol.11, no.4, pp.22, 27, July 2013.
- [6] M. Shahidehpour and S. Pullins, "Is the Microgrid Buzz Real?" in IEEE Electrification Magazine, vol. 2, no. 1, pp. 2-5, March 2014.
- [7] J. M. Guerrero, J. C. Vasquez, J. Matas, L. G. de Vicuna and M. Castilla, "Hierarchical Control of Droop-Controlled AC and DC Microgrids—A General Approach Toward Standardization," in IEEE Transactions on Industrial Electronics, vol. 58, no. 1, pp. 158-172, Jan. 2011.
- [8] A. Bidram and A. Davoudi, "Hierarchical Structure of Microgrids Control System," in IEEE Transactions on Smart Grid, vol. 3, no. 4, pp. 1963-1976, Dec. 2012.
- [9] Y. A. R. I. Mohamed and A. A. Radwan, "Hierarchical Control System for Robust Microgrid Operation and Seamless Mode Transfer in Active Distribution Systems," in IEEE Transactions on Smart Grid, vol. 2, no. 2, pp. 352-362, June 2011.
- [10] H. Karimi, "Islanding Detection and Control of an Islanded Electronically Coupled Distributed Generation Unit," Ph.D., Univ. Toronto, Dept. of ECE., 2007.
- [11] D. E. Olivares et al., "Trends in Microgrid Control," in IEEE Transactions on Smart Grid, vol. 5, no. 4, pp. 1905-1919, July 2014.

- [12] A. Madureira, C. Moreira, and J. Peças Lopes, "Secondary load-frequency control for microGrids in islanded operation," in Proc. ICREPQ, Frankfurt, Germany, 2005, pp. 1–4.
- [13] B. Awad, J. Wu, and N. Jenkins, "Control of distributed generation," *Elektrotechnik & Informationstechnik*, vol. 125, no. 12, pp. 409–414, 2008.
- [14] A. Mehrizi-Sanir and R. Iravani, "Secondary control for microgrids using potential functions: Modeling issues," in Proc. CYGRE, 2009, pp. 182.1–182.9.
- [15] K. Vanthournout, K. De Brabandere, E. Haesen, J. Van den Keybus, G. Deconinck, and R. Belmans, "Agora: Distributed tertiary control of distributed resources," in Proc. 15th Power Syst. Comput. Conf., Liege, Belgium, Aug. 22–25, 2005.
- [16] A. G. Madureira and J. A. Peças Lopes, "Voltage and reactive power control in MV networks integrating MicroGrids," in Proc. ICREPQ, Seville, Spain, 2007.
- [17] H. Karimi, H. Nikkhajoei, and M. R. Iravani, "Control of an electronically-coupled distributed resource unit subsequent to an islanding event," *IEEE Trans. Power Del.*, vol. 23, no. 1, pp. 493–501, Jan. 2008.
- [18] F. Katiraei, M. R. Iravani, and P. W. Lehn, "Micro-grid autonomous operation during and subsequent to islanding process," *IEEE Trans. Power Del.*, vol. 20, no. 1, pp. 248–257, Jan. 2005.
- [19] H. Karimi, A. Yazdani, and M. R. Iravani, "Negative-sequence current injection for fast islanding detection of a distributed resource unit," *IEEE Trans. Power Electron.*, vol. 23, no. 1, pp. 298–307, Jan. 2008.
- [20] F. Blaabjerg, R. Teodorescu, M. Liserre, and A. V. Timbus, "Overview of control and grid synchronization for distributed power generation systems," *IEEE Trans. Ind. Electron.*, vol. 53, no. 5, pp. 1398–1409, Oct. 2006.
- [21] F. Gao and M. R. Iravani, "A control strategy for a distributed generation unit in grid-connected and autonomous modes of operation," *IEEE Trans. Power Del.*, vol. 23, no. 2, pp. 850–859, Apr. 2008.
- [22] K. D. Brabandere, B. Bolsens, J. V. den Keybus, A. Woyte, J. Driesen, and R. Belmans, "A voltage and frequency droop control method for parallel inverters," *IEEE Trans. Power Electron.*, vol. 22, no. 4, pp. 1107–1115, Jul. 2007.
- [23] Y. Li, D. M. Vilathgamuwa, and P. C. Loh, "Design, analysis, and real-time testing of a controller for multibus microgrid system," *IEEE Trans. Power Electron.*, vol. 19, no. 5, pp. 1195–1204, Sep. 2004.
- [24] C. K. Sao and P. W. Lehn, "Autonomous load sharing of voltage source converters," *IEEE Trans. Power Del.*, vol. 20, no. 2, pp. 1009–1016, Apr. 2005.

- [25] P. Piagi and R. H. Lasseter, "Autonomous control of microgrids," in Proc. IEEE Power and Energy Soc. General Meet., Jun. 2006.
- [26] H. Nikkhajoei and R. H. Lasseter, "Distributed generation interface to the CERTS microgrid," IEEE Trans. Power Del., vol. 24, no. 3, pp. 1598–1608, Jul. 2009.
- [27] M. C. Chandorkar, D. M. Divan, and R. Adapa, "Control of parallel connected inverters in standalone ac supply systems," IEEE Trans. Ind. Appl., vol. 29, no. 1, pp. 136–143, Jan./Feb. 1993.
- [28] M. Prodanović and T. C. Green, "High-quality power generation through distributed control of a power park microgrid," IEEE Trans. Ind. Electron., vol. 53, no. 5, pp. 1471–1482, Oct. 2006.
- [29] N. Pogaku, M. Prodanovic, and T. C. Green, "Modeling, analysis and testing of autonomous operation of an inverter-based micro-grid," IEEE Trans. Power Electron., vol. 22, no. 2, pp. 613–625, Mar. 2007.
- [30] J. M. Guerrero, L. Hang, and J. Uceda, "Control of distributed uninterruptible power supply systems," IEEE Trans. Ind. Electron., vol. 55, no. 8, pp. 2845–2859, Aug. 2008.
- [31] C. -L. Chen, Y. Wang, J. -S. Lai, Y.-S. Lee, and D. Martin, "Design of parallel inverters for smooth mode transfer microgrid applications," IEEE Trans. Power Electron., vol. 25, no. 1, pp. 6–15, Jan. 2010.
- [32] A. Micallef, M. Apap, C. Spiteri-Staines, J. M. Guerrero, and J. C. Vasquez, "Reactive power sharing and voltage harmonic distortion compensation of droop controlled single phase islanded microgrids," IEEE Trans. Smart Grid, vol. 5, no. 3, pp. 1149–1158, 2014.
- [33] M. Savaghebi, A. Jalilian, J. C. Vasquez, and J. M. Guerrero, "Secondary control for voltage quality enhancement in microgrids," IEEE Trans. Smart Grid, vol. 3, no. 4, pp. 1893–1902, 2012.
- [34] A. Mehrizi-Sani and R. Iravani, "Potential-function based control of a microgrid in islanded and grid-connected models," IEEE Trans. Power Syst., vol. 25, no. 4, pp. 1883–1891, Nov. 2010.
- [35] J. Machowski, J. W. Bialek, and J. R. Bumby, Power System Dynamics, 2nd ed. Wiley, 2008.
- [36] Q. Shafiee, J. M. Guerrero and J. C. Vasquez, "Distributed Secondary Control for Islanded Microgrids—A Novel Approach," in IEEE Transactions on Power Electronics, vol. 29, no. 2, pp. 1018-1031, Feb. 2014.
- [37] M. Savaghebi, A. Jalilian, J. C. Vasquez and J. M. Guerrero, "Secondary Control Scheme for Voltage Unbalance Compensation in an Islanded Droop-Controlled Microgrid," in IEEE Transactions on Smart Grid, vol. 3, no. 2, pp. 797-807, June 2012.

- [38] D. Yazdani, A. Bakhshai, G. Joos, and M. Mojiri, "A nonlinear adaptive synchronization technique for grid-connected distributed energy sources," *IEEE Trans. Power Electron.*, vol. 23, pp. 2181–2186, Jul. 2008.
- [39] B. P. McGrath, D. G. Holmes, and J. J. H. Galloway, "Power converter line synchronization using a discrete Fourier transform (DFT) based on a variable sample rate," *IEEE Trans. Power Electron.*, vol. 20, pp. 877–884, Jul. 2005.
- [40] S. J. Lee, H. Kim, S. K. Sul, and F. Blaabjerg, "A novel control algorithm for static series compensators by use of PQR instantaneous power theory," *IEEE Trans. Power Electron.*, vol. 19, pp. 814–827, May 2004.
- [41] D. Jovcic, "Phase-locked loop system for FACTS," *IEEE Trans. Power Syst.*, vol. 18, pp. 1116–1124, Aug. 2003.
- [42] A. Yazdani and R. Iravani, "A unified dynamic model and control for the voltage source converter under unbalanced grid conditions," *IEEE Trans. Power Del.*, vol. 21, pp. 1620–1629, Jul. 2006.
- [43] M. Andreasson, D. V. Dimarogonas, H. Sandberg, and K. H. Johansson, "Distributed control of networked dynamical systems: Static feedback, integral action and consensus," *IEEE Trans. Autom. Control*, vol. 59, no. 7, pp. 1750–1764, 2014.
- [44] Y. Wang, Z. Chen, X. Wang, Y. Tian, Y. Tan and C. Yang, "An Estimator-Based Distributed Voltage-Predictive Control Strategy for AC Islanded Microgrids," in *IEEE Transactions on Power Electronics*, vol. 30, no. 7, pp. 3934-3951, July 2015.
- [45] Y. B. Wang, Y. J. Tian, X. F. Wang, Z. Chen, and Y. D. Tan, "Kalman-filter- based state estimation for system information exchange in a multi-bus islanded microgrid," in *Proc. 7th IET Int. Conf. Power Electron., Mach. Drives*, Apr. 8–11, 2014, pp. 1–6.
- [46] Y. B. Wang, X. F. Wang, Z. Chen, Y. J. Tian, and Y. D. Tan, "A communication-less distributed voltage control strategy for a multi-bus islanded AC microgrid," in *Proc. Int. Power Electron. Conf.*, May 18–21, 2014, pp. 3538–3545.
- [47] J. M. Guerrero, J. C. Vasquez, J. Matas, M. Castilla and L. Garcia de Vicuna, "Control Strategy for Flexible Microgrid Based on Parallel Line-Interactive UPS Systems," in *IEEE Transactions on Industrial Electronics*, vol. 56, no. 3, pp. 726-736, March 2009.
- [48] Q. Shafiee, C. Stefanovic, T. Dragicevic, P. Popovski, J. C. Vasquez, and J. [68] M. Guerrero, "Robust networked control scheme for distributed secondary control of islanded microgrids," *IEEE Trans. Ind. Electron.*, vol. 61, no. 10, pp. 5363–5374, Oct. 2014.
- [49] A. Bidram, A. Davoudi, F. L. Lewis, and Z. Qu, "Secondary control of microgrids based on distributed cooperative control of multi-agent systems," *IET Gener., Transmiss. Distrib.*, vol. 7, pp. 822–831, Aug. 2013.

- [50] A. Bidram, A. Davoudi, F. L. Lewis, and J. M. Guerrero, "Distributed cooperative secondary control of microgrids using feedback linearization," *IEEE Trans. Power Syst.*, vol. 28, no. 3, pp. 3462–3470, Aug. 2013.
- [51] A. Bidram, F. L. Lewis and A. Davoudi, "Distributed Control Systems for Small-Scale Power Networks: Using Multiagent Cooperative Control Theory," in *IEEE Control Systems*, vol. 34, no. 6, pp. 56-77, Dec. 2014.
- [52] H. Bouattour, J. W. Simpson-Porco, F. Dorfler, and F. Bullo, "Further results on distributed secondary control in microgrids," *IEEE Conf. Decision Control*, 2013, pp. 1514–1519.
- [53] J. W. Simpson-Porco, F. Dorfler, F. Bullo, Q. Shafiee, and J. M. Guerrero, "Stability, power sharing, and distributed secondary control in droop- controlled microgrids," *Proc. IEEE Smart Grid Commun. Symp.*, 2013, pp. 672–677.
- [54] J. W. Simpson-Porco, F. Dorfler, and F. Bullo, "Synchronization and power sharing for droop-controlled inverters in islanded microgrids," *Automatica*, vol. 49, pp. 2603–2611, Jun. 2013.
- [55] J. W. Simpson-Porco, Q. Shafiee, F. Dörfler, J. C. Vasquez, J. M. Guerrero and F. Bullo, "Secondary Frequency and Voltage Control of Islanded Microgrids via Distributed Averaging," in *IEEE Transactions on Industrial Electronics*, vol. 62, no. 11, pp. 7025-7038, Nov. 2015.
- [56] F. L. Lewis, H. Zhang, K. Hengster-Movric, and A. Das, "Cooperative Control of Multi-Agent Systems: Optimal and Adaptive Design Approaches," Berlin, Germany: Springer-Verlag, 2014.
- [57] A. L. D. Franco, H. Bourles, E. R. De Pieri and H. Guillard, "Robust nonlinear control associating robust feedback linearization and  $H_\infty$  control," in *IEEE Transactions on Automatic Control*, vol. 51, no. 7, pp. 1200-1207, July 2006.
- [58] F. Guo, C. Wen, J. Mao and Y. D. Song, "Distributed Secondary Voltage and Frequency Restoration Control of Droop-Controlled Inverter-Based Microgrids," in *IEEE Transactions on Industrial Electronics*, vol. 62, no. 7, pp. 4355-4364, July 2015.
- [59] F. Lin, M. Fardad and M. R. Jovanović, "Design of Optimal Sparse Feedback Gains via the Alternating Direction Method of Multipliers," in *IEEE Transactions on Automatic Control*, vol. 58, no. 9, pp. 2426-2431, Sept. 2013.
- [60] W Ren, Y Cao, "Distributed coordination of multi-agent networks: emergent problems, models, and issues," 1st edition New York; London; : Springer-Verlag; 2011;2010;.
- [61] A. Sarlette and R. Sepulchre, "Consensus optimization on manifolds," *SIAM J. Control Optim.*, vol. 48, no. 1, pp. 56–76, 2009.
- [62] V. D. Blondel and J. N. Tsitsiklis, "A survey of computational complexity results in systems and control," *Automatica*, vol. 36, no. 9, pp. 1249–1274, 2000.

- [63] H. S. Witsenhausen, "A counterexample in stochastic optimum control," *SIAM Journal on Control*, vol. 6, no. 1, pp. 131–147, 1968.
- [64] F. Lin, M. Fardad and M. R. Jovanović, "Algorithms for Leader Selection in Stochastically Forced Consensus Networks," in *IEEE Transactions on Automatic Control*, vol. 59, no. 7, pp. 1789-1802, July 2014.
- [65] C.-H. Fan, J. L. Speyer, and C. R. Jaensch, "Centralized and decentralized solutions of the linear-exponential-Gaussian problem," *Automatic Control, IEEE Transactions on*, vol. 39, no. 10, pp. 1986–2003, 1994.
- [66] X. Qi, M. V. Salapaka, P. G. Voulgaris, and M. Khammash, "Structured optimal and robust control with multiple criteria: A convex solution," *Automatic Control, IEEE Transactions on*, vol. 49, no. 10, pp. 1623– 1640, 2004.
- [67] M. Rotkowitz and S. Lall, "A characterization of convex problems in decentralized control," *Automatic Control, IEEE Transactions on*, vol. 51, no. 2, pp. 274–286, 2006.
- [68] P. Shah and P. Parrilo, "H<sub>2</sub>-optimal decentralized control over posets: A state space solution for state-feedback," in *Decision and Control (CDC), 2010 49th IEEE Conference on*, 2010, pp. 6722–6727.
- [69] S. Schuler, P. Li, J. Lam, and F. Allgower, "Design of structured dynamic output-feedback controllers for interconnected systems," *International Journal of Control*, vol. 84, no. 12, pp. 2081–2091, 2011.
- [70] S. Schuler, U. Munz, and F. Allgower, "Decentralized state feedback control for interconnected systems with application to power systems," *Journal of Process Control*, 2013.
- [71] K. Dvijotham, E. Theodorou, E. Todorov, and M. Fazel, "Convexity of optimal linear controller design," in *Proceedings of the Control and Decision Conference*, 2013.
- [72] K. Dvijotham, E. Todorov, and M. Fazel, "Convex structured controller design," *CoRR*, vol. abs/1309.7731, 2013.
- [73] S Schuler, P Li, J Lam, F Allgöwer, "Design of structured dynamic output-feedback controllers for interconnected systems," *International Journal of Control*, 2011.
- [74] S Schuler, U Münz, F Allgöwer, "Decentralized State Feedback Control for Interconnected Process Systems," *IFAC Proceedings Volumes*, 2012.
- [75] P. L. D. Peres and J. C. Geromel, "An alternate numerical solution to the linear quadratic problem," *IEEE Trans. Autom. Control*, vol. 39, pp. 198–202, 1994.
- [76] S. Boyd, N. Parikh, E. Chu, B. Peleato, and J. Eckstein, "Distributed optimization and statistical learning via the alternating direction method of multipliers," *Found. Trends Mach. Learning*, vol. 3, no. 1, pp. 1–124, 2011.

- [77] S. Boyd and L. Vandenberghe, *Convex Optimization*. Cambridge, U.K.: Cambridge Univ. Press, 2004.
- [78] N. Motee and A. Jadbabaie, "Optimal control of spatially distributed systems," *IEEE Trans. Automat. Control*, vol. 53, no. 7, pp. 1616–1629, Jul. 2008.
- [79] P. V. Kokotovic, H. K. Khali, and J. O'Reilly, *Singular Perturbation Methods in Control: Analysis and Design*, ser. TJ213.K3924, 1999.
- [80] D. Naidu, *Singular Perturbation Methodology in Control Systems*, Dec. 1987.
- [81] M. Rasheduzzaman, J. A. Mueller and J. W. Kimball, "Reduced-Order Small-Signal Model of Microgrid Systems," in *IEEE Transactions on Sustainable Energy*, vol. 6, no. 4, pp. 1292-1305, Oct. 2015.
- [82] E. A. A. Coelho, P. Cortizo, and P. F. D. Gracia, "Small signal stability for parallel-connected inverters in stand-alone ac supply systems," *IEEE Trans. Ind. Appl.*, vol. 38, no. 2, pp. 533–542, Mar./Apr. 2002.
- [83] M. Rasheduzzaman, J. A. Mueller and J. W. Kimball, "An Accurate Small-Signal Model of Inverter- Dominated Islanded Microgrids Using dq Reference Frame," in *IEEE Journal of Emerging and Selected Topics in Power Electronics*, vol. 2, no. 4, pp. 1070-1080, Dec. 2014.
- [84] J. M. Undrill, "Dynamic stability calculations for an arbitrary number of interconnected synchronous machines," *IEEE Trans. Power Appar. Syst.*, vol. PAS-87, no. 3, pp. 835–845, Mar. 1968.
- [85] RE Skelton, *Dynamic systems control: linear systems analysis and synthesis*, New York: Wiley; 1988.
- [86] A. C. Antoulas and D. C. Sorensen, "Approximation of large-scale dynamical systems: An overview," *App. Math. Comp. Science*, vol. 11, no. 5, p. 1093–1122, 2001.
- [87] CL Phillips, JM Parr, *Feedback control systems*, 5th ed. Boston: Prentice Hall; 2011.
- [88] J. Hahn and T. F. Edgar, "An improved method for nonlinear model reduction using balancing of empirical gramians," *Comp. Chem. Eng.*, vol. 26, no. 10, p. 1379–1397, 2002.
- [89] A. Bidram, A. Davoudi and F. L. Lewis, "A Multiobjective Distributed Control Framework for Islanded AC Microgrids," in *IEEE Transactions on Industrial Informatics*, vol. 10, no. 3, pp. 1785-1798, Aug. 2014.
- [90] S. Dasgupta, S. N. Mohan, S. K. Sahoo and S. K. Panda, "A Plug and Play Operational Approach for Implementation of an Autonomous-Micro-Grid System," in *IEEE Transactions on Industrial Informatics*, vol. 8, no. 3, pp. 615-629, Aug. 2012.

- [91] Q. Shafiee, J. C. Vasquez and J. M. Guerrero, "Distributed secondary control for islanded MicroGrids - A networked control systems approach," IECON 2012 - 38th Annual Conference on IEEE Industrial Electronics Society, Montreal, QC, 2012, pp. 5637-5642.
- [92] F. Lin, "Structure identification and optimal design of large-scale networks of dynamical systems," Ph.D. dissertation, Dept. Elect. Eng., Univ. of Minnesota, Minneapolis, MN, 2012.
- [93] H. Al Hassan, "Fault Protection and Reduced-Order Modeling for Secondary Controller Design of Inverter-Based Microgrids," Ph.D. dissertation, Dept. Elect. Eng., Univ. of Pittsburgh, Pittsburgh, PA, 2018.
- [94] K. J. Åström and R. M. Murray, Feedback Systems: An Introduction for Scientists and Engineers. Princeton: Princeton University Press, 2008.
- [95] H. A. Al Hassan, T. Alharbi, S. A. Morello, Z. Mac and B. M. Grainger, "Linear Quadratic Integral Voltage Control of Islanded AC Microgrid Under Large Load Changes," 2018 9th IEEE International Symposium on Power Electronics for Distributed Generation Systems (PEDG), Charlotte, NC, 2018, pp. 1-5.
- [96] Bong-Hwan Kwon, Jin-Ha Choi and Tae-Won Kim, "Improved single-phase line-interactive UPS," in IEEE Transactions on Industrial Electronics, vol. 48, no. 4, pp. 804-811, Aug. 2001.